

**Total Maximum Daily Loads for Dioxins
in the Houston Ship Channel**

**Contract No. 582-0-80121
Work Order No. 582-0-80121-07**

Final Report

Prepared by
*University of Houston
Parsons Water&Infrastructure
PBS&J*

Principal Investigators
*Hanadi Rifai
Randy Palachek
Paul Jensen*

PREPARED IN COOPERATION WITH THE
TEXAS COMMISSION ON ENVIRONMENTAL QUALITY AND
U.S. ENVIRONMENTAL PROTECTION AGENCY

The preparation of this report was financed through grants from the U.S. Environmental Protection Agency through the Texas Commission on Environmental Quality

TCEQ Contact:
Larry Koenig
TMDL Team
P.O. Box 13087, MC - 203
Austin, Texas 78711-3087
lkoenig@tceq.state.tx.us

November, 2005

TABLE OF CONTENTS

LIST OF TABLES.....	vi
LIST OF FIGURES	xi
TABLE OF CONTENTS	2
UNIT SYMBOLS, ABBREVIATIONS, AND CONVERSIONS.....	17
chapter 1	1
INTRODUCTION.....	1
1.1 PROBLEM STATEMENT.....	2
1.2 PROJECT DESCRIPTION.....	3
1.3 DESCRIPTION OF THE REPORT	4
CHAPTER 2.....	6
QUALITY ASSURANCE PROJECT PLAN	6
2.1 AMENDMENTS TO THE APPROVED QAPP.....	6
2.2 QUALITY CONTROL ACTIVITIES.....	7
2.3 QC ISSUES	11
2.3.1 Wet Deposition Sample Mishandling.....	11
2.3.2 Holding Times.....	11
2.3.3 Wet Deposition Sample Duration.....	12
2.3.4 Field Duplicates.....	12
2.3.5 Laboratory Duplicates	15
CHAPTER 3.....	17
MONITORING AND DATA COLLECTION	17
3.1 DESCRIPTION OF SAMPLING ACTIVITIES	18
3.1.1 Assessment of Current Levels and Trends of Dioxins in the Houston Ship Channel	18

3.1.2	Assessment of Major Sources, Transport and Fate of Dioxins in the Houston Ship Channel	35
3.1.3	Gather Information to Support Modeling	48
3.2	SAMPLING RESULTS	50
3.2.1	Assessment of Current Levels and Trends of Dioxins in the Houston Ship Channel	52
3.2.2	Assessment of Major Sources, Transport and Fate of Dioxins in the Houston Ship Channel	146
3.2.3	Flow Measurements in Support of Modeling Activities	182
3.3	COLLECTION OF SEDIMENT DATA TO SUPPORT MODELING ACTIVITIES	198
CHAPTER 4		233
DATA ANALYSIS		233
4.1	SITE-SPECIFIC BIOACCUMULATION FACTORS AND WATER QUALITY TARGETS	233
4.1.1	Development of Site-specific Bioaccumulation Factors	233
4.1.2	Development of Site-specific Biota-Sediment Accumulation Factors	261
4.1.3	Combined Bioaccumulation and Biota to Sediment Accumulation Factors	273
4.1.4	Texas Statewide Water Quality Criterion	284
4.1.5	Tissue Residue Criterion	286
4.1.6	Water Quality Target Calculations for Dissolved PCDD/Fs in Water	287
4.1.7	Water Quality Target Calculations for PCDD/Fs in Water	288
4.1.8	Water Quality Target Calculations for PCDD/Fs in Sediments	294
4.1.9	Observed Target Exceedance Rates	297
4.2	SPATIAL TRENDS	299
4.2.1	Longitudinal Profiles	299
4.2.2	Multivariate Analysis	305
4.3	TEMPORAL TRENDS	328
4.3.1	Historical versus Current Data	328
4.3.2	Time Trends of Current Data	340

4.4	SEASONAL TRENDS	342
4.5	COMPARISON OF DIOXIN DATA AMONG THE THREE SAMPLED MEDIA.....	350
4.5.1	All data	350
4.5.2	Principal Component Analysis	355
4.6	ANALYSIS OF AIR DATA	359
4.6.1	Vapor-to-particle Partitioning	372
4.6.2	Temporal Trend	375
4.6.3	Spatial Trends.....	382
4.6.4	Source Identification	384
4.6.5	Dry Deposition versus Ambient Air Concentrations.....	398
4.6.6	Analysis of Various Air Matrices.....	402
4.6.7	Deposition Loads.....	403
4.7	ANALYSIS OF RUNOFF DATA	407
4.7.1	Runoff Concentrations versus Physical Properties.....	407
4.7.2	Runoff versus Soil/Sediment Profiles.....	407
CHAPTER 5.....		412
MODEL DEVELOPMENT		412
5.1	MEGA-TX MODEL OF THE HOUSTON SHIP CHANNEL	412
5.1.1	Conceptual Model and Schematic	412
5.1.2	Input Data.....	416
5.1.3	Output Data	433
5.1.4	Sensitivity Analysis	440
5.2	WASP SIMPLIFIED MODEL	440
5.2.1	Conceptual Model	448
5.2.2	Channel Segmentation.....	449
5.2.3	Input Parameters.....	449

5.2.4	Model Runs	466
5.3	WASP TRANSIENT MODEL.....	474
5.3.1	Channel Segmentation.....	474
5.3.2	Hydraulic Input.....	474
5.3.3	WASP Model Development.....	481
CHAPTER 6.....		484
STAKEHOLDER/PUBLIC EDUCATION AND INVOLVEMENT.....		484
6.1	SUMMARY OF SUPPORT ACTIVITIES	484
6.2	TECHNICAL PRESENTATIONS AT STAKEHOLDER MEETINGS	485
6.3	PUBLIC OUTREACH	485
CHAPTER 7.....		487
PCB ASSESSMENT.....		487
7.1	PCB WATER QUALITY STANDARDS	488
7.2	PCB ANALYTICAL QUANTIFICATION	489
7.3	SUMMARY OF PCB RESULTS IN THE HOUSTON SHIP CHANNEL	489
7.3.1	In-stream Water	490
7.3.2	Sediment.....	495
7.3.3	Tissue.....	500
7.4	ANALYSIS OF PCB DATA IN THE HOUSTON SHIP CHANNEL	508
7.4.1	BAF/BSAF Calculations	508
7.4.2	Spatial Trends.....	517
7.5	SUMMARY OF AROCLOR RESULTS IN THE HOUSTON SHIP CHANNEL.....	520
7.6	USE SUPPORT AND RISK ASSESSMENT	532
7.7	RECOMMENDATIONS.....	540
CHAPTER 8.....		Error! Bookmark not defined.
SUMMARY AND CONCLUSIONS.....		Error! Bookmark not defined.

APPENDIX A - QUALITY ASSURANCE

APPENDIX B - DIOXIN LABORATORY RESULTS FOR SPRING 2004 SAMPLES

APPENDIX C - SEDIMENT LOAD STUDY

APPENDIX D - BACKGROUND FOR STATISTICAL ANALYSES

APPENDIX E - MODELING FILES

LIST OF TABLES

<u>TABLE #</u>	<u>TITLE</u>	<u>PAGE #</u>
Table 2.1	Standardized Flags Assigned to Data	8
Table 2.2	Percentage Data Packages Reviewed	10
Table 2.3a	Percent Deviation of the Field Duplicates collected in Spring 2004	13
Table 2.3b	Percent Deviation of the Field Duplicates collected in Summer 2004	14
Table 2.3c	Percent Deviation of the Field Duplicates collected in Fall 2004	15
Table 3.1	Number of Samples Collected in for Current Levels and Trend Analysis	20
Table 3.2	Summary of Water, Sediment, and Tissue Sampling in WO7	23
Table 3.3	Catfish Tissue Samples Collected from HSC & Upper Galveston Bay	32
Table 3.4	Blue Crab Tissue Samples Collected from HSC & Upper Galveston Bay	33
Table 3.5	Number of Samples Collected in Support of Sources and Transport Assessment	38
Table 3.6	Summary of Locations for Flow Measurements	51
Table 3.7	Field Measurements during Water Sampling Activities	53
Table 3.8	Physical Characteristics of Water Samples	61
Table 3.9	Total Dioxin Concentrations in Water	65
Table 3.10	Field Measurements during Sediment Sampling Activities	73
Table 3.11	Physical Characteristics of Sediment Samples	76
Table 3.12	Total Dioxin Concentrations in Sediment	78
Table 3.13	Total Dioxin Concentrations in Catfish	87
Table 3.14	Total Dioxin Concentrations in Crabs	88
Table 3.15a	Physical Data for Station 11261	93

Table 3.15b	Radiochemical Data for Station 11261.....	94
Table 3.16a	Physical Data for Station 15244.....	101
Table 3.16b	Radiochemical Data for Station 15244.....	102
Table 3.17a	Physical data for Station 11193.....	108
Table 3.17b	Radiochemical Data for Station 11193.....	109
Table 3.18a	Physical Data for Station 15979.....	114
Table 3.18b	Radiochemical Data for Station 15979.....	115
Table 3.19a	Physical Data for Station 11270.....	119
Table 3.19b	Radiochemical data for Station 11270.....	120
Table 3.20a	Physical data for Station FW1.....	124
Table 3.20b	Radiochemical Data for Station FW1.....	125
Table 3.21a	Physical data for Station 16499.....	130
Table 3.21b	Radiochemical Data for Station 16499.....	131
Table 3.22a	Physical Data for Station 13337.....	135
Table 3.22b	Radiochemical data for Station 13337.....	136
Table 3.23	Summary of Sediment Accumulation Rates.....	140
Table 3.24	Total Dioxin Concentrations in Sediment Cores.....	141
Table 3.25	Total Dioxin Concentrations in Water from Tributaries.....	151
Table 3.26	Dioxin Concentrations in Ambient Air.....	152
Table 3.27	Concentrations of PCDD/PCDFs with respect to Particle Size.....	157
Table 3.28	Dry Deposition fluxes at Clinton Drive and Lang Road sites (December 2003- April 2004)	160

Table 3.29	Wet Deposition Flux Clinton Drive (December 2003-April 2004).....	163
Table 3.30	Dry and Wet Deposition Fluxes at Clinton Drive (September 2004-February 2005) 166	
Table 3.31	Bulk Deposition Fluxes of Dioxins (pg/m ² /day)	167
Table 3.32	Field Measurements during Runoff Sampling Activities	169
Table 3.33	Physical Characteristics of Runoff Samples.....	170
Table 3.34	Physical Characteristics of Soil/Sediment Samples collected during Runoff Sampling	172
Table 3.35	Total Dioxin Concentrations in Runoff.....	173
Table 3.36	Dioxins in Houston Urban Sediment during Runoff Conditions	180
Table 3.37	Dioxins in Houston Urban Sediment Prior to Runoff Sampling.....	181
Table 3.38	Dioxins in Houston Soil collected during Runoff Conditions.....	185
Table 3.39	Dioxins in Houston Soil Prior to Runoff Sampling.....	186
Table 3.40	Average Flows for Each Event.....	193
Table 3.41	Regression Results.....	196
Table 3.42	EMC TSS Values for Various Land Uses	200
Table 3.43	TSS Loads to the Houston Ship Channel from Newell et al. (1992)	201
Table 3.44	Summary of TSS EMC Data from Storm Water Management Joint Task Force	201
Table 3.45	Estimated Annual TSS and VSS Loads to the Houston Ship Channel	218
Table 3.46	Sediment Data from 2002 and 2003 Intensive Surveys	229
Table 3.47	Estimated Annual Volume and Mass of Solids Accumulation in Houston Ship Channel	230

Table 3.48 Sediment and Organic Balances 231

LIST OF FIGURES

<u>FIGURE #</u>	<u>TITLE</u>	<u>PAGE #</u>
Figure 3.1	Locations for Water Sampling in WO7.....	22
Figure 3.2	Locations for Sediment Sampling in WO7.....	25
Figure 3.3	Sediment Locations Sampled in Summer 2004.....	26
Figure 3.4	Sampled Locations in the San Jacinto River in Summer 2005	27
Figure 3.5a	Sampled Locations in Segment 1007 in Summer 2005.....	28
Figure 3.5b	Sampled Locations in Segment 1006 in Summer 2005.....	28
Figure 3.6	Locations for Catfish and Crab Sampling in WO7.....	31
Figure 3.7	Locations of Sediment Cores.....	36
Figure 3.8	Locations for Ambient Air and Wet/Dry Deposition Sampling in WO7	39
Figure 3.9	Runoff Sampling Locations.....	44
Figure 3.10	Rainfall Totals for 24-hour Period Prior to Beginning of Sampling from HCOEM	46
Figure 3.11	Rainfall Hyetographs and Flow During Runoff Events	47
Figure 3.12	Locations for Flow Measurements	49
Figure 3.13	Verical Profiles of Field Parameters (in-stream).....	63
Figure 3.14	Total TEQ Concentrations in Water.....	66
Figure 3.15	Comparison of Dioxin Concentrations in Shallow and Deep Water Samples	68
Figure 3.16	Fugacity Ratios.....	70
Figure 3.17	Organic-carbon Normalized TEQ Concentrations in Sediment.....	80
Figure 3.18	Dioxin Concentrations in High-resolution Sediment samples	82

Figure 3.19	Organic-carbon Normalized Concentrations from High-Resolution Sediment Sampling	83
Figure 3.20	Principal Component Analysis Results for the High-resolution Sediment Samples	84
Figure 3.21	Dioxin Concentrations along Transect at Station 15979	86
Figure 3.22	TEQ Concentrations in Catfish	89
Figure 3.23	TEQ Concentrations in Crabs	90
Figure 3.24	Grain Size Distribution for Core Sediment at Station 11261	95
Figure 3.25	$^{210}\text{Pb}_{\text{xs}}$ and ^7Be Data for Station 11261	95
Figure 3.26	Porosity and POC Data for Station 11261	96
Figure 3.17	POC vs. ^7Be for Station 11261	96
Figure 3.28	^7Be Modeling Data for Station 11261	98
Figure 3.29	$^{210}\text{Pb}_{\text{xs}}$ Modeling Data for Station 11261	98
Figure 3.30	^7Be and $^{210}\text{Pb}_{\text{xs}}$ based Chronologic Profile for Station 11261	99
Figure 3.31	Grain Size Distribution for Core Sediment at Station 15244	103
Figure 3.32	$^{210}\text{Pb}_{\text{xs}}$ and ^7Be Data for Station 15244	103
Figure 3.33	Porosity and POC Data for Station 15244	104
Figure 3.34	$^{210}\text{Pb}_{\text{xs}}$ Modeling Data for Station 15244	104
Figure 3.35	^{137}Cs Data for Station 15244	106
Figure 3.36	$^{239,240}\text{Pu}$ Data for Station 15244	106
Figure 3.37	$^{210}\text{Pb}_{\text{xs}}$ based Chronologic Profile for Station 15244	107
Figure 3.38	Grain Size Distribution for Core Sediment at Station 11193	107

Figure 3.39	$^{210}\text{Pb}_{\text{xs}}$ and ^7Be data for Station 11193	110
Figure 3.40	Porosity and POC Data for Station 11193.....	110
Figure 3.41	$^{210}\text{Pb}_{\text{xs}}$ Modeling Data for Station 11193	112
Figure 3.42	^{137}Cs Data for Station 11193	112
Figure 3.43	$^{210}\text{Pb}_{\text{xs}}$ based Chronologic Profile for Station 11193	113
Figure 3.44	Grain Size Distribution for Core Sediment at Station 15979.....	113
Figure 3.45	$^{210}\text{Pb}_{\text{xs}}$ and ^7Be data for Station 15979	116
Figure 3.46	Porosity and POC Data for Station 15979.....	116
Figure 3.47	$^{210}\text{Pb}_{\text{xs}}$ based Chronologic Profile for Station 15979	118
Figure 3.48	Grain Size Distribution for Core Sediment at Station 11270.....	118
Figure 3.49	$^{210}\text{Pb}_{\text{xs}}$ dat for Station 11270.....	121
Figure 3.50	Porosity and POC Data for Station 11270.....	121
Figure 3.51	^{137}Cs Data for Station 11270	122
Figure 3.52	Grain Size Distribution for Core Sediment at Station FW!.....	126
Figure 3.53	$^{210}\text{Pb}_{\text{xs}}$ and ^7Be Data for Station FW1	126
Figure 3.54	Porosity and POC Data for Station FW1.....	127
Figure 3.55	$^{210}\text{Pb}_{\text{xs}}$ Modeling Data for Station FW1	127
Figure 3.56	^{137}Cs Data for Station FW1	129
Figure 3.57	$^{210}\text{Pb}_{\text{xs}}$ based Chronologic Profile for Station FW1.....	129
Figure 3.58	Grain Size Distribution for Core Sediment at Station 16499	132
Figure 3.59	$^{210}\text{Pb}_{\text{xs}}$ and ^7Be data for Station 16499	132
Figure 3.60	Porosity and POC Data for Station 16499.....	134

Figure 3.61	²¹⁰ Pb _{xs} Chronologic Profile for Station 16499.....	134
Figure 3.62	Grain Size Distribution for Core Sediment at Station 13337	137
Figure 3.63	²¹⁰ Pb _{xs} and ⁷ Be Data for Station 13337	137
Figure 3.64	Porosity and POC Data for Station 13337.....	138
Figure 3.65	²¹⁰ Pb _{xs} Modeling Data for Station 13337	138
Figure 3.67	Dioxin Concentrations in Sediment Cores	144
Figure 3.68	Chronologies of Dioxin Concentrations.....	145
Figure 3.69	Chronologies of Dioxin Concentrations Normalized to maximum Concentrations	147
Figure 3.70	Vertical Profiles of Field Parameters (tributaries)	148
Figure 3.71	Ambient Air Profiles of Dioxins and Furans.....	154
Figure 3.72	ΣTexas-TEQ Distribution by Particle Size	158
Figure 3.73	Dry Deposition Profiles at Clinton Drive and Lang Road Sites (First Dry and Wet Deposition Experiment).....	161
Figure 3.74	Wet Deposition Profile at Clinton Drive (First Dry and Wet Deposition Experiment)	164
Figure 3.75	Wet and Dry Deposition at Clinton Drive (Second Dry and Wet Deposition Experiment)	168
Figure 3.76	Bulk Deposition Profile.....	171
Figure 3.77	Dissolved-Phase Profile of Dioxins.....	175
Figure 3.78	Suspended-Phase (1 micron) Profile of Dioxins	176
Figure 3.79	Suspended-Phase (40 micron) Profile of Dioxins	177

Figure 3.80	Distribution of Total Dioxin Mass in Houston Urban Runoff	178
Figure 3.81	Distribution of TEQ in Houston Urban Runoff.....	178
Figure 3.82	Fraction Contribution of Dioxins in Houston Sediment during Runoff and Dry Conditions	182
Figure 3.83	Fraction Contribution of Dioxins in Houston Grass Soil during Runoff Conditions	187
Figure 3.84	Fraction Contribution of Dioxins in Houston Forest Soil during Runoff Conditions	188
Figure 3.85	Fraction Contribution of Dioxins in Houston Residential Soil during Runoff Conditions	189
Figure 3.86	Fraction Contribution of Dioxins in Houston Transitional Soil during Runoff Conditions	190
Figure 3.87	Fraction Contribution of Dioxins in Houston Urban Soil during Runoff Conditions	191
Figure 3.88	Measured and Predicted Flow in the HSC	197
Figure 3.89	Locations of USGS Gages and Sampling Stations.....	203
Figure 3.90	Relationship between TSS and Flow.....	205
Figure 3.91	Relationship between VSS and Flow	210
Figure 3.92	Distributions Of Flow Normalized W.R.T. Drainage Area.....	215
Figure 3.93	Regression Lines of TSS Against Normalized Flow.....	217
Figure 3.94	Map of Houston Ship Channel	223
Figure 3.95	Maintenance Dredging Contract Reaches and Periods	224

Figure 3.97 Average Sediment Accumulation Rates by Decades 227

UNIT SYMBOLS, ABBREVIATIONS, AND CONVERSIONS

Symbol or abbreviation	Text	Unit Equivalence	Unit Type
°C	degrees celcius		temperature
kg	kilograms	10 ³ grams	mass
g	grams	454 grams ~ 1 pound	mass
mg	milligrams	10 ⁻³ grams	mass
µg	micrograms	10 ⁻⁶ grams	mass
ng	nanograms	10 ⁻⁹ grams	mass
pg	picograms	10 ⁻¹² grams	mass
fg	femtograms	10 ⁻¹⁵ grams	mass
L	liter	3.78 liters ~ 1 gallon	volume
mL	milliliter	10 ⁻³ liters	volume
mBq	millibecquerel	27 microcuries (mCi)	radioactivity
µg/L	micrograms per liter	~10 ⁻⁹ , or 1 ppb	mass/volume concentration
ng/L	nanograms per liter	~10 ⁻¹² , or 1 ppt	mass/volume concentration
pg/L	picograms per liter	~10 ⁻¹⁵ , or 1 ppq	mass/volume concentration
ng/kg	nanograms per kilogram	=10 ⁻¹² , or 1 ppt	mass/mass concentration
mg/g	milligrams per gram	10 ⁻³	mass/mass concentrations
g/cm ²	gram per square centimeter		cumulative mass
mBq/g	millibecquerel per gram		radioactivity
ppm	parts per million	10 ⁻⁶	unitless concentration
ppb	parts per billion	10 ⁻⁹	unitless concentration
ppt	parts per trillion	10 ⁻¹²	unitless concentration
ppq	parts per quadrillion	10 ⁻¹⁵	unitless concentration

CHAPTER 1

INTRODUCTION

Polychlorinated dibenzo-*p*-dioxins (PCDDs) and dibenzofurans (PCDF) and polychlorinated biphenyls (PCBs) are halogenated aromatic compounds that have been widely found in the environment. The PCDDs include 75 congeners and PCDFs include 135 different congeners. Only 7 out of the 75 PCDD congeners and 10 of the 135 PCDF congeners have been identified as having dioxin-like toxicity. There are 209 PCB congeners, of which 13 are identified as having dioxin-like toxicity. These dioxin-like compounds are highly toxic and persistent environmental contaminants and, consequently, have received a great deal of attention by environmental regulators and researchers.

Dioxin (the term used to refer to dioxin-like compounds) presents a likely cancer hazard to humans (U. S. Environmental Protection Agency, 2000a) and can cause health problems even at extremely low doses. Reproductive problems, behavioral abnormalities, and alterations in immune functions are among the health effects caused by exposure to dioxin. Because dioxin-like compounds have been proven to bioaccumulate in biological tissues, particularly in animals, the major route of human exposure is through the food chain. Thus, several food advisories have been issued across the United States to prevent people from consuming unhealthful doses of these compounds.

1.1 PROBLEM STATEMENT

Section §303(d) of the Clean Water Act requires all states to identify waters that do not meet, or are not expected to meet, applicable water quality standards and develop a list of such waters known as the §303(d) list. For each listed water body that does not meet a standard, states must develop a total maximum daily load (TMDL) for each pollutant that has been identified as contributing to the impairment of water quality in that water body. The Texas Commission of Environmental Quality (TCEQ) is responsible for ensuring that TMDLs are developed for impaired surface waters in Texas. The ultimate goal of these TMDLs is to restore the quality of the impaired water bodies such that water quality standards are met.

A seafood consumption advisory for catfish and blue crabs in the upper portion of Galveston Bay and the Houston Ship Channel (HSC) was issued by the Texas Department of Health in September of 1990 as a result of dioxin found in fish and crab tissue. The HSC system was subsequently placed on the §303(d) list and a TMDL study was initiated by the TCEQ. Segments placed on the §303(d) list include the San Jacinto River Tidal (Segment 1001), Houston Ship Channel (Segments 1005, 1006, 1007), Tabbs Bay (Segment 2426), San Jacinto Bay (Segment 2427), Black Duck Bay (Segment 2428), Scott Bay (Segment 2429), Burnett Bay (Segment 2430), and Barbours Cut (Segment 2436). In addition, Upper Galveston Bay (Segment 2421), Segment 2438 (Bayport Channel), and Segment 901 (Cedar Bayou Tidal) were included in the §303(d) list and are part of this TMDL study, even though they are not part of the HSC system. The overall purpose of this project is to develop a TMDL for dioxin in the Houston Ship Channel System, including upper Galveston Bay, and a plan for managing dioxins to

correct existing water quality impairments and maintain good water quality in the future. The project also includes an assessment of existing PCB levels in the channel to determine the scope and nature of PCB impairment.

1.2 PROJECT DESCRIPTION

The dioxin TMDL study has been divided into several phases to ensure a cost-effective, flexible and logical project development.

Phases I and II have been completed and final reports submitted to TCEQ. Phase I was aimed at assessing current conditions and identifying the deficiencies in dioxin data in the HSC. Phase I resulted in the development of a work plan for Phases II and III of the project. Two work orders were completed for Phase I. Work Order 1 encompassed an assessment of current dioxin levels and trends in the Project area, an assessment of major sources and fate and transport of dioxin in the environment, and development of a work plan and cost estimate for Phases II and III of the TMDL. The scope of work also included participation in the stakeholder process for the dioxin TMDL. The second work order (TNRCC Work Order No. 582-0-80121-03) was aimed at incorporating recent information that became available from EPA and other State agencies into the project workplan.

Phase II of the TMDL study (TNRCC Work Order No. 582-0-80121-04) included the following tasks: 1) identification of water quality targets; 2) monitoring and data collection in the Houston Ship Channel (for dioxins and PCBs); 3) modeling the fate and transport of dioxin in the Houston Ship Channel; 4) participation in the stakeholder process; and 5) developing load allocation scenarios.

Phase III of the TMDL study is currently underway (TCEQ Work Order No. 582-0-80121-07). Work Order 7 incorporates data evaluation, additional data collection, system-wide modeling, and load assessments. There are seven main tasks to be completed in WO7:

1. Project administration;
2. Development of a Quality Assurance Project Plan (QAPP) for additional data collection;
3. Conducting dioxin monitoring and data collection in the Houston Ship Channel area;
4. Incorporating collected data into dioxin TMDL models developed in WO4;
5. Participation in stakeholder involvement with the dioxin TMDL project;
6. TMDL allocations; and
7. Evaluation of PCB data gathered to date and assessment of the need for a PCB TMDL.

1.3 DESCRIPTION OF THE REPORT

This document constitutes the Final Report for Work Order No. 582-0-80121-07 (Contract Number 582-0-80121) of the Dioxin TMDL Project and summarizes the activities undertaken by the University of Houston, in conjunction with Parsons and PBS&J during the period September 1, 2003 to August 31, 2005.

This report compiles the seven quarterly reports submitted to TCEQ in compliance with the Work Order and adds the activities completed during the last quarter of the project. The topics in the report are organized according to the tasks specified in Work Order 582-0-80121-07.

The approved Quality Assurance Project Plan (QAPP) for the sampling activities conducted for this project and its approved amendments are addressed in Chapter 2 and

Appendix A of this report. Chapter 2 also presents a description of the quality control activities conducted and lists the quality control issues encountered throughout the project.

Chapter 3 describes the monitoring and data collection activities conducted to assess current levels of dioxins in the HSC and to evaluate sources of dioxins to the HSC system. Along with the description of sampling activities, a summary of analytical results is presented in Chapter 3. Chapter 3 also includes an update of the section describing the collection of sediment data to support modeling that had been previously included in the Final Report for WO4. The update incorporates sediment data collected in the Houston Ship Channel in recent years.

Chapter 4 presents the development of site-specific values for water quality targets for this TMDL project. A quantification of site-specific bioaccumulation factors (BAFs) and biota-to-sediment accumulation factors (BSAFs) is also detailed in Chapter 4. In addition, Chapter 4 presents analyses of the entire dioxin dataset to evaluate spatial, temporal, and seasonal trends.

Modeling activities are summarized in Chapter 5. Data in Chapter 5 describe the methods and technical approaches followed to set up a QUAL-TX, a simplified WASP, and a transient WASP model for dioxins in the HSC system.

A list of activities completed in support of stakeholder activities during WO7 is presented in Chapter 6. This chapter also includes copies of the presentations given by members of the project team at stakeholder meetings.

An assessment of the PCB data gathered in WO4 along with recommendations for TMDL needs is included in Chapter 7. Finally, Chapter 8 presents a summary and conclusions of project activities completed under Work Order No. 7.

CHAPTER 2

QUALITY ASSURANCE PROJECT PLAN

The goal of this task is to develop a plan for additional data collection that met the needs for the TMDL. The quality assurance project plan was prepared based on the proposed monitoring activities outlined in task 3 of the work plan for Work Order 7. A first draft of the Quality Assurance Project Plan for data collection was submitted to TCEQ on September 19, 2003. Comments from TCEQ on the first draft were received and addressed prior to November 11, 2003. The revised QAPP was approved by TCEQ and submitted to EPA on December 9, 2003. EPA approved and signed the QAPP on January 24, 2004. An annual update compiling the original QAPP and the approved amendments was submitted to TCEQ on January 24, 2005. The annual update was approved by TCEQ on March 9, 2005 and by EPA on April 22, 2005.

2.1 AMENDMENTS TO THE APPROVED QAPP

Two amendments to the approved QAPP and one amendment to the Annual Update were developed and submitted to TCEQ. The first amendment added high-resolution sediment sampling in segments 1001 and 1006 aimed at identifying the possible causes of elevated dioxin levels in those segments. The second amendment included additional dioxin runoff data collection and evaluation of a surrogate estimation method for dioxins in runoff. The amendment also extended the sampling time for air sampling and increased the deposition sampler surface area to minimize non-detects. Amendment No. 1 was approved on July 1, 2004 and Amendment No. 2 was approved on August 19, 2004.

In addition to compiling the original QAPP and approved Amendments, the annual update submitted on January 2005 included flow measurements using and Acoustic Doppler Profilers (ADP) to support modeling activities. Finally, an Amendment to the annual update was submitted on July 11, 2005. This final Amendment added more high-resolution sediment sampling in segments 1001, 1006, and 1007 to characterize sediment “hot spots” within the project area and support the search for unknown sources of dioxins. This Amendment was approved on July 12, 2005 through a non-substantive change request.

Appendix A of this report includes the Annual Update as well as the final Amendment.

2.2 QUALITY CONTROL ACTIVITIES

The quality assurance/quality control (QA/QC) tasks that were conducted during Work Order 7 included monitoring/coordinating sample deliveries to the laboratories, verifying laboratory compliance with the QAPP, and verification of data packages. There were no noncompliant issues encountered in the shipping and receiving of the samples collected in Fall and Summer 2004. All samples were received by the laboratories without incident and were within the temperature range specified in the QAPP. In Spring 2004, there were two instances in which the sample IDs were mislabeled in the chain-of-custody (COC). The water sample collected on 3/12/04 was labeled 11342 instead of 13342. The water sample collected on 4/2/04 was mistakenly labeled as 11302, the correct ID is 11287. In both cases, the station IDs were corrected in the database. In Summer 2005, two sediment sample containers broke during shipment (Sites 10 and 12). New samples were collected at those two sites and submitted to the laboratories for analysis.

There were no non-compliance issues encountered in the data verification conducted for dioxin samples collected in 2004 and 2005.

Due to the complexity of the dioxin/furan analysis, many different data qualifiers (flags) are used by the various laboratories. Standardization of these flags was necessary to allow for accurate and consistent qualification of the data. The flags that have been assigned to the data by the project team are given in Table 2.1.

Table 2.1 Standardized Flags Assigned to Data

Flag	Description
B	Blank contamination (result is less than twenty times the amount found in the associated blank).
U	Target analyte is not detected above the method detection level (MDL) in the sample.
J	Result is between the method detection limit (MDL) and the reporting level (RL) or the value is to be considered an estimate due to quality control issues involved in the analysis.
UJ	Analyte was not detected but the result is an estimate due to non compliant QC.
R	Sample result is to be rejected and is considered unusable.

These flags are consistent with those given in the USEPA Contract Laboratory Program National Functional Guidelines for Organic Data Review dated February 1994.

The analyses of all the samples have been in compliance with the QAPP. There have been a few instances when the reporting levels have been elevated because they were either based on the signal to noise ratio of each sample injection or due to matrix interferences. When

interferences have caused a higher than normal reporting level, the laboratories have reported the analyte as non-detect and the reporting level as the maximum estimated possible concentration that could be in the sample based on the peak area of the interference. This practice is recommended in the original EPA method. Method blanks have also been reported with detectable amounts of target analytes. Several method blanks have been reported with detectable amounts of target analytes. However, all of the concentrations reported in the method blank were within the acceptable criteria given in the QAPP for blanks and all data were considered usable.

All reviewed analytical data for dioxins/furans complies with the QA/QC requirements outlined in the QAPP. The QA/QC requirements outlined in the QAPP include: holding times, method blanks, initial calibration curves, ambient water reporting limits (AWRL) verification, laboratory control sample (LCS), field duplicates, matrix spikes/matrix spike duplicates, laboratory duplicates, continuing calibration samples, surrogates, and internal standards. In the sample results reviewed, no data were rejected. The percent data verification completed for each laboratory per matrix for the different sampling events is summarized in Table 2.2.

There was a non-compliant issue with the samples analyzed by NWDLS consisting of the exceedance of holding times for a group of samples as described in Section 2.3.2 below.

Table 2.2 Percentage Data Packages Reviewed

Laboratory	Media	# samples collected	Results reviewed
<i>Spring 2004</i>			
PSC/Maxxam Analytical	Water	30	100%
PSC/Maxxam Analytical	Catfish	37	100%
PSC/Maxxam Analytical	Crab	29	100%
Pace Analytical	Sediment	21	100%
<i>Summer 2004</i>			
PSC/Maxxam Analytical	Water	7	100%
Pace Analytical	Sediment	21	100%
<i>Fall 2004</i>			
PSC/Maxxam Analytical	Water	28	100%
PSC/Maxxam Analytical	Catfish	19	100%
PSC/Maxxam Analytical	Crab	19	100%
Pace Analytical	Sediment	19	100%
Pace Analytical	Sediment cores	102	94% ^a
<i>Runoff (Fall 2004 to Summer 2005)</i>			
PSC/Maxxam Analytical	Water	24 (8 sites)	88% ^b
Pace Analytical	Sediment/soil	41	95% ^b
<i>Air (Fall 2003 to Summer 2005)</i>			
Alta	Ambient air	18	94% ^c
Alta	Particle size	21	100%
Alta	Dry deposition	13	92% ^c
PSC/Maxxam Analytical	Wet deposition	3	67% ^c
PSC/Maxxam Analytical	Bulk deposition	2	50% ^c

^aSix additional core samples (deepest for each core) were submitted for analysis in August 2005. Results have not been received.

^bResults for the last runoff sample have not been received from the laboratory.

^cThe last sample is being collected (June to December 2005)

2.3 QC ISSUES

2.3.1 Wet Deposition Sample Mishandling

The XAD-2 column resin column that collected wet deposition at site C-408 (Lang Road) and delivered to PSC Analytical Services on April 23, 2004 was not handled appropriately. As a consequence the sample was unusable. The Project QAO requested a Corrective Action Report from the laboratory including: (1) a statement of what occurred, (2) an explanation of what caused the problem(s), and (3) an explanation of corrective measures taken to ensure the error would not re-occur. PSC Analytical Services is preparing the report.

2.3.2 Holding Times

When verifying the data packages received from NWDLS, it was noticed that the holding times for total dissolved solids (TDS) and Volatile Solids analyses were exceeded in a number of occasions by 2-3 days (holding time as per the QAPP is 7 days for both analyses). Data for TDS or volatile solids are not used in the dioxin data analysis, but per the QAPP, the project team is required to analyze for those parameters and report data to TRACS. The number of samples that exceeded the holding time is listed in parenthesis:

- TDS: Spring 04 (2), Summer 04 (2), Fall 04 (15)
- Volatile Solids: Spring 04 (9), Fall 04 (9).

Results for samples that exceeded the holding time were not reported to TRACS.

2.3.3 Wet Deposition Sample Duration

The wet deposition sample was intended to be collected and analyzed as a six-month composite sample using two co-located samplers. Sample collection proceeded as planned, the columns were changed three times for each sampler for a total of 6 XAD-resin samples to be combined. However, because all the columns were spiked prior to deployment as indicated in the method, it was not possible to combine all six of them for a single analysis because the amount of spike will overwhelm the GC unit and increase the detection limits. Thus, only the first pair of co-located XAD-2 columns deployed in the field (i.e. a 2 month-sample) were combined and analyzed for dioxins. The remaining columns are being combined and analyzed in pairs. A second field effort to collect a six-month wet deposition sample was initiated in early June 2005 and is currently on-going.

2.3.4 Field Duplicates

A field duplicate is defined as a split sample (or measurement) from the same location, collected in immediate succession (after homogenization), using identical techniques. Field duplicates were collected at a frequency of 7.1 % or higher¹.

Table 2.3a summarizes the relative percent deviation of the field duplicates (FRPD) for dioxin samples collected during Spring 2004. As can be observed, the average FRPDs for dioxins are 17, 30, 9, 39, and 49% for dissolved, suspended sediment, bottom sediment, catfish, and crab,

¹Field duplicate frequency required as per QAPP is 5% or higher.

Table 2.3a Percent Deviation of the Field Duplicates collected in Spring 2004

Matrix	Dioxins ^a (%)			Total TEQ (%)		
	min	max	mean ^b	min	max	mean ^b
Dissolved	0	49	17 ± 4	6	36	16 ± 42
Suspended	0	65	30 ± 7	6	57	33 ± 64
Sediment	0	37	9 ± 3	3	4	4 ± 6
Catfish	4	103	39 ± 12	22	73	42 ± 67
Crab	5	144	49 ± 15	3	12	41 ± 89

^a Percent deviation was calculated for each of the 17 dioxin-like congeners, only detected concentrations were used.

^b Mean ± Confidence interval ($\alpha=0.05$)

A complete table with all the FRPD calculations by sample is included in Appendix A.

respectively, when the comparison is based on each individual congener. When the comparison is based on total TEQ, the average FRPDs were 16, 33, 4, 42, and 41%, for dissolved, suspended sediment, bottom sediment, catfish, and crab, respectively.

Table 2.3b includes the relative percent deviation of the field duplicates (FRPD) for dioxin samples collected during Summer 2004. As can be observed, the average FRPDs for dioxins are 7, 3, and 98% for dissolved, suspended sediment, and bottom sediment, respectively, when the comparison is based on each individual congener. When the comparison is based on total TEQ, the average FRPDs were 3, 2, and 71%, for dissolved, suspended sediment, and bottom sediment, respectively. The high percent deviation observed in bottom sediment duplicates is due to samples collected at location 11193 that probably were not adequately homogenized.

Table 2.3b Percent Deviation of the Field Duplicates collected in Summer 2004

Matrix	Dioxins ^a (%)			Total TEQ (%)		
	min	max	mean ^b	min	max	mean ^b
Dissolved	0	20	7 ± 5	na ^c	na ^c	3 ^c
Suspended	0	9	3 ± 2	na ^c	na ^c	2 ^c
Sediment	0	161	99 ± 26	7	135	71 ± 125

^a Percent deviation was calculated for each of the 17 dioxin-like congeners, only detected concentrations were used.

^b Mean ± Confidence interval ($\alpha=0.05$)

^c Only 1 duplicate was collected. The mean value corresponds to the measured FRPD for the collected duplicate. A complete table with all the FRPD calculations by sample is included in Appendix A.

Table 2.3c includes the relative percent deviation of the field duplicates (FRPD) for dioxin samples collected during Fall 2004. As can be observed, the average FRPDs for dioxins are 9, 6, 11, 23, and 39% for dissolved, suspended sediment, bottom sediment, catfish, and crab, respectively, when the comparison is based on each individual congener. When the comparison is based on total TEQ, the average FRPDs were 21, 5, 8, 9, and 53%, for dissolved, suspended sediment, bottom sediment, catfish, and crab, respectively.

The approved QAPP requires the FRPD be 50% or less. Thus, water, sediment, and catfish field duplicates that exceeded the criteria were flagged as estimates.

The relative percent deviation criterion was met for all field duplicates for conventional analyses in water. The 50% FRPD criterion for conventional analyses was met for most sediment field duplicates with the exception of four values for grain size analysis that were flagged as estimates and were not reported to TRACS.

Table 2.3c Percent Deviation of the Field Duplicates collected in Fall 2004

Matrix	Dioxins ^a (%)			Total TEQ (%)		
	min	max	mean ^b	min	max	mean ^b
Dissolved	1	20	9 ± 5	5	37	21 ± 0.3
Suspended	1	21	6 ± 3	0	10	5 ± 0.1
Sediment	0	30	11 ± 3	2	14	8 ± 0.1
Catfish	7	74	23 ± 7	8	10	9 ± 0.1
Crab	5	120	39 ± 11	49	57	53 ± 0.1

^a Percent deviation was calculated for each of the 17 dioxin-like congeners, only detected concentrations were used.

^b Mean ± Confidence interval ($\alpha=0.05$)

A complete table with all the FRPD calculations by sample is included in Appendix A.

It is noted that the duplicates for crab samples collected in Spring 2004 were prepared using different individuals than the parent sample (i.e. two complete sets of crabs were collected at the same location and time). Therefore, these field duplicates are not actually a measure of the precision of the sampling and analytical methods but rather a measure of the variation in the chemical composition among individuals.

2.3.5 Laboratory Duplicates

There was a set of sediment samples for which the % RPD for laboratory duplicates was 11.4%. As per the approved QAPP, the % RPD for total organic carbon (TOC) in sediment should not exceed 10%. However, the 10% value is too low as indicated by the % RPD for TOC in water (20%). Furthermore, the Surface Water Quality Monitoring (SWQM) QAPP has a 30% RPD criterion for TOC in sediment as indicated by the TCEQ Project Management and QC Section. Therefore, it was considered that the TOC results for the aforementioned set of sediment

samples were valid, met the QC criterion, and could be both reported to TRACS and used for dioxin data analyses.

CHAPTER 3

MONITORING AND DATA COLLECTION

The monitoring and data collection task encompasses two main subtasks: (i) monitoring and data collection to assess current levels of dioxins in the HSC, and (ii) sampling to evaluate sources of dioxins to the HSC system. This chapter summarizes the sampling activities conducted between September 1, 2003 and August 31, 2005. In addition, the chapter includes a summary of the sampling results and presents an analysis of the gathered data. Four “major” sampling events were completed in support of this task. The first event (Spring 2004) was conducted between March 9 and May 8, 2004. The second sampling event (Summer 2004) was initiated on August 2, 2004 and was completed on August 31, 2004. Sampling for the third sampling event (Fall 2004) was conducted between October 19 and December 2, 2004. Finally, the fourth sampling event (Summer 2005) was completed between August 15 and August 30, 2005. In addition to the major sampling events, continuous air/deposition sampling was conducted between December 2003 and August 2005; sediment core sampling was conducted between May 21, 2004 and February 17, 2005; and runoff sampling was conducted between December 16, 2004 and July 14, 2005.

Monitoring conducted as part of Work Order 7 yielded a total of 71 in-stream water samples, 98 sediment samples, 53 catfish tissue samples, 47 crab tissue samples, 106 sediment core samples, 8 runoff samples, 41 soil samples, 18 ambient air samples, 13 dry deposition samples, 3 wet deposition samples, 2 bulk deposition samples, and 21 particulate air samples.

A description of the methods and technical approach undertaken to accomplish the sampling tasks is presented below. All the sampling and analysis procedures employed for this task followed those specified in the approved QAPP.

3.1 DESCRIPTION OF SAMPLING ACTIVITIES

3.1.1 Assessment of Current Levels and Trends of Dioxins in the Houston Ship Channel

The main purpose of this task is to confirm the severity, spatial and temporal extent of the current impairment and to determine whether water quality is improving or deteriorating for each segment listed. The goals include: (i) using the data results to verify whether dioxin concentrations are above the criteria and where, and/or how much dioxin levels must decline to meet the criteria, (ii) identifying historical increases and declines in dioxin levels that may be related to changes in sources over time, and (iii) characterizing other segments/waterbodies, such as side bays, where dioxin levels have not been previously measured.

During the Spring 2004 sampling event, 17 in-stream sites were sampled for ambient water, 18 sites for sediments, and 28 sites for catfish and crab tissue. For the Summer 2004 sampling event, 15 in-channel locations were sampled for sediments, and 4 locations for ambient water (in two of them water was sampled at 2 different depths). In addition, sediment was sampled in a transect at location 15979 to assess the difference in dioxins levels between the center of the channel and the banks. During the Fall 2004 sampling event, 17 in-stream locations were sampled for ambient water and sediments, and 28 locations for catfish and crab tissue. Finally, during the Summer 2005 sampling event, 40 sediment samples and 1 sediment core were collected. Additionally, 8 sediment cores were collected for geochronological and dioxin

analyses during WO7. Table 3.1 includes a summary of the total number of samples collected for WO7.

Samples were shipped to the laboratories to be analyzed for dioxins (EPA method 1613B) and conventional parameters. The following sections present a summary of sampling sites, media, and sampling procedures.

3.1.1.1 In-channel Water Sampling

Water sampling was conducted using the high-volume technique to allow for detection of concentrations below the reporting limit for the analytical method (10 pg/L for 2378-TCDD). Using this technique allows concentrating dioxins from large volumes of water to obtain measurable quantities. The high-volume system uses a stainless steel column packed with hydrophobic polymeric resin beads through which large volumes of water can be passed. Since dioxins are very hydrophobic, they rapidly sorb onto the resin, making it possible to completely collect the dissolved dioxins from the sampled water. Later, in the laboratory, the dioxins are recovered from the resin by extraction with a nonpolar organic solvent. Dioxins associated with suspended particulate matter were collected on a fiber glass filter, which was also extracted later in the laboratory.

For this TMDL, the project team used a commercially-available Infiltrax 300 high-volume sampling system manufactured and sold by Axys Environmental Systems of Sydney, British Columbia.

Table 3.1 Number of Samples Collected in for Current Levels and Trend Analysis

Matrix	Spring 2004			Summer 2004			Fall 2004			Summer 2005		
	# sites	QC samples ^a	total # samples	# sites	QC samples ^a	total # samples	# sites	QC samples ^a	total # samples	# sites	QC samples ^a	total # samples
In-channel water - <i>XAD Column</i>	17	3	20	2, 2(2) ^b	2	8	17	3	20			
- <i>Filter</i>	17	3	20	2, 2(2) ^b	2	8	17	3	20			
Sediment	18	6	24	15,1(5) ^c	4	24	17	3	20	32	8	40
Tissue - <i>Catfish</i>	28	4	32	0	0	0	17	4	21			
- <i>Crab</i>	26	2	28	0	0	0	17	2	19			
Sediment core	2 (11) ^d	2	24	2 (11) ^d	2	24	4 (11) ^d	4	48	5(1),1(5) ^d		10

^a Field duplicates, field blanks and recovery columns specified in the QAPP.

^b 2 sites were sampled at 2 depths (surface and bottom).

^c Sediment samples were collected along a transect (5 samples) at one location.

^d Numbers in parentheses correspond to the number of core sections analyzed for dioxins.

Water sampling was conducted following the guidelines set forth in the QAPP for the dioxin project. A pumping rate of about 1.6 L/min was selected for this project based on the manufacturer's recommendations to avoid incomplete capture of the dissolved analytes by the resin trap (breakthrough). The target volume of water was 700 L, which allows reporting limits as low as 0.014 pg/L for 2378-TCDD. This target volume was achieved for all but one sample. The exception was station 11357 (Buffalo Bayou at San Felipe Rd) for which the pumping rate could not be maintained above 1 L/min due to the high solids content that constantly plugged the pre-filter; after 8 hours of pumping only 326 L were processed.

A total of 19 locations in the main channel were sampled for ambient water. Fifteen locations were sampled twice (Spring and Fall 2004), two locations were sampled three times (Spring, Summer, and Fall 2004), and 2 locations were sampled once (Summer 2004) to determine dioxin levels in water (dissolved and suspended). Figure 3.1 shows the locations of the sampled sites. Table 3.2 includes a description of the sampled sites as well as the sampled volume for each station.

In addition to measuring dioxin concentrations at each location, grab water samples were collected to be analyzed for TSS (total suspended solids), TDS (total dissolved solids), DOC (dissolved organic carbon content), and TOC (total organic carbon content). Field probe parameters (i.e., pH, temperature, dissolved oxygen, conductivity, and salinity) were measured using a YSI sonde (6920 or 600-XLM).

3.1.1.2 Sediment Sampling

Sediment samples were collected using a stainless steel Ponar dredge. Prior to collection at each sample site, the dredge, stainless steel spoon, and polyethylene or stainless steel

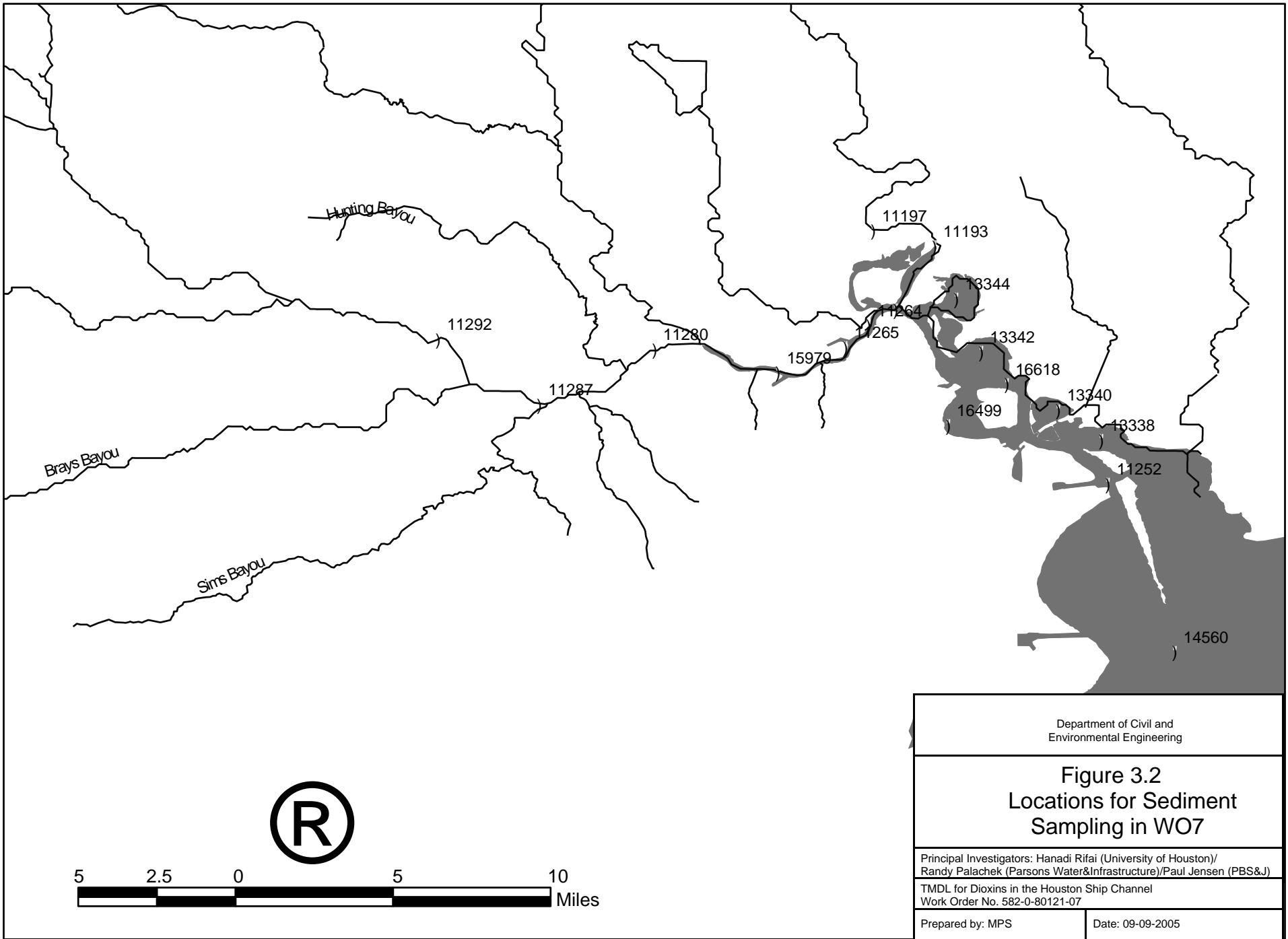
tray/mixing bowl were rinsed with deionized water, then ambient water. Samples were collected and deposited into a stainless bowl. A minimum of three grab samples were composited using the top 5 centimeters of sediment, mixed thoroughly with a clean stainless steel spoon, and deposited into a labeled, pre-cleaned amber glass jar with a Teflon seal. A separate sample of the same mixture was prepared for solids and TOC analysis. Multiple grab samples from the dredged channel and both banks at a given stream location were collected and composited into a single sample. Sampling procedures and handling followed the requirements specified in the QAPP for the project.

Sediment samples were collected at a total of 17 locations in the Ship Channel, San Jacinto River, Upper Galveston Bay, and side bays during Spring and Fall 2004 (Figure 3.2). One location was sampled once during the Spring 2004 event. During Summer 2004, 15 locations in segments 1001, 1005, and 1006 were sampled to obtain detailed concentration profiles and 1 location was sampled along a transect to measure differences in concentrations across the width of the channel (Figure 3.3). High-resolution sampling conducted in Summer 2005 included 32 locations shown in Figures 3.4 and 3.5. Table 3.2 includes a description of the sampled sites.

Standard field parameters (DO, pH, temperature, conductivity, and salinity) were measured at the time of sample collection using a YSI sonde (6920 or 600XLM).

3.1.1.3 Tissue Sampling

Tissue was sampled along with water and sediment to obtain data on bioaccumulation and/or transport of dioxin. For this sampling component, fish fillets and edible crab portions were collected, processed, and analyzed.



Department of Civil and Environmental Engineering

Figure 3.2
Locations for Sediment Sampling in WO7

Principal Investigators: Hanadi Rifai (University of Houston)/ Randy Palachek (Parsons Water&Infrastructure)/Paul Jensen (PBS&J)

TMDL for Dioxins in the Houston Ship Channel
 Work Order No. 582-0-80121-07

Prepared by: MPS

Date: 09-09-2005

Figure 3.4 Sampled Locations in the San Jacinto River in Summer 2005

Figure 3.5a Sampled Locations in Segment 1007 in Summer 2005

Figure 3.5b Sampled Locations in Segment 1006 in Summer 2005

Species that were sampled included hardhead catfish (*Arius felis*), blue catfish (*Ictalurus furcatus*), and blue crabs (*Callinectes sapidus*). Sample size for fish and crabs was approximately 100 g. All tissue sample collections were conducted using procedures that are consistent with those documented in the *TCEQ Surface Water Quality Monitoring Procedures Manual* (TCEQ, 2003) and according to the QAPP for this project.

Gill nets or a fishing line with bait (shrimp or chicken) were used to catch sufficient catfish to obtain 100 grams of muscle tissue. A minimum of three catfish were collected from each selected sample site to give a representative sample. A total length of 300 mm was targeted for collection for catfish. After each station collection, fish were separated, placed into a plastic bag, and placed into a cooler with ice. Once all fish samples were collected, the sampled fish were taken to the U of H field office, measured, weighed, and processed. Collected fish were filleted with a clean stainless steel knife, packed in clean foil with the dull side facing the tissue and placed into individual Ziploc® bags. Fillets were taken from the left side of the fish and, in most cases, the right side was used as a duplicate sample. All Ziploc® bags were labeled and frozen. All fish samples were packed in dry ice for shipment to the analytical laboratory. The fish tissue samples of a single species collected at a single station were composited into a single sample for analysis.

Crab tissue was harvested from blue crabs using standard plastic coated wire mesh crab traps. A minimum of three blue crabs, and typically five, were collected from each selected sample site to give a representative sample. Blue crabs with a carapace width of 125 mm and greater were targeted. Caught crabs were measured and weighed, and their edible tissue was

separated, composited, wrapped in aluminum foil, placed in a labeled Ziploc® bag, and frozen prior to shipment to the laboratory.

Preparation of tissue samples was performed in a clean working area at the U of H field office. Prior to sample preparation for each sampled site, all equipment including plastic cutting boards, stainless steel knives, scales, etc. were cleaned with distilled water, acetone, distilled water rinse, and allowed to air dry. Samples were prepared on polypropylene cutting boards that had been covered in aluminum foil with the dull side of the foil exposed. This foil was replaced after each sample was processed.

Tissue samples were packed on dry ice and shipped to the laboratory via overnight courier. Samples remained frozen until the laboratory confirmed that samples could be shipped, received and processed in the required time frame. The field teams retained a sample sized aliquot of the right side fillets of most fish samples (except the duplicate samples), and a portion of the crab tissue was kept frozen at the University of Houston field office until results were obtained and confirmed.

During WO7, 17 locations were sampled for catfish tissue twice and 11 locations were sampled once (Figure 3.6 and Table 3.2). Similarly, crab samples were collected two times from 17 locations and once from 9 locations. The locations sampled for crabs are shown in Table 3.2 and Figure 3.6. It is noted that there were two sites (stations 11347-Buffalo Bayou and 11382-Whiteoak Bayou) where no crabs were found during Spring 2004. This explains the discrepancy in the total number of sites sampled for crab tissue between the QAPP (28) and Table 3.1 of this report (26). Tables 3.3 and 3.4 present a summary of species, weight, and length of individuals composited to make catfish and crab samples, respectively.

Figure 3.6 Locations for Catfish and Crab Sampling in WO7

Table 3.3 Catfish Tissue Samples Collected from HSC & Upper Galveston Bay

Table 3.4 Blue Crab Tissue Samples Collected from HSC & Upper Galveston Bay

3.1.1.4 Sediment Core Sampling

The ability to collect sediment cores that are adequate to address the objectives of the project has been challenging, considering the heavily impacted and commercially active nature of the Houston Ship Channel (HSC), upper Galveston Bay and the lower San Jacinto River, where this research is focused. Numerous field trips were necessitated to acquire usable cores: 5/21/04 - Reconnaissance trip: project team visited all of the prospective field sites to determine where it may be best to attempt coring.

6/16/04 - Sampling trip 1: Five aqueous sampling sites were visited and a total of 15 cores were collected. Of these, the core collected at station 11261 was appropriate to begin processing for analytical work.

8/4/04 - Sampling trip 2: Five aqueous sampling sites were visited and a total of 10 cores were collected. Of these, the core collected at station 15244 was appropriate to begin processing for analytical work.

8/30/04 - Sampling trip 3: Five aqueous sampling sites were visited and a total of 6 cores were collected. Of these, cores collected at stations 11193 and 15979 were chosen to begin processing for analytical work.

10/18/04 – Sampling trip 4: Three sampling sites were visited and a total of 3 cores were collected. Of these, station 11270 was chosen for processing.

11/8/04 – Sampling trip 5: Two sampling sites were visited and a total of 6 cores were collected. Of these, none were deemed satisfactory for processing by UH researchers.

12/10/04 – Sampling trip 6: Two forested wetland sites within the lower reaches of the Trinity River floodplain were visited and a total of 4 cores were collected. Of these, station FW1 was chosen for processing.

2/17/05 – Sampling trip 7: Six sites were visited and three were sampled. Out of that a total of 11 cores were collected, cores from stations 16499 and 13337 were chosen for processing.

All sub-aqueous cores have been collected by divers. The 6" diameter PVC core sleeves were driven into the sediments to refusal, capped and stored upright for transportation to the laboratory where they were immediately processed. Replicate x-ray trays were collected in the same fashion at each station to allow for preliminary examination of the stratigraphy at each site, in an effort to process only those cores that may yield useful results. Each selected core was then sectioned at 1cm intervals using a sterilized spatula to avoid cross-contamination. Sediment aliquots for dioxin determination were stored in amber bottles at 4°C until delivery to the laboratory. Figure 3.7 shows the locations of the collected sediment cores.

3.1.2 Assessment of Major Sources, Transport and Fate of Dioxins in the Houston Ship Channel

The objective of this task is to assess the relative importance of the potential sources of dioxin in the HSC and its transport and fate in the environment. This task addresses tributary water sampling, air deposition (dry and wet) measurements, and stormwater runoff sampling.

During WO7, 11 locations at the mouths of major tributaries were sampled using high-volume units twice (Spring and Fall 2004). Ambient air and dry deposition sampling was

Figure 3.7 Locations of Sediment Cores

conducted at two locations 4 times and at 1 location 4 times, respectively. Wet deposition was sampled at one location three times and bulk deposition twice. In addition, eight locations were sampled for stormwater runoff. Table 3.5 includes a summary of the total number of samples collected in WO7 for assessing major sources of dioxin to the HSC.

A description of the sampling locations, media, frequency, and sampling methodology is presented in the following sections.

3.1.2.1 Water Sampling

In-stream water samples were collected at the confluences of the tributaries with the main system to assess dioxin levels that are coming from the tributary or are "background" concentrations. During Spring and Fall 2004, a total of 11 sites were sampled for water using the high-volume technique (Figure 3.1 and Table 3.2). Sample collection followed the procedure described in section 3.1.1.1 of this report and was consistent with the requirements specified in the QAPP for the project.

3.1.2.2 Air Sampling

During WO7, ambient air concentrations of dioxins and furans were monitored intermittently between December 2003 and August 2005 at two sampling locations: Clinton Drive (C403) and Lang Road (C408) (Figure 3.8). Due to the ultra trace levels of dioxins in the air, monthly and bi-monthly sampling events were planned to obtain enough sample volume for dioxin analysis.

Wet and dry deposition was concurrently measured at Clinton Dr and Lang Road from December 2003 to April 2004 and at Clinton Dr from September 2004 to February 2005 and from June to December 2005 (ongoing sampling). Likewise bulk deposition was measured at

Table 3.5 Number of Samples Collected in Support of Sources and Transport Assessment

Matrix	Winter-Spring 2004			Summer-Fall 2004			Winter-Spring-Summer 2005		
	# sites	QC samples ^a	total # samples	# sites	QC samples ^a	total # samples	# sites	QC samples ^a	total # samples
Water from tributaries - <i>XAD Column</i>	11	2	13	11	0	11			
- <i>Filter</i>	11	1	12	11	0	11			
Air - <i>Ambient</i>	2(4) ^c	3(2) ^{c,d}	14	1(2) ^c	0	2	1(2) ^{c,e}	0	2
- <i>Particulate(by size)</i>	2(6) ^f	1(2) ^c	14	1(6) ^f	1	7			
- <i>Dry Deposition</i>	2(3),1(1) ^c	1(2) ^c	9	1(2) ^c	0	2	1(2) ^{c,e}	0	2
- <i>Wet Deposition</i>	1(1) ^c	0	1	1(1) ^c	0	1	1(1) ^{c,e}	0	1
- <i>Bulk Deposition</i>				1(1) ^c	0	1	1(1) ^{c,e}	0	1
<i>Runoff</i> - <i>XAD Column</i>				1	0	1	7	0	7
- <i>Filter^g</i>				1(2) ^g	0	2	7(2) ^g	0	14
- <i>Soil</i>				1(1) ^c	0	1	7(1) ^c	0	7
- <i>Sediment</i>				1(6) ^h	0	6	7(5) ^h	0	35

^a Field duplicates, field blanks and recovery columns specified in the QAPP

^b Including samples collected in previous quarter

^c Number in parentheses and italics indicates sampling frequency

^d QC samples (duplicates at both sites plus a blank) were collected only for the two first sampling events

^e The last sample is being collected (June 2005 to December 2005)

^f Number is parentheses and italics indicate number of particle-size stages

^g 1-µm and 40-µm were analyzed separately, number in parenthesis indicate number of filters per site

^h Number in parentheses and italics indicate number of land use types sampled per site

Figure 3.8 Locations for Ambient Air and Wet/Dry Deposition Sampling in WO7

Clinton Dr. twice (including an ongoing event). In addition to ambient air, the distribution of dioxins by particle size was sampled at Clinton Dr. three times. Samples were sent to the selected laboratories to be analyzed for dioxins using EPA method TO-9A (ambient air, particulate size, and dry deposition) and EPA 1613B (wet and bulk deposition).

Ambient air samples were collected using high-volume samplers designed to collect both vapor and particle bound phases. In these samplers, air is first drawn through a quartz micro-fiber filter (QFF) where atmospheric particles of $>0.1 \mu\text{m}$ in diameter are trapped. Air then passes through a polyurethane foam plug (PUF) used to remove the vapors from the air stream. Quartz filters were replaced on a weekly-basis to avoid significant pressure drops through the system. So, for example, at the end of a monthly event, a sample consisting of 4 QFF filters and 1 PUF were shipped to the laboratory for dioxin analysis. The airflow rate was calibrated to $0.25 \text{ m}^3/\text{min}$ prior to initiation of the sampling event. At this flow rate, a minimum of 6000 m^3 of air was processed during the sampling period. The sampler motors were replaced every 500 hours of operation to avoid motor malfunctions that might cause loss of sample. QFFs were baked at 400°C for 5 hours and dried in a clean atmosphere prior to use. Likewise, the PUF adsorbent plugs were subjected to a 16-hour Soxhlet extraction with acetone at approximately 4 cycles per hour to ensure cleanliness. The PUF plugs are then air dried in a clean atmosphere, placed in glass cartridges, and spiked with $^{37}\text{Cl}_4\text{-}2378\text{-TCDD}$. The PUF plugs are wrapped in aluminum foil for protection from light prior to their use in the field.

Wet/Dry deposition samples were collected using modified automated precipitation collectors. Because these samplers were originally designed to collect only rain samples for wet deposition, they have been modified to include dry deposition sample collection. The modified

sampler consists of two separate compartments where rainwater (wet event) and falling particles (dry event) are collected. The sampler is equipped with a rain sensor and a controller. The controller records the time corresponding to the total and dry events. The dry deposition compartment consists of an inverted translucent glass fiber Frisbee with a sharp edge ($<10^\circ$) mounted on a mechanical actuator. The edge design minimizes abrupt interruptions of the wind path that might affect the deposition process. The face of the Frisbee exposed to the ambient air is covered with a one-foot diameter disk of Velcro brand loop material to collect the falling particles. When raining, the sampler is designed to automatically retract the dry deposition Frisbee, cover it with a lid, and expose the rain collector compartment. During dry periods, the rain collector is covered and the dry deposition disk is exposed to the environment. The rain collector compartment consists of an aluminum funnel with an area of 0.212 m^2 and a depth of 0.46 m . This funnel is connected to a XAD-2 resin column, wrapped in aluminum foil, where dioxins/furans are removed from the rainwater stream. To avoid losses and/or potential degradation of the sample, the dry deposition Velcro brand loop sampling material was replaced on a weekly basis.

The bulk (wet + dry) deposition sampler is an open-aluminum funnel with an area of 0.372 m^2 . Similarly to the wet/dry deposition units, the funnel is connected to a XAD-2 resin column wrapped in aluminum foil. The columns are regularly replaced with fresh ones. The used columns are wrapped in aluminum foil and then stored at 4°C in darkness. At the end of the sampling event, the columns are composited and analyzed for dioxins and furans.

Particle size distribution of associated dioxins and total organic carbon (TOC) samples (in ambient air) were collected using two high-volume total suspended particle (TSP) pumping

systems equipped with five-stage cascade impactors. Aerosol particles were separated into six size fractions on glass- and quartz-fiber filters according to the following equivalent cutoff diameters: first stage >7.2 µm, second stage 7.2-3 µm, third stage 3.0-1.5 µm, fourth stage 1.5-0.95 µm, fifth stage 0.95-0.49 µm and backup filter <0.49 µm. Slotted glass and quartz-fiber filters (SQFF) were used as collection substrates. Similarly to QFFs used in the collection of ambient air samples of dioxins, the filters were baked at 400°C for 5 hours and dried in a clean atmosphere prior to use. The cascade impactors were adjusted to run at a flow rate of 1.13 m³/min. The samplers were programmed to run 6 days/week, 4 weeks/month. On the seventh day, the filters were replaced to avoid significant pressure drops. Similarly to ambient air samplers, the motors were replaced every 500 hours of operation to avoid motor malfunctions that might cause loss of sample.

3.1.2.3 Runoff Sampling

For storm water sampling, ten tentative sites were selected from 25 Harris County Flood Control District (HCFCD) candidate drainage ditches. All sites have the following characteristics:

- No dry weather flow;
- Channelized (or pipe) cross section with easy to establish stage-discharge relationship;
- Safe and adequate access (e.g., roadway overpass that is amenable to lane closure or other off-road parking and working areas);
- More than 50% of the drainage area with the same land use/land cover;
- More than 50% of the drainage area with the same soil type; and
- Close to air sampling sites.

All sites were visited prior to sampling to ascertain access, identify safety issues, and to deploy stage markings for later use. During WO7, eight locations (Figure 3.9) were sampled for stormwater runoff using a high-volume unit (Infiltrax 300). Sampling typically proceeded in the following manner:

First, using radar images and weather reports, a sampling team mobilized to a preselected sampling site in advance of the storm. Upon arrival at the sampling site, the booster pump and discharge line were placed in the stream and sampling was initiated using the high-volume equipment that was located in a suitable location on the bank. The gear pump on the Infiltrax drew from the stainless steel reservoir while the booster pump continuously pumped runoff water from the channel. This arrangement was required due to the low suction lift capability of the Infiltrax unit gear pump. The team continued sampling until the desired sample size (i.e. 700 L) was achieved. The standard high-volume equipment was supplemented with extractable 40 micron pre-filters installed before the standard 1 micron filters to extend filter run times under heavy solids loading and minimize primary filter changes. All filters and pre-filters used during the processing of a sample were collected for dioxin analysis.

During sample volume collection, grab samples were collected every 15 minutes. Equal amounts of all samples (250 mL) were combined into one large container and stored on ice. The composited volume was used to obtain sub-samples for total suspended solids, total dissolved solids, total organic carbon, and dissolved organic carbon. Water level and flow measurements were recorded during the event as well.

In addition, up to five surface soil and one drainage ditch sediment samples were collected from within each of the eight runoff sampling drainage areas, generating a total of forty-one

Figure 3.9 Runoff Sampling Locations

samples. Each of the five samples within the runoff sampling drainage areas was collected from different land use categories (for example, near highways or residential areas) to have a good representation of the area. The samples were analyzed for dioxins, organic content, and particle size distribution. The dioxin concentrations observed in each of the sampling land use category will then be used as indicative of the concentrations elsewhere in the drainage area with the same land uses. Average concentrations in soil will be used along with the TSS event mean concentrations to develop a surrogate runoff load estimation method.

Figure 3.10 shows the Harris County Office of Emergency Management (OEM) rain gauges with the recorded rainfall amounts 24 hours prior to sampling. Figure 3.11 shows the amount of rain recorded prior to, during, and after the sampling event, along with the stream flow for each sampled location.

Sampling at location SS-10 (located in east Houston on an unnamed tributary to Hunting Bayou) was undertaken on December 16, 2004. A total of 707 L of stormwater runoff were processed at SS-10. Sampling at location SS-13, located in Baytown on an unnamed tributary to Goose Creek, was conducted on January 13, 2005. Total volume pumped at SS-13 was 709 L. Sampling at station SS-9, located in northeast Houston on an unnamed tributary to Greens Bayou, was undertaken on February 7, 2005. A total of 698 L of water were pumped at SS-9. Sampling at station SS-15, located in west Houston on an unnamed tributary to Brays Bayou, was conducted on February 24, 2005. The total volume sampled at SS-15 was 700 L. Sampling at SS-14 (located in east Houston on an unnamed tributary to Brays Bayou) was undertaken on March 2, 2005. A total volume of 700 L was processed at SS-14. Station SS-16, located in southwest Houston on an unnamed tributary to Sims Bayou, was sampled on March 16, 2005. A total of 700 L of water

**Figure 3.10 Rainfall Totals for 24-hour Period Prior to Beginning of Sampling from
HCOEM**

Figure 3.11 Rainfall Hyetographs and Flow During Runoff Events

were pumped through the Infiltrax unit at SS-16. Station SS-8, located in northwest Houston on an unnamed tributary to White Oak Bayou, was sampled on May 29-30, 2005. Total sample volume at SS-8 was 708 L. Sampling at station SS-7, located in west Houston on Buttermilk Creek, a tributary to Spring Branch, was undertaken on July 14, 2005. A total of 617 L of stormwater runoff were collected at SS-7.

3.1.3 Gather Information to Support Modeling

Flow measurements were conducted using an acoustic doppler profiler on a line towed boat configuration (RiverCat®) to provide data for model development. Flows and velocities were measured across transects in the HSC and major tributaries between 6 and 8 times each. Measurements were conducted at 15 locations (shown in Figure 3.12) following the standard operating procedure (SOP) included in the approved QAPP. Measured flows were used to establish a relationship between flow and the change in tide height. These relationships can be used to predict flow at any time from the change in tide height.

Flow calibration of the model requires flow data from several in-stream locations as well as from major tributaries. The flow at any point was assumed to be equal to the sum of tributary inflows, wastewater discharges, tidally-driven water movements, and runoff to the system downstream of tributary flow gages. Other minor factors affecting flow include groundwater gain and loss, water withdrawals, evaporation, and direct rainfall. Using the tide/flow relationships and tide height data, together with tributary inflow data from USGS gages, and runoff estimates from the HSPF model, it would be possible to predict and model flow over long time periods (days, months, or years) at intervals as short as six minutes. The tidally-driven currents are expected to

Figure 3.12 Locations for Flow Measurements

be the dominant flows, and understanding the relationship between flow and tide cycle is key to predicting flows.

Up to seven simultaneous flow/tide height measurements were performed at each of the locations in Figure 3.5 to develop the required relationships between flow and tide height. Each time flow was measured, a minimum of 4 different flow readings was collected to assure data of adequate quality. In addition, flow measurements were collected under a variety of tidal conditions, including rising and falling tides. The timing of the measurements was also important. Measurements were made at flood, ebb, and slack tide conditions to the extent possible. Also, because the relationships could be weakened if tributary inflows change substantially during the period in which flow measurements were made, the flow measurements were performed in dry weather conditions. Table 3.6 lists the locations at which sampling was conducted as well as the measured parameters.

3.2 SAMPLING RESULTS

This section provides a summary of data collected as part of Work Order 7. The data include field water parameters (dissolved oxygen, pH, salinity, and water temperature), physical characteristics of water and sediment samples, and dioxin levels for the collected samples.

To date, 100% of the results for dioxin for Spring, Summer, and Fall 2004, and Spring 2005 samples have been received and verified, while dioxins results for the Summer 2005 samples have not been received as of this writing.

Table 3.6 Summary of Locations for Flow Measurements

3.2.1 Assessment of Current Levels and Trends of Dioxins in the Houston Ship Channel

3.2.1.1 In-stream Water Quality Sampling

Table 3.7 provides a summary of field parameters measured during in-channel water sampling activities and Table 3.8 presents the results of the physical properties of water-column samples analyzed by North Water District Laboratory Services (NWDLS). Vertical profiles of field parameters are shown in Figure 3.13. Data in Figure 3.13 indicate that, in general, stations in the main channel exhibited thermal and/or salinity stratification, while stations in the side bays showed little change in temperature and salinity with depth. This is relevant for bottom sediment-water partitioning calculations.

A summary of dioxin/furan concentrations in water samples collected in WO7 and the resulting Texas-TEQ levels is provided in Table 3.9. It is noted that PSC Analytical reported dissolved (XAD-2 resin) and suspended (filter) levels on a mass basis (in picograms), thus, dissolved and suspended concentrations were calculated by dividing those results by the sampled volume and adding them up to obtain the total concentration in water presented in Table 3.9. Maps illustrating total TEQ concentrations in water for the Spring and Fall 2004 sampling events are shown in Figure 3.14. Overall, dioxin concentrations in water for Spring 2004 varied between 0.089 and 1.252 pg TEQ/L with an average value of 0.409 pg TEQ/L. Dioxin concentrations in water samples collected in Fall 2004 varied between 0.075 and 0.877 pg TE/L with an average value of 0.34 pg TEQ/L. It is noted that dioxin levels in water exceeded the water quality standard (0.0933 pg TEQ/L) at 94% of the locations sampled in Spring 2004 and 94% of the locations sampled in Fall 2004. The highest TEQ levels in the Spring samples were measured at stations

Table 3.7 Field Measurements during Water Sampling Activities

T 3.7 (2)

T 3.7 (3)

T 3.7 (4)

T 3.7 (5)

T 3.7 (6)

T 3.7 (7)

T 3.7 (8)

Table 3.8 Physical Characteristics of Water Samples

T 3.8 (2)

Figure 3.13 Verical Profiles of Field Parameters (in-stream)

Figure 3.13 (2)

Table 3.9 Total Dioxin Concentrations in Water

Figure 3.14 Total TEQ Concentrations in Water

11193 (segment 1001) and 15979 (segment 1006), while the highest TEQ concentrations in Fall samples were measured at stations 11261 (segment 1005) and 15979 (segment 1006).

Analysis of dioxin data in bottom sediments and water column collected in 2002-2003 indicated “disequilibrium” between these two media. However, it is noted that the collected data correspond to shallow water and there is the possibility of thermal and salinity-driven stratification in the channel. To address whether or not dioxin concentrations in the HSC are at equilibrium between bottom sediments and the water column, the project team gathered samples to develop vertical profiles of dioxins at two locations (Figure 3.1) during the Summer 2004. Dioxin concentrations for the vertical profiles are included in Table 3.9. A graphical comparison between shallow and deep dioxin concentrations is presented in Figure 3.15. As can be seen in Figure 3.15, deep concentrations were generally higher than shallow concentrations, with average deep/shallow ratios of up to 1.69 and 1.54 for locations 11193 and 15979, respectively (maximum ratios were 2.85 and 2.67, respectively). The only exceptions were 1234789-HpCDF at station 11193 and 123789-HxCDF at station 15979 for which the shallow concentrations were higher than those measured in the deep samples.

To investigate if dioxins are at equilibrium at the local scale among different phases in the HSC, fugacity calculations were completed for the different 2378-PCDD/Fs for the two locations sampled in Summer 2004. Fugacity is the tendency of a compound to "escape" from one phase to another (Mackay, 1991) and is linearly related to concentration by

$$C=Z*f \tag{3.1}$$

Figure 3.15 Comparison of Dioxin Concentrations in Shallow and Deep Water Samples

where C is the concentration of a chemical in a given phase, Z is the fugacity capacity [mol/m³Pa], and f is fugacity [Pa]. The fugacity capacity can be calculated using the following equations (Mackay, 1991):

$$\text{Water: } Z = \frac{1}{H} \quad \text{or} \quad Z = \frac{C_s}{P_s} \quad (3.2)$$

$$\text{Solid Sorbent: } Z = \frac{K_p \rho_s}{H} \quad \text{or} \quad Z = \frac{K_{oc} f_{oc} \rho_s}{H} \quad (3.3)$$

where H is the Henry's law constant [Pa m³/mol], C_s is the aqueous solubility [mol/m³], P_s is the vapor pressure [Pa], K_p is the partitioning coefficient [L/kg], K_{oc} is the organic carbon-normalized partitioning coefficient [L/kg-oc], f_{oc} is the fraction organic carbon [uniteless], and ρ_s is density [kg/L].

Equilibrium organic carbon partitioning coefficients (K_{oc}) were calculated using a linear model with 95% confidence limits developed by Seth et al. (1999):

$$\log K_{oc} = 1.03 \log K_{ow} - 0.61 \quad (3.4)$$

Using Equation (3.4), measured individual concentrations, and the estimated fugacity capacities, it is possible to estimate congener-specific fugacities (f) for each of the collected samples. The tendency for a specific compound to partition from one phase to another can be evaluated by the ratio of its fugacities in the two respective phases. The fugacity ratios between the suspended and dissolved phases (f_{sus}/f_w) and between bottom sediments and dissolved phase (f_{sed}/f_w) equal 1 at equilibrium.

Figures 3.16a and b show the suspended/dissolved and sediment/dissolved fugacity ratios for selected 2378-substituted PCDD/Fs, respectively. There is a lack of equilibrium at the suspended-dissolved and sediment-dissolved interfaces for most of the congeners as indicated by

Figure 3.16 Fugacity Ratios

the large range of fugacity ratios depicted in Figure 3.16. An f_s/f_w ratio greater than 1 indicates that the organic compound has a tendency to move from the particulate phase to the dissolved phase, while an f_s/f_w ratio smaller than 1 indicates a tendency of the compound to move from the dissolved to the particulate phase. Using shallow water data, fugacity ratios for the 2378-substituted dioxins varied from 0.02 to 4.77 with an average of 0.47 for the suspended-dissolved interface and from 0.19 to 39.7 with an average of 4.03 for the bottom sediment-dissolved interface. Similarly, dioxin data in deep water samples yielded fugacity ratios varying from 0.001 to 3.35 with an average of 0.26 for the dissolved-suspended interface and from 0.03 to 15.35 with an average of 1.60 for the bottom sediment-dissolved interface.

Data in Figures 3.16a suggest that 2378-TCDD is close to equilibrium at location 11193, while a dissolved→ particulate flux is expected at location 15979 as indicated by f_s/f_w ratios lower than 1. Data in Figure 3.16b indicate that 2378-TCDD is close to equilibrium between the bottom sediments and the dissolved phase (deep) at location 15979, whereas a bottom sediment→ dissolved flux is expected at location 11193. For almost all the remaining congeners, ratios lower than 1 were measured for the dissolved-suspended interface. The only exceptions were 2378-TCDF and 12378-PeCDF. For the bottom sediment-dissolved interface (Figure 3.16b), on the other hand, ratios greater than 1 were measured for some PCDFs and ratios lower than 1 for the higher chlorinated PCDDs. In addition, as can be seen in Figure 3.16b, 12378-PeCDD, 123478-HxCDF, 123678-HxCDF, 234678-HxCDF, 1234678-HpCDF, and 1234789-HpCDF are close to equilibrium between the bottom sediments and dissolved (deep) phases.

During Summer 2004, two additional locations in the upper watershed were sampled to obtain boundary dioxin data for calibration purposes (Stations 11142 and 11357 in Figure 3.1).

Table 3.9 presents a summary of dioxin/furan concentrations and the resulting Texas-TEQ levels for the samples collected in the upper watershed. Calculated Texas-TEQ levels were 0.055 pg/L and 0.074 pg/L for locations 11142 (Buffalo Bayou at Barker Dam) and 11357 (Buffalo Bayou at San Felipe), respectively. It is noted that dioxin levels in both locations were below the Texas WQS of 0.0933 pg/L.

A database of water sampling results reported by PSC/ Maxxam Analytical Laboratory is included in Appendix B1.

3.2.1.2 In-channel Sediment Sampling

Table 3.10 presents water column parameters obtained during the sediment sampling effort and Table 3.11 summarizes the results of the physical properties of sediment samples analyzed by NWDLS.

A summary of dioxin levels in sediment and their corresponding Texas-TEQs are presented in Table 3.12. Maps illustrating total TEQ concentrations in sediment for the Spring and Fall 2004 sampling events are shown in Figure 3.17. For the Spring 2004, dioxin levels in sediment varied from 0.92 to 451.4 ng TEQ/kg-dry wt. (dry weight), with an average value of 42.7 ng TEQ/kg-dry wt. Organic carbon (OC)-normalized levels ranged from 183.7 to 24,008 ng TEQ/kg-oc, with a mean value of 2,701 ng TEQ/kg-oc. TEQ. It is noted that the data are influenced by three relatively high values. A better estimate of central tendency, in this case, is probably the median which is equal to 1,048 ng TEQ/kg-oc. Likewise, TEQ concentrations in sediments collected in Fall 2004 varied ranged from 0.5 to 846.3 ng/kg-dry wt., with an average value of 68.8 ng/kg-dry wt. Organic carbon-normalized levels ranged from 247.1 to 30,551 ng/kg-oc, with a median value of 1,433 ng/kg-oc. The highest TEQ levels in the Spring samples

Table 3.10 Field Measurements during Sediment Sampling Activities

T 3.10 (2)

T 3.10 (3)

Table 3.11 Physical Characteristics of Sediment Samples

T 3.11 (2)

Table 3.12 Total Dioxin Concentrations in Sediment

T 3.12 (2)

Figure 3.17 Organic-carbon Normalized TEQ Concentrations in Sediment

were measured at locations 11280 (segment 1007) and 11193 (segment 1001), whereas the highest TEQ concentrations in Fall samples were measured at locations 11280 (segment 1007) and 16499 (segment 2427).

Dioxin results of high-resolution sediment sampling, conducted in Summer 2004 to pinpoint the location of unidentified major sources near stations 15979 and 11193, are included in Table 3.12. Total TEQ concentrations varied between 8.07 and 92.38 ng/kg-dry wt. with an average of 22.57 ng/kg-dry wt. Figure 3.18 shows the distribution of Texas TEQ in sediment samples and Figure 3.19 shows profiles of oc-normalized 2378-TCDD and TEQ concentrations at the 15 sampling locations. The highest organic-carbon normalized TEQ concentrations were observed at stations 11268 and 18389 for segments 1006 and 1001, respectively. Both 2378-TCDD and TEQ levels at station 18389 (~1 km upstream of station 11193) are significantly higher than those observed at the remaining locations in segment 1001, which might suggest the presence of an identified source of 2378-TCDD. This finding prompted additional high-resolution sediment sampling at the bend in San Jacinto River (1001) as discussed in Section 3.1.1.2. In the main channel results suggest additional unidentified sources might be present in the vicinity of 11280 and between 11269 and 11267.

The high-resolution data from Summer 2004 were analyzed using Principal Component and Cluster Analysis Techniques to determine if the fingerprints for the various locations were different (Figure 3.20). As shown in Figure 3.20, almost all the locations exhibited similar fingerprints, the only exception is station 11267 that seems to form its own cluster (relatively high concentrations of 1234678-HpCDF and OCDF), thus suggesting a different source from the other stations.

Figure 3.18 Dioxin Concentrations in High-resolution Sediment samples

Figure 3.19 Organic-carbon Normalized Concentrations from High-Resolution Sediment Sampling

Figure 3.20 Principal Component Analysis Results for the High-resolution Sediment Samples

In addition to high-resolution sediment sampling, five samples along a transect at location 15979 were collected during the Summer 2004 to evaluate the difference in dioxin concentrations between the dredged channel and the channel banks. Concentrations of dioxins along the transect are presented in Table 3.12 and depicted in Figure 3.21. Data show that the concentrations in the main channel are higher than those measured at the banks.

Results from the sediment sampling conducted during Summer 2005 are not available as of this writing and will be discussed in the next quarterly report.

A database of sediment results reported by Pace Analytical Laboratory is included in Appendix B1.

3.2.1.3 Tissue Sampling

A summary of dioxin levels in catfish and crab samples and their corresponding TEQs are presented in Tables 3.13 and 3.14, respectively. Total TEQ concentrations in tissue are mapped in Figures 3.22 and 3.23 for catfish and crab, respectively. Spring 2004 tissue samples varied from 0.19 to 19.64 ng TEQ/kg-wet wt. for catfish and from 0.37 to 8.61 ng TEQ/kg-wet wt. for crabs, with average values of 5.68 and 3.32 ng TEQ/kg-wet wt., respectively. Similarly, TEQ concentrations in Fall 2004 ranged from 0.93 to 27.4 ng/kg-wet wt. for catfish, and from 1.32 to 12.08 ng/kg-wet wt. for crabs, with respective average values of 9.39 and 6.93 ng/kg-wet wt. Lipid-normalized concentrations² in catfish and crabs showed average values of 11.39 and 6.82 ng TEQ/kg-wet wt. in Spring 2004, and 13.1 and 16.19 ng TEQ/kg-wet wt. in Fall 2004.

² Fish samples normalized to 3% lipids and crab samples to 2% lipids.

Figure 3.21 Dioxin Concentrations along Transect at Station 15979

Table 3.13 Total Dioxin Concentrations in Catfish

Table 3.14 Total Dioxin Concentrations in Crabs

Figure 3.22 TEQ Concentrations in Catfish

Figure 3.23 TEQ Concentrations in Crabs

The health-based standard of 0.47 ng TEQ/kg (derived from the Texas WQS) was exceeded in 96% of the Spring 2004 samples (for both catfish and crabs) and in all tissue samples collected in Fall 2004. In Spring 2004, locations 11300 (Vince Bayou) and 15979 (segment 1006) showed the highest dioxin catfish concentrations, while locations 11273 (Patrick Bayou) and 16618 (segment 1005) presented the highest dioxin concentrations in crabs. The highest dioxin concentrations in tissue collected in Fall 2004 were found at locations 11252 (segment 1005) and 11280 (segment 1007) for catfish, and 11193 (segment 1001) and 11252 (segment 1005) for crabs. It is noted that tissue was not sampled in tributaries during Fall 2004.

A database with results from tissue samples reported by PSC Philip Analytical Laboratory is provided in Appendix B1.

3.2.1.4 Sediment Core Sampling

Physical and Geochronological Analyses. This section presents the results for the eight cores selected for sediment dating analysis. It is noted that:

- Unsupported or excess ^{210}Pb ($^{210}\text{Pb}_{\text{xs}}$) is derived from atmospheric fallout and is the constituent of interest in terms of modeling sediment accumulation. Supported ^{210}Pb is that fraction of the isotope derived by the in situ radioactive decay of its progenitor, ^{226}Ra . The determination of $^{210}\text{Pb}_{\text{xs}}$ is outlined in more detail in subsequent sections.
- Cumulative mass depth is used here and is a mass based assessment of depth, as opposed to cm or some other one dimensional unit. Mass depth = [(1 – porosity) * density * interval thickness], where the density is assumed = 2.5 g cm^{-3} and the typical interval thickness = 1 cm. Cumulative mass depth is the summation of mass depth over the interval of interest.

- Reported concentrations of $^{239,240}\text{Pu}$ have been corrected to account for a small, above background anomaly, most likely resulting from slight contamination of an acid bath. The concentrations of $^{239,240}\text{Pu}$ in samples where no ^{137}Cs was found have been combined as an average value (0.022 ± 0.009 mBq/g), which was then subtracted from all reported values of $^{239,240}\text{Pu}$.

Station 11261

Summary physical and radiochemical data for this station are shown in Tables 3.15a and b. X-radiograph and the core grain size distribution are shown in Figure C-1 and listed in Table C-1 of Appendix C. The core grain size distribution is shown in Figure 3.24 and listed in Table 3.15a. For this and all stations, $^{210}\text{Pb}_{\text{xs}}$ is defined as total ^{210}Pb – deepest ^{210}Pb values in the core, where equilibrium is assumed between ^{210}Pb and its progenitor, ^{226}Ra (Walsh and Nittrouer 2003, Kim and Rejmankova 2002, Craft and Richardson 1993, Binford 1990). Here, the mean ^{210}Pb value over the depth interval of 23 – 48 cm was used as the supported value (10.93 ± 1.00 mBq g^{-1}). Deep penetration of ^7Be to 20 cm (Figure 3.25) could be interpreted as either deep mixing or rapid sedimentation. The absence of a distinct ^{137}Cs peak (Table 3.13b), the layered structure of POC and porosity (Table 3.15a, Figure 3.26) and the close correlation of ^7Be activity concentrations with POC concentrations (Figure 3.27) are all consistent with rapid sedimentation, and inconsistent with deep mixing. This station appears to have experienced recent and very rapid sedimentation. The very low concentrations of $^{239,240}\text{Pu}$ also support rapid and recent sedimentation here (Table 3.15b).

Sediment accumulation rates using both ^7Be and $^{210}\text{Pb}_{\text{xs}}$ have been determined using the constant flux-constant sedimentation (CF-CS) model (Yeager *et al.* 2004), where sedimentation

Table 3.15a Physical Data for Station 11261

Table 3.15b Radiochemical Data for Station 11261

Figure 3.24 Grain Size Distribution for Core Sediment at Station 11261

Figure 3.25 $^{210}\text{Pb}_{\text{xs}}$ and ^7Be Data for Station 11261

Figure 3.26 Porosity and POC Data for Station 11261

Figure 3.27 POC vs. ⁷Be for Station 11261

rates can be calculated assuming steady state conditions and at relatively constant porosity, using:

$$[I(z)] = [I(0)]^{-\alpha z} \quad (3.5a)$$

$$\alpha = \frac{\lambda}{S} \quad (3.5b)$$

where $[I(z)]$ and $[I(0)]$ represent ^7Be or $^{210}\text{Pb}_{\text{xs}}$ concentration at depth z and at the sediment-water interface, respectively; S = sediment accumulation rate ($\text{g cm}^{-2} \text{ yr.}^{-1}$) and λ = decay constant of each isotope ($^{210}\text{Pb} = 0.031 \text{ yr.}^{-1}$ and $^7\text{Be} = 4.75 \text{ yr.}^{-1}$). Figures 3.28 and 3.29 show the semi-log plots of each isotope over depth, from which sediment accumulation rates were derived. The time frame over which each isotope is valid in terms of modeling sedimentation rates is equal to approximately seven times its half-life, so ^7Be represents a one year time frame while $^{210}\text{Pb}_{\text{xs}}$ represents over one hundred years. Sediment accumulation rates for this station were determined to be $143.94 \pm 109.39 \text{ g cm}^{-2} \text{ yr.}^{-1}$ (or $113.10 \pm 87.08 \text{ cm yr.}^{-1}$) in the upper 20 cm ($0 - 26.95 \text{ g cm}^{-2}$) via ^7Be and beneath this depth to be $2.82 \pm 1.30 \text{ g cm}^{-2} \text{ yr.}^{-1}$ (or $1.94 \pm 0.89 \text{ cm yr.}^{-1}$) via $^{210}\text{Pb}_{\text{xs}}$. It thus appears that the upper 20 cm was deposited over a ≈ 2.5 -month time frame, considering the half-life of ^7Be (53 d). Sedimentation below 26.95 g cm^{-2} was determined by applying a weighted average technique, where the average $\log ^{210}\text{Pb}_{\text{xs}}$ for the upper region ($0 - 26.95 \text{ g cm}^{-2}$) was used as the first point of the plot.

The chronology of the sediment profile is represented in Figure 3.30. As previously discussed, the upper 20 cm ($0 - 26.95 \text{ g cm}^{-2}$) was deposited over several months, based on ^7Be data. This upper region chronology was determined by applying the constant flux model (CF)

Figure 3.28 ^7Be Modeling Data for Station 11261
Figure 3.29 $^{210}\text{Pb}_{\text{xs}}$ Modeling Data for Station 11261

Figure 3.30 ^7Be and $^{210}\text{Pb}_{\text{xs}}$ based Chronologic Profile for Station 11261

(Robbins 1978, Appleby and Oldfield 1978), which is defined as:

$$t = -\frac{1}{\lambda} \ln \left[1 - \frac{\Sigma(m)}{\Sigma(\infty)} \right] \quad (3.6)$$

where t = time (yr.), λ = ^7Be decay constant (4.75 yr.^{-1}), $\Sigma(m) = \int_0^m A(u)du = \int_0^t F_7 e^{-\lambda t} dt$, $\Sigma(\infty) = F_7/\lambda$ and $F_7 = ^7\text{Be}$ flux ($\text{mBq cm}^{-2} \text{ yr.}^{-1}$). Since $^{210}\text{Pb}_{\text{xs}}$ data at this station is sporadic, the CF model is not applicable for sediment below 20 cm. The chronology below this depth is determined by applying the longer term $^{210}\text{Pb}_{\text{xs}}$ based sedimentation rate.

Station 15244

Summary physical and radiochemical data for this station are listed in Tables 3.16a and b. X-radiograph and the core grain size distribution are shown in Figure C-2 and listed in Table C-1 of Appendix C. The grain size distribution for the core is shown in Figure 3.31 and summarized in Table 3.16a. The mean ^{210}Pb value over the depth interval of 6 – 30 cm was used as the supported value ($23.05 \pm 1.73 \text{ mBq g}^{-1}$). This station shows nearly ideal profiles for ^7Be and $^{210}\text{Pb}_{\text{xs}}$ (Figure 3.32), indicating that mixing over the short term is constrained to the very upper section of the sediment profile (< 3 cm) at most, and that the profile represents over 100 years of deposition. This interpretation is supported by porosity and POC data (Figure 3.33), that indicate little mixing at depth and a stable, accumulating sedimentary setting.

Sediment accumulation rates using $^{210}\text{Pb}_{\text{xs}}$ have been determined using the CF-CS model, as previously described. Figure 3.34 shows the semi-log plot of $^{210}\text{Pb}_{\text{xs}}$ over depth, from which a sediment accumulation rate was derived. Sediment accumulation at this station based on $^{210}\text{Pb}_{\text{xs}}$ is $0.24 \pm 0.10 \text{ g cm}^{-2} \text{ yr.}^{-1}$ (or $0.31 \pm 0.13 \text{ cm yr.}^{-1}$). Sediment accumulation rates have also been

Table 3.16a Physical Data for Station 15244

Table 3.16b Radiochemical Data for Station 15244

Figure 3.31 Grain Size Distribution for Core Sediment at Station 15244

Figure 3.32 $^{210}\text{Pb}_{\text{xs}}$ and ^7Be Data for Station 15244

Figure 3.33 Porosity and POC Data for Station 15244

Figure 3.34 $^{210}\text{Pb}_{\text{xs}}$ Modeling Data for Station 15244

determined using ^{137}Cs (Table 3.16b) by:

$$S = \frac{D_{pk}}{T} \quad (3.7)$$

where S = sediment accumulation rate ($\text{g cm}^{-2} \text{ yr.}^{-1}$), D_{pk} = mass depth (g cm^{-2}) at which the ^{137}Cs maxima occurs (1963) and T = time (yr.). This model is based on the assumption of limited vertical mobility of cesium in sediments (Huntley *et al.* 1995, Winkels *et al.* 1998, Valero-Garces *et al.* 1999). Sediment accumulation rates at this station based on ^{137}Cs are $0.26 \pm 0.03 \text{ g cm}^{-2} \text{ yr.}^{-1}$ (or $0.27 \pm 0.05 \text{ cm yr}^{-1}$), are very close to those determined using $^{210}\text{Pb}_{\text{xs}}$ (Figure 3.35). This rate is further supported by $^{239,240}\text{Pu}$ data, whose temporal input function and particle reactive nature allow for the same approach as for ^{137}Cs . Sediment accumulation rates at this station based on $^{239,240}\text{Pu}$ are $0.18 \pm 0.01 \text{ g cm}^{-2} \text{ yr.}^{-1}$ (or $0.26 \pm 0.03 \text{ cm yr}^{-1}$) (Figure 3.36).

The chronology of the sediment profile is represented in Figure 3.37 and was determined using $^{210}\text{Pb}_{\text{xs}}$ data and the constant flux (CF) model, as previously discussed.

Station 11193

Summary physical and radiochemical data for station 11193 are listed in Tables 3.17a and b. X-radiograph and the grain size distribution for the core are shown in Figure C-3 and listed in Table C-2 of Appendix C. The grain size distribution for this core is shown in Figure 3.38 and summarized in Table 3.17a. ^7Be data (Table 3.17b, Figure 3.39) suggest that short term mixing is confined to the very surface layer of sediment here (0 – 2 cm). For this station, the mean ^{210}Pb value over the depth interval of 30 – 40 cm was used as the supported value ($8.34 \pm 0.78 \text{ mBq g}^{-1}$), $^{210}\text{Pb}_{\text{xs}}$ is shown in Figure 3.39. The interpretation of limited mixing is supported by porosity and POC data (Figure 3.40).

Figure 3.35 ^{137}Cs Data for Station 15244
Figure 3.36 $^{239,240}\text{Pu}$ Data for Station 15244

Figure 3.37 $^{210}\text{Pb}_{\text{xs}}$ based Chronologic Profile for Station 15244

Figure 3.38 Grain Size Distribution for Core Sediment at Station 11193

Table 3.17a Physical data for Station 11193

Table 3.17b Radiochemical Data for Station 11193

Figure 3.39 $^{210}\text{Pb}_{\text{xs}}$ and ^7Be data for Station 11193
Figure 3.40 Porosity and POC Data for Station 11193

Sediment accumulation rates using $^{210}\text{Pb}_{\text{xs}}$ have been determined using the CF-CS model, as previously described. Figure 3.41 shows the semi-log plot of $^{210}\text{Pb}_{\text{xs}}$ over depth, from which a sediment accumulation rate was derived. Only the upper section of the profile was modeled, as the lower portion of the profile does not show exponential decline (see Figure 3.39), likely due to mixing or very rapid sedimentation that occurred in the past, prior to the upper most, exponential portion's deposition. Sediment accumulation at this station based on $^{210}\text{Pb}_{\text{xs}}$ is $0.18 \pm 0.09 \text{ g cm}^{-2} \text{ yr.}^{-1}$ (or $0.21 \pm 0.11 \text{ cm yr.}^{-1}$). Sediment accumulation rates have been determined using ^{137}Cs as described previously (Figure 3.42), $0.20 \pm 0.02 \text{ g cm}^{-2} \text{ yr.}^{-1}$ (or $0.21 \pm 0.02 \text{ cm yr.}^{-1}$), very close to those determined using $^{210}\text{Pb}_{\text{xs}}$ (Figure 3.41).

The extrapolated chronology of the sediment profile is represented in Figure 3.43 and was determined using $^{210}\text{Pb}_{\text{xs}}$ data and the constant flux (CF) model, as previously discussed.

Station 15979

Summary physical and radiochemical data for station 15979 are presented in Tables 3.18a and b. X-radiograph and the core grain size distribution are shown in Figure C-4 and listed in Table C-2 of Appendix C. The grain size distribution for this core is shown in Figure 3.44 and summarized in Table 3.18a. ^7Be (Table 3.18b, Figure 3.45) data suggest that short term mixing is confined to the near surface (0 – 2 cm). For this station, the mean ^{210}Pb value over the depth interval of 28 – 35 cm was used as the supported value ($6.69 \pm 0.66 \text{ mBq/g}$), $^{210}\text{Pb}_{\text{xs}}$ is shown in Figure 3.45. The possibility of longer term, episodic mixing or rapid sedimentation is indicated by the grain size distribution (increased sand composition with depth, Figure 3.44) and irregular $^{210}\text{Pb}_{\text{xs}}$ and POC profiles (Figures 3.45 and 3.46, respectively).

The use of $^{210}\text{Pb}_{\text{xs}}$ to determine sediment accumulation rates for this core is not

Figure 3.41 $^{210}\text{Pb}_{\text{xs}}$ Modeling Data for Station 11193

Figure 3.42 ^{137}Cs Data for Station 11193

Figure 3.43 $^{210}\text{Pb}_{\text{xs}}$ based Chronologic Profile for Station 11193

Figure 3.44 Grain Size Distribution for Core Sediment at Station 15979

Table 3.18a Physical Data for Station 15979

Table 3.18b Radiochemical Data for Station 15979

Figure 3.45 $^{210}\text{Pb}_{\text{xs}}$ and ^7Be data for Station 15979
Figure 3.46 Porosity and POC Data for Station 15979

appropriate, since the distribution of ^{137}Cs suggests that sediment beneath 10.43 g cm^{-2} (10 cm, Table 3.18b) is older than 1953 (year when appreciable ^{137}Cs was detected at the earth's surface) or is comprised of older sediment which has been mixed into the profile. An average rate of sediment accumulation has been determined using ^{137}Cs based on this premise, $0.20 \pm 0.03 \text{ g cm}^{-2} \text{ yr}^{-1}$ (or $0.18 \pm 0.02 \text{ cm yr}^{-1}$).

The extrapolated chronology of the sediment profile is represented in Figure 3.47 and was determined based on the average sedimentation rate as determined using ^{137}Cs .

Station 11270

Summary physical and radiochemical data for station 11270 are presented in Tables 3.19a and b. X-radiograph and the core grain size distribution are shown in Figure C-5 and listed in Table C-3 of Appendix C. The grain size distribution for this core is shown in Figure 3.48 and summarized in Table 3.19a; note the dominance of the sand fraction in the near surface, indicative of a recent depositional event. The absence of ^7Be (Table 3.19b) suggests a mixed setting where “old” sediment (relative to the half life of ^7Be) has been deposited over the last few years. For this station, the mean ^{210}Pb value over the depth interval of 38 – 43 cm was used as the supported value ($5.95 + 0.54 \text{ mBq/g}$); $^{210}\text{Pb}_{\text{xs}}$ is shown in Figure 3.49. The $^{210}\text{Pb}_{\text{xs}}$ profile is also indicative of mixing or rapid sedimentation. The presence of high quantities of $^{210}\text{Pb}_{\text{xs}}$ deep in the profile suggests the possibility that the sediment profile has been affected by high energy depositional events. Episodic deposition events are also indicated by other evidence, including high $^{210}\text{Pb}_{\text{xs}}$ values at depth and an irregular profile for POC (Figure 3.50) as well as a chaotic ^{137}Cs profile (Table 3.19b, Figure 3.51) and very low values for $^{239,240}\text{Pu}$ (Table 3.19b).

A rigorous determination of sedimentation rates derived from any of the isotopes

Figure 3.47 $^{210}\text{Pb}_{\text{xs}}$ based Chronologic Profile for Station 15979

Figure 3.48 Grain Size Distribution for Core Sediment at Station 11270

Table 3.19a Physical Data for Station 11270

Table 3.19b Radiochemical data for Station 11270

Figure 3.49 $^{210}\text{Pb}_{\text{xs}}$ dat for Station 11270
Figure 3.50 Porosity and POC Data for Station 11270

Figure 3.51 ¹³⁷Cs Data for Station 11270

quantified herein is impossible for this station, as is a chronological determination. However, the ^{137}Cs data (Figure 3.51) indicate that the interval over which appreciable ^{137}Cs is found at least 13 g cm^{-2} , deposited in less than 50 years, suggesting at least $0.65\text{ g cm}^{-2}\text{ yr}^{-1}$ of equivalent continuous sediment accumulation. It must be emphasized that lateral transport events are typical in this system, as evidenced by the number of sites visited and cores collected that showed evidence of either mixing or strong depositional and/or erosional events.

Station FW1

A wetland core was selected and identified as an essential component of the research, in that such a core, if collected from a stable area nearby but not in the HSC system could provide background (atmospheric input) data for dioxins. The data from the core, combined with chronological information from radionuclide studies would significantly contribute to the overall project objectives (in particular the "legacy" issue). Summary physical and radiochemical data for station FW1 are presented in Tables 3.20a and b. X-radiograph and the core grain size distribution are shown in Figure C-6 of Appendix C and listed in Table 3.20a. The grain size distribution for the core is shown in Figure 3.52 and summarized in Table 3.20a. The mean ^{210}Pb value over the depth interval of 20 – 41 cm was used as the supported value ($9.50 \pm 0.92\text{ mBq g}^{-1}$). This station shows nearly ideal profiles for ^7Be and $^{210}\text{Pb}_{\text{xs}}$ (Figure 3.53), indicating that mixing over the short term is constrained to the very upper section of the sediment profile (< 2 cm) at most. This interpretation is supported by porosity and POC data (Figure 3.54) that indicate little mixing at depth and a stable sedimentary setting. Of note is the high concentration of POC in the near surface, an expected scenario in a forested wetland.

Sediment accumulation rates using $^{210}\text{Pb}_{\text{xs}}$ have been determined using the CF-CS model,

Table 3.20a Physical data for Station FW1

Table 3.20b Radiochemical Data for Station FW1

Figure 3.52 Grain Size Distribution for Core Sediment at Station FW!

Figure 3.53 $^{210}\text{Pb}_{\text{xs}}$ and ^7Be Data for Station FW1

Figure 3.54 Porosity and POC Data for Station FW1
Figure 3.55 ²¹⁰Pb_{xs} Modeling Data for Station FW1

as previously described. Figure 3.55 shows the semi-log plot of $^{210}\text{Pb}_{\text{xs}}$ over depth, from which a sediment accumulation rate was derived. Only the upper portion of the profile was modeled (0 – 19 cm), as it is representative of the exponential decay of $^{210}\text{Pb}_{\text{xs}}$ here. Sediment accumulation at this station based on $^{210}\text{Pb}_{\text{xs}}$ is $0.21 \pm 0.12 \text{ g cm}^{-2} \text{ yr}^{-1}$ (or $0.14 \pm 0.08 \text{ cm yr}^{-1}$). Sediment accumulation rates have been determined using ^{137}Cs as previously discussed. The sediment accumulation rate at this station based on ^{137}Cs is $0.18 \pm 0.04 \text{ g cm}^{-2} \text{ yr}^{-1}$ (or $0.13 \pm 0.03 \text{ cm yr}^{-1}$), very close to that determined using $^{210}\text{Pb}_{\text{xs}}$ (Figure 3.56). Of note here is the double peak in the ^{137}Cs profile. In addition to the expected peak corresponding to maximum global fallout of ^{137}Cs in 1963, a second, smaller but distinct peak is present and corresponds to the Chernobyl accident which occurred in the former Soviet Union in 1986, further testament to the very stable setting at this core. Using this peak as an additional chronologic marker yields a sediment accumulation rate of $0.21 \pm 0.08 \text{ g cm}^{-2} \text{ yr}^{-1}$ (or $0.19 \pm 0.05 \text{ cm yr}^{-1}$).

The chronology of the sediment profile is represented in Figure 3.57 and was determined using $^{210}\text{Pb}_{\text{xs}}$ data and the constant flux (CF) model, as previously discussed.

Station 16499

Summary physical and radiochemical data for station 16499 are presented in Tables 3.21a and b. X-radiograph and the core grain size distribution are shown in Figure C-7 and listed in Table C-3 of Appendix C. The grain size distribution for this core is shown in Figure 3.58 and summarized in Table 3.21a. The mean ^{210}Pb value over the depth interval of 39 – 41 cm was used as the supported value ($8.64 \pm 0.91 \text{ mBq g}^{-1}$). Profiles of ^7Be and $^{210}\text{Pb}_{\text{xs}}$ (Figure 3.59) suggest a very recent, stable sedimentary setting, overlying what appears to be a previously mixed or rapidly deposited profile, as evidenced by the homogenized $^{210}\text{Pb}_{\text{xs}}$ data after approximately 4 cm

Figure 3.56 ^{137}Cs Data for Station FW1
Figure 3.57 $^{210}\text{Pb}_{\text{xs}}$ based Chronologic Profile for Station FW1

Table 3.21a Physical data for Station 16499

Table 3.21b Radiochemical Data for Station 16499

Figure 3.58 Grain Size Distribution for Core Sediment at Station 16499

Figure 3.59 $^{210}\text{Pb}_{\text{xs}}$ and ^7Be data for Station 16499

depth. This interpretation is supported by POC data (Figure 3.60) that indicate a stable sedimentary setting at the near surface only.

The use of $^{210}\text{Pb}_{\text{xs}}$ to determine sediment accumulation rates for this core is not appropriate due to the homogenized nature of the $^{210}\text{Pb}_{\text{xs}}$ profile and the persistence of appreciable ^{137}Cs with depth (29 cm, Table 3.21b). As such, an average rate can be obtained as was done for station 15979, using the lowest occurrence of ^{137}Cs as representative of 1953 (year which appreciable ^{137}Cs was detected at the earth's surface). An average rate of sediment accumulation of $0.31 \pm 0.01 \text{ g cm}^{-2} \text{ yr}^{-1}$ (or $0.56 \pm 0.02 \text{ cm yr}^{-1}$) has been determined using ^{137}Cs based on this premise.

The extrapolated chronology of the sediment profile is represented in Figure 3.61 and was determined based on the average sedimentation rate as determined using ^{137}Cs .

Station 13337

Summary physical and radiochemical data for station 13337 are presented in Tables 3.22a and b. X-radiograph and the core grain size distribution are shown in Figure C-8 and listed in Table C-4 of Appendix C. The grain size distribution for this core is shown in Figure 3.62 and summarized in Table 3.22a. The mean ^{210}Pb value over the depth interval of 38 – 44 cm was used as the supported value ($29.67 \pm 2.73 \text{ mBq g}^{-1}$). This station shows a nearly ideal profile for ^7Be , indicating very little mixing at the surface in the short term and a steadily declining $^{210}\text{Pb}_{\text{xs}}$ profile with depth (Figure 3.63). This interpretation is supported by porosity and POC data (Figure 3.64) that indicate little mixing at the near surface and in general, a gradual decline in concentrations of POC moving down section.

Sediment accumulation rates using $^{210}\text{Pb}_{\text{xs}}$ have been determined using the CF-CS model, described previously. Figure 3.65 shows the semi-log plot of $^{210}\text{Pb}_{\text{xs}}$ over depth, from which a

Figure 3.60 Porosity and POC Data for Station 16499
Figure 3.61 $^{210}\text{Pb}_{\text{xs}}$ Chronologic Profile for Station 16499

Table 3.22a Physical Data for Station 13337

Table 3.22b Radiochemical data for Station 13337

Figure 3.62 Grain Size Distribution for Core Sediment at Station 13337

Figure 3.63 $^{210}\text{Pb}_{\text{xs}}$ and ^7Be Data for Station 13337

Figure 3.64 Porosity and POC Data for Station 13337

Figure 3.65 ²¹⁰Pb_{xs} Modeling Data for Station 13337

Figure 3.66 $^{210}\text{Pb}_{\text{xs}}$ based chronologic profile for station 13337

sediment accumulation rate was derived. Sediment accumulation at this station based on $^{210}\text{Pb}_{\text{xs}}$ is $0.46 \pm 0.14 \text{ g cm}^{-2} \text{ yr.}^{-1}$ (or $0.97 \pm 0.30 \text{ cm yr.}^{-1}$). While additional data will refine the ^{137}Cs approach, taking the deepest significant ^{137}Cs point (40 cm, Table 3.22b) as 1953 yields an average sediment accumulation rate that is close to that determined via $^{210}\text{Pb}_{\text{xs}}$, i.e., $0.37 \pm 0.01 \text{ g cm}^{-2} \text{ yr.}^{-1}$ (or $0.77 \pm 0.02 \text{ cm yr.}^{-1}$).

The chronology of the sediment profile is represented in Figure 3.66 and was determined using $^{210}\text{Pb}_{\text{xs}}$ data and the constant flux (CF) model, as previously discussed.

A summary of accumulation rates for the eight sediment cores is presented in Table 3.23. Data indicate that core 11261 presented the highest sedimentation rate, while the wetland location (FW1) exhibited the lowest sedimentation rate. Cores 15979 and 11270 exhibited high mixing, whereas the remaining cores presented mixing limited to the upper sections.

Table 3.23 Summary of Sediment Accumulation Rates

Core	Accumulation Rate (cm/yr)	Comments
11261	113.10 ± 87.08	Recent and rapid sedimentation
15244	0.31 ± 0.13	Stable, shallow mixing
11193	0.21 ± 0.11	Limited mixing
15979	0.18 ± 0.02	Episodic mixing
11270	Could not be calculated	High mixing
FW1	0.14 ± 0.08	Stable, shallow mixing
16499	0.56 ± 0.02	Stable, shallow mixing
13337	0.97 ± 0.30	Stable, shallow mixing

Dioxin Analyses. Dioxin results for eight sediment cores are included in Table 3.24. Overall, total TEQ concentrations varied from 0.27 to 238.9 ng/kg-dry wt. Average TEQ concentrations for cores 11261, 15244, 11193, 15979, 11270, FW1A, 13337, and 16499 were 6.32, 5.03, 12.77,

Table 3.24 Total Dioxin Concentrations in Sediment Cores

T 3.24 (2)

9.44, 91.80, 0.56, 9.23, and 12.38 ng/kg-dry wt., respectively. As expected, the “cleanest” core was that collected from a wetland (FW1A), while the most contaminated core was retrieved from location 11270.

Figure 3.67 shows vertical profiles of selected organic carbon-normalized 2378-substituted congeners and TEQ for all eight cores. It can be seen in Figures 3.67a, d, and e that all the congeners follow the same pattern for cores 11261, 15979, and 11270, with significant peaks at the 8-cm, 7-cm, and 12-cm depth intervals, respectively. These cores are also characterized by a relatively high presence of 2378-TCDF when compared to the other congeners (except OCDD). It is noted that core 11270 exhibited the highest concentrations (up to 15 times its counterparts for the remaining cores). Likewise, cores 15244, 11193, 13337, and 16499 showed similar fairly consistent pattern among the selected congeners (Figures 3.67b, c, g, and h), with significant peaks for all the congeners but OCDD in the top 5 cm of the cores and a second peak in the intervals around 20-cm. 12378-PeCDD and 23478-PeCDF in this group of cores exhibited very “flat” profiles, with concentrations significantly lower than those for the other congeners. Concentrations for core FW1A (Figure 3.67f) showed no significant peaks, with the exception of OCDD that showed a peak at the 10-cm interval. The profiles at FW1A exhibited a slight increase with depth. It is also noted that this core showed the lowest concentrations with most of the congeners below the detection limit.

Figure 3.68 presents the vertical distribution of 2378-TCDD, 2378-TCDF, Σ PCDD and Σ PCDF concentrations in seven of the collected cores³ versus the estimated year of deposition (derived from $^{210}\text{Pb}_{\text{xs}}$ and ^{137}Cs profiles). The longest time coverage of the sediment cores was

³ Estimation of age was not possible for core 11270 due to mixing.

Figure 3.67 Dioxin Concentrations in Sediment Cores

Figure 3.68 Chronologies of Dioxin Concentrations

about 150 years (sample 13337-35cm). It is noted that geochronology analyses for the deepest intervals were not undertaken, but when the age vs. depth curves were extrapolated coverages of up to 800 years were estimated. Data in Figure 3.68 show that surprisingly the oldest interval concentrations appear to be as high or slightly higher than those measured in the surface intervals. This could indicate the presence of other sources prior to the construction of the HSC (1909).

Figure 3.69 shows vertical distribution of selected compounds normalized to the maximum (=100%). It can be seen in Figure 3.69 that the maximum concentration of 2378-TCDD and 2378-TCDF was located in the oldest (deepest) sediment layers for cores 11193, 13337, and 15979. Additional samples at greater depths are being analyzed for dioxins to confirm this observation.

A database of dioxin results for the sediment cores as reported by Pace Analytical is included in Appendix B2.

3.2.2 Assessment of Major Sources, Transport and Fate of Dioxins in the Houston Ship Channel

3.2.2.1 Water Sampling

Results from field and conventional parameters for water samples collected in the main tributaries are included in Tables 3.7 and 3.8, respectively. Vertical profiles of temperature, pH, and salinity are shown in Figure 3.70. Salinity data in Figure 3.70 indicate that the profiles for most stations are similar, reflecting nearly freshwater at the surface and an increase in salinity with depth. The exceptions are stations 11272 (Carpenter Bayou), 11300 (Vince Bayou), 11347

Figure 3.69 Chronologies of Dioxin Concentrations Normalized to maximum Concentrations

Figure 3.70 Vertical Profiles of Field Parameters (tributaries)

F 3.70 (2)

(Buffalo Bayou) and 11382 (Whiteoak Bayou), where the salinity profile is more uniform, with concentrations close to 0 ‰.

Dioxin results from the water samples collected at main tributaries are included in Table 3.25. Total TEQ concentrations in water from tributaries are mapped in Figure 3.14. Dioxin levels in water samples collected at the mouth of 11 tributaries during Spring 2004 varied from 0.044 to 1.824 pg TEQ/L, while the Fall 2004 concentrations varied from 0.069 to 1.430 pg TEQ/L. The average concentrations were 0.389 pg TEQ/L for Spring 2004 and 0.332 pg TEQ/L for Fall 2004. These averages are very similar to those calculated for in-channel samples (0.409 and 0.340 pg TEQ/L for the Spring and Fall 2004, respectively). Location 11273 (Patrick Bayou) exhibited the highest dioxin levels for both Spring and Fall 2004. Nine of the 11 (82%) tributary locations exceeded the Texas water quality standard (0.0933 pg/L) in Spring 2004, while eight of them (73%) exceeded the standard in Fall 2004. Location 11382 (Whiteoak Bayou) was the only one that did not exceed the WQ standard in both samples.

3.2.2.2 Air Sampling

Ambient Air Concentrations

The total ambient air dioxin concentrations along with the concentrations of the 17 individual 2378-substituted congeners at the two air monitoring stations measured as part of WO7 are presented in Table 3.26. Total ambient air dioxin concentrations measured in WO7 ranged from 668 to 1,518 fg/m³ at Clinton Drive (C403), and from 486 to 1,559 fg/m³ at Lang Road (C408). Average dioxin concentrations at Clinton Drive for the Dec/03-Apr/04 and Sep/04-Feb/05 periods (mean±standard deviation) were 1159 ± 342, and 1083 ± 387 fg/m³, respectively. Similarly, the average total ambient air concentration measured at Lang Road during the Dec/03-

Table 3.25 Total Dioxin Concentrations in Water from Tributaries

Table 3.26 Dioxin Concentrations in Ambient Air

Apr/04 sampling periods was $972 \pm 497 \text{ fg/m}^3$.

The higher chlorinated congeners such as 1234678-HpCDD, 1234678-HpCDF, OCDF, and especially OCDD were consistently found at both sites as the congeners making the major contribution to the total ambient air dioxin concentration. In most of the cases, the contribution of OCDD was found to be >50% at all stations during the period sampled (see Figure 3.71). Concentrations for OCDD of up to $1,024 \text{ fg/m}^3$ were measured in the Houston area at the Lang Road site in the January/04 event. In contrast, 2378-TCDD had a very low contribution to the total dioxin concentration during the sampled period. A maximum concentration of 1.6 fg/m^3 was detected for this congener at the Clinton Drive site (this site is located in the industrial area and near major highways) in the February-March/04 event.

In terms of Σ TEQ concentrations, values were found fluctuating from 7 to 20 fg/m^3 at Clinton Drive and from 6 to 21 fg/m^3 at Lang Road. The congeners 12378-PeCDD and 23478-PeCDF were consistently found to be the major contributors to the Σ Texas-TEQ concentration. Contributions of up to 23 and 22% were observed for 12378-PeCDD at Clinton Drive and Lang Road, respectively. Similarly, contributions of up to 31 and 33% were found for 23478-PeCDF at the same sites, respectively. Finally, 2378-TCDD contributions to the total TEQ were up to 15 and 20%, for the aforementioned sites, respectively.

Particle Size Distribution of Associated Dioxins

Bi-monthly particle size data of associated dioxins samples were collected from September 2004 to February 2005 at Clinton Drive (C403). Three sampling events were completed: September/04-October/04, November/04-December/04, and January/04-February/05. The airborne particles were separated into the following size ranges: >7.2, 7.2-3.0, 3.0-1.5, 1.5-

Figure 3.71 Ambient Air Profiles of Dioxins and Furans

F 3.71 (2)

0.95, 0.95-0.49, <0.49 μm in aerodynamic diameter (d_{ae}) as mentioned previously.

The concentrations (fg/m^3) of individual dioxin and furan congeners, and organic and elemental carbon determined in the different particle size ranges are summarized in Table 3.27. The concentrations of the higher chlorinated congeners were significantly higher than those of the less chlorinated congeners at all stages. OCDD was the most prominent congener for the full size range analyzed in this study. Lower chlorinated congeners were found associated with the smallest fraction of particles (i.e., 0.95-0.49 and <0.49 μm). Fine particles ($d_{ae} < 2.5 \mu\text{m}$) are known to be produced predominantly from gas-to-particle conversion and from incomplete combustion (anthropogenic sources such as diesel fueled vehicles). The congener 2378-TCDD was primarily found bound to particles with $d_{ae} < 0.49 \mu\text{m}$ in November/04-December/04 and January/05-February/05 events at concentrations of 0.2 and 0.1 fg/m^3 , respectively.

The total dioxin particle-phase concentration was found to be mostly associated to the range sizes 0.95-0.49 and <0.49 μm in the three events. In fact, the combined contributions of these two stages to the total dioxin particle-phase concentrations observed in the three consecutive events were 84, 94, and 90%, respectively.

From the particle size ranges analyzed in this study, particles with $d_{ae} > 7.2 \mu\text{m}$ were characterized by having the highest deposition velocities. At this particle size range, OCDD, 1234678-HpCDD, 1234678-HpCDF, and OCDF were consistently found dominating the dioxin mass profile. In fact, more than 98% of the total dioxin mass detected at this specific size range (>7.2 μm) was attributed to these four congeners.

Total TEQ data in Table 3.27 indicated that the highest concentrations were observed in the particle sizes rich in lower chlorinated congeners (0.95-0.49 and <0.49 μm). Concentrations

Table 3.27 Concentrations of PCDD/PCDFs with respect to Particle Size

fluctuating from 0.9 to 2.5 fg Σ Texas-TEQ/m³ and from 1.7 and 8.5 fg Σ Texas-TEQ/m³ were observed for these two particle sizes, respectively. A combined contribution of these two particle sizes of >87% to the Σ Texas-TEQ was found (see Figure 3.72).

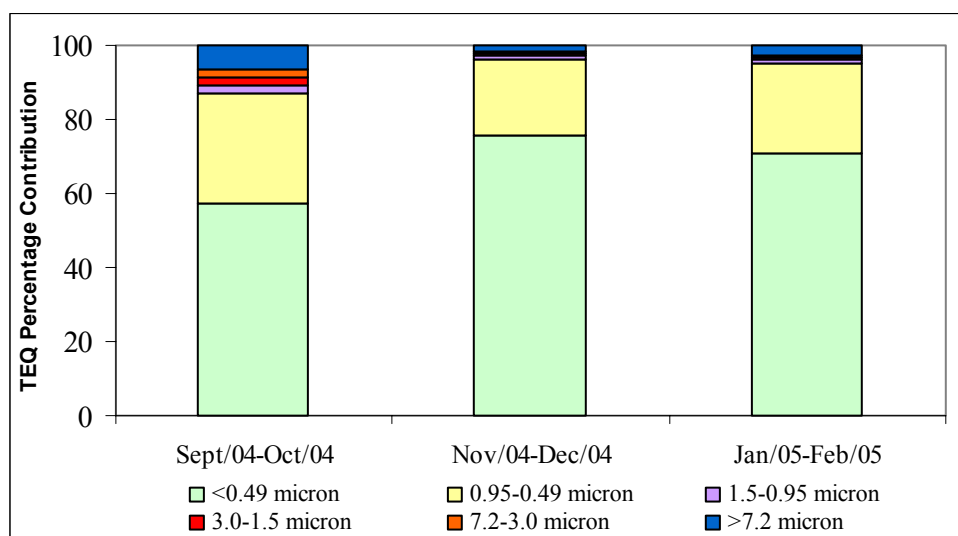


Figure 3.72 Σ Texas-TEQ Distribution by Particle Size

Total organic carbon (TOC), elemental carbon (EC), and total carbon (TC) concentrations are also summarized in Table 3.27. Significant concentrations of OC and EC were consistently found in particles with sizes >7.2 μ m, 0.95-0.49 μ m, and <0.49 μ m. EC, a characteristic constituent of fine particles and diesel emissions (soot), was consistently and predominantly found in particles <0.49 μ m.

Dry and Wet Deposition

First Dry and Wet Deposition Experiment

Monthly dry deposition samples were concurrently collected at Clinton Drive and Lang Road from December 2003 to April 2004 in four different sampling events: December/03-

January/04, January/04-February/04, February/04-March/04, and March/04-April/04. Results of this experiment are summarized in Table 3.28. Total dry deposition was observed to fluctuate from 305 to 376 and from 95 to 155 $\text{pg}/\text{m}^2/\text{day}$ at Clinton Drive and Lang Road, respectively. A *t*-test was conducted to establish if there is any statistical significant difference in the dry deposition process between these two sites. The test, carried out at an $\alpha=0.05$ significance level, demonstrated the existence of spatial variability of the dry deposition.

None of the lower chlorinated congeners were found in the dry deposition sample. In contrast, the higher chlorinated congeners, 1234678-HpCDD, 1234678-HpCDF, OCDF and especially OCDD were found to dominate the dry deposition profile. A contribution of up to 88% of the total dry deposition flux was attributed to OCDD, followed by 1234678-HpCDD with 10% (Figure 3.73). This result is in agreement with those obtained from the particle size distribution of associated dioxin samples where the stage containing the largest particles ($>7.2 \mu\text{m}$) was dominated by the higher chlorinated congener (in particular OCDD). Particles in this range (coarse mode particles) are generated mostly by mechanical processes such as grinding, wind, or erosion.

Results for the wet deposition sample collected (December/03-April/04) at Clinton Dr is listed in Table 3.29. A total wet deposition flux of $2,873 \text{ pg}/\text{m}^2/\text{day}$ was measured at that specific location. In the case of wet deposition, 123478-HxCDF, 123678-HxCDD, 1234678-HpCDD, OCDD, 2378-TCDF, 123478-HxCDF, 123678-HxCDF, 234678-HxCDF, OCDF were detected in rain. OCDD, as seen in dry deposition, was the most prominent congener with a contribution of 81% to the total wet deposition flux (Figure 3.74). It is noted that 2378-TCDF, a compound existing predominantly in the vapor phase, was detected in rain at a concentration of 99 fg/L .

**Table 3.28 Dry Deposition fluxes at Clinton Drive and Lang Road sites (December 2003-
April 2004)**

Figure 3.73 Dry Deposition Profiles at Clinton Drive and Lang Road Sites (First Dry and Wet Deposition Experiment)

F 3.73 (2)

Table 3.29 Wet Deposition Flux Clinton Drive (December 2003-April 2004)

Figure 3.74 Wet Deposition Profile at Clinton Drive (First Dry and Wet Deposition Experiment)

These results show that rain, while intermittent, is an important process that removes dioxins from the atmosphere.

The individual contributions of the observed wet and dry deposition fluxes of dioxins were combined to obtain a total deposition flux for the Houston area. To do this, the wet deposition flux was adjusted by accounting for the fraction of time during the sampling period with rain and the remaining fraction of time was used to adjust the dry deposition flux. This weighting allowed totaling the individual contributions of both deposition processes. An analysis of rain data at the monitoring station for the period sample revealed that precipitation of 0.01” or more occurred approximately 7% of the time. Therefore, a total deposition flux of 527 pg/m²/day was estimated for the Houston area. This value translated to a Texas-TEQ flux of 0.41 pg/m²/day.

Second Dry and Wet Deposition Experiment

Although dioxins and furans were detected in the dry and wet deposition samples, a number of congeners were not detected especially in the dry deposition. Therefore, a second experiment was undertaken from September/04 to February/05. In this case, co-located samplers were installed at Clinton Drive to increase the collection area. Similarly, bi-monthly sampling events were designed with the purpose of increasing the amount of sample to minimize non-detects. Thus, dioxin samples were collected in three bi-monthly events: September/04-October/04, November/04-December/04, and January/05-February/05.

Results of the second dry and wet deposition experiment are summarized in Table 3.30. For the dry deposition samples, the higher chlorinated congeners, 1234678-HpCDD, OCDF, 1234678-HpCDF, and OCDF were consistently detected. In the case of the wet deposition sample, more congeners were detected in comparison with the first deposition experiment. The

Table 3.30 Dry and Wet Deposition Fluxes at Clinton Drive (September 2004-February 2005)

congeners 2378-TCDD, 12378-PeCDD, and 123789-HxCDF were still missing from wet deposition. In both dry/wet deposition, OCDD followed by 1234678-HpCDD were, once again, identified as the major contributors to the total wet and dry deposition fluxes (Figure 3.75).

Similarly to the first wet and dry deposition experiment, the contributions of the wet and dry deposition fluxes of the second experiment were combined to obtain a total deposition flux. In this case, 4% of the total time sampled showed precipitation of 0.01 inches or more. A total deposition flux of 787 pg/m²/day was estimated for the Houston area. This value translated to a Texas-TEQ flux of 0.50 pg/m²/day.

Bulk Deposition

The combined contribution (bulk) of deposition of dioxins in the Houston area was studied concurrently with the second dry and wet deposition experiment (September/04-February/05) at the Clinton Drive site. The fluxes for the detected congeners are summarized in Table 3.31.

Table 3.31 Bulk Deposition Fluxes of Dioxins (pg/m²/day)

Congener	Bulk Deposition Flux
2,3,7,8-TCDD	<0.1
1,2,3,7,8-PeCDD	0.3
1,2,3,4,7,8-HxCDD	0.6
1,2,3,6,7,8-HxCDD	0.8
1,2,3,7,8,9-HxCDD	1
1,2,3,4,6,7,8-HpCDD	27
OCDD	207
2,3,7,8-TCDF	0.6
1,2,3,7,8-PeCDF	0.2
2,3,4,7,8-PeCDF	0.2
1,2,3,4,7,8-HxCDF	0.6
1,2,3,6,7,8-HxCDF	0.6
2,3,4,6,7,8-HxCDF	0.3
1,2,3,7,8,9-HxCDF	<0.04
1,2,3,4,6,7,8-HpCDF	4.0
1,2,3,4,7,8,9-HpCDF	0.2
OCDF	11
Σ(PCDD+PCDF)	255

Figure 3.75 Wet and Dry Deposition at Clinton Drive (Second Dry and Wet Deposition Experiment)

Table 3.32 Field Measurements during Runoff Sampling Activities

2378-TCDD and 123789-HxCDF were the only two congeners not detected in the bulk deposition sample. The profile was found to be dominated by the higher chlorinated congeners (Figure 3.76). A total bulk deposition flux of 255 pg/m²/day was measured at Clinton Drive. This flux translated to 0.71 pg TEQ/m²/day.

Load calculations from dry, wet, and bulk deposition will be presented in Chapter 4. A database of air sampling results is included in Appendix B3.

3.2.2.3 Runoff Sampling

Stormwater Runoff Samples

Table 3.32 provides a summary of field parameters measured during runoff sampling activities. Table 3.33 presents a summary of physical characteristics of storm water samples collected as of this writing. A summary of physical characteristics of soil/sediment samples collected during runoff sampling is included in Table 3.34.

Table 3.33 Physical Characteristics of Runoff Samples

Sampling Site	Date	TSS (mg/L)	TDS (mg/L)	TOC (mg/L)	DOC (mg/L)
SS-10	12/16/2004	66	NA	10.9	10.4
SS-13	01/13/2005	70.4	276	9.12	8.04
SS-9	02/07/2005	39.2	288	16.8	16.2
SS-15	02/24/2005	74.8	NA	9.19	9.04
SS-16	03/16/2005	<4.0	391	8.79	8.54
SS-14	03/22/2005	122	214	8.1	7.22
SS-8	05/29/2005	244	145	8.56	8.48
SS-7	07/14/2005	27.6	97	8.64	8.15

NA= Not available, sample volume not sufficient for analysis

Results for dioxins in Houston urban runoff samples in both dissolved and suspended (1 and 40 µm) phases collected at different locations are summarized in Table 3.35. Total TEQ

Figure 3.76 Bulk Deposition Profile

**Table 3.34 Physical Characteristics of Soil/Sediment Samples collected during Runoff
Sampling**

Table 3.35 Total Dioxin Concentrations in Runoff

concentrations varied between 0.019 and 0.491 pg/L, with an average of 0.255 pg/L. Seven of the eight samples (88%) exceeded the Texas WQS of 0.0933 pg/L. It is noted that the concentrations measured in runoff were at or below the levels measured in the in-stream water of the HSC.

The profiles in both phases (dissolved and suspended) were dominated by the higher chlorinated congeners OCDD, 1234678-HpCDD, and OCDF. Particularly for OCDD, this congener contributed over 82% of the total dioxin mass that was observed in both phases (dissolved and suspended) at all monitoring sites. The congener 2378-TCDD was detected only in the 1- and 40- μm suspended phases with average contributions of (mean \pm std) 0.018 ± 0.021 and 0.024 ± 0.040 % to the total dioxin mass, respectively. Dioxin profiles for the dissolved and suspended (1 μm and 40 μm) phases are illustrated in Figures 3.77 to 3.79.

The general distribution of the total dioxin mass between the dissolved and suspended phases is depicted in Figure 3.80. It is noted that approximately between 78 and 96% of the total dioxin mass was associated with the particulate phase (1 and 40 μm). This characteristic is similar to the distribution of the dioxin congeners in the particle and gas phases in the ambient air where over 70% of the total dioxin mass was detected bound to atmospheric particles. A comparison between the 1- and 40 μm suspended-phase samples showed that with the exception of sites SS-15 and SS-8, the total dioxin mass was mainly bound to fine particles (<1 μm). Particles in the size range (<2.5 μm) are known to be the result of anthropogenic activities such as diesel-fueled vehicle emissions.

Similar to the distribution of the total dioxin mass between the suspended and dissolved phases, the TEQ distribution is illustrated in Figure 3.81. On average, approximately 80% of the total TEQ (suspended + dissolved) was found associated with particulate matter. 12378-PeCDD,

Figure 3.77 Dissolved-Phase Profile of Dioxins

Figure 3.78 Suspended-Phase (1 micron) Profile of Dioxins

Figure 3.79 Suspended-Phase (40 micron) Profile of Dioxins

Figure 3.80 Distribution of Total Dioxin Mass in Houston Urban Runoff

Figure 3.81 Distribution of TEQ in Houston Urban Runoff

123789-HxCDD, and 23478-PeCDF were found as the major contributors to the total TEQ in the dissolved and suspended phases. The combined average contributions of these three congeners to the TEQs in the dissolved, and 1- and 40-mm suspended phases were 48.8 ± 2.2 , 48.2 ± 4.7 , and 47.9 ± 4.9 %, respectively. Likewise, 2378-TCDD was found contributing respectively an average of 7.6 ± 3.1 , 7.6 ± 3.5 , and 8.8 ± 6.8 % to the total TEQ.

Soil/sediment Samples

One sediment sample and up to five soil samples were collected from the drainage area of each of the runoff sites. The soil samples were representative of different land uses: forest, grass, urban, transitional, and residential. Transitional soil refers to a sample collected from a boundary between two defined land uses. Tables 3.36 and 3.37 provide a summary of the dioxin results obtained for sediment samples that were collected during runoff conditions and prior to runoff sampling in September-October/2004. As shown in Tables 3.36 and 3.37, sediment concentrations ranged from 0.27 (SS-16) to 2.75 ng TEQ/kg-dry wt (SS-10) under runoff conditions, and from 0.35 (SS-16) to 4.28 (SS-9) ng TEQ/kg-dry wt. for samples collected prior to runoff. Total TEQ concentrations for sediment samples collected during runoff conditions were additionally normalized by TOC content. Concentrations fluctuating from 18.4 (SS-8) to 261 (SS-9) ng TEQ/kg-oc were determined. It was noted that while 2378-TCDD was found below the detection limit in the set of sediment samples collected during runoff conditions, this same congener was detected in only one of the soil samples collected prior to runoff sampling (i.e., SS-9) (Table 3.37) at a concentration of 0.33 ng/kg-dry wt. This concentration of 2378-TCDD represented a contribution of ~8% to the total TEQ.

The individual contribution of each congener to the total dioxin sediment dioxin mass

Table 3.36 Dioxins in Houston Urban Sediment during Runoff Conditions

Table 3.37 Dioxins in Houston Urban Sediment Prior to Runoff Sampling

concentration both during runoff sampling and prior to runoff sampling is depicted in Figure 3.82. The higher chlorinated congeners were found to be the major contributors to the total dioxin mass concentration. The combined contribution of 1234678-HpCDD, OCDD, 1234678-HpCDF, and OCDF to the total dioxin sediment dioxin mass concentration at all of the sites was found to be >95%. Similarly, 2378-TCDD was found to contribute with <0.3% to the total dioxin mass concentration. The profiles shown in Figure 3.82 resemble the profiles found for dioxins in ambient air; mainly, the higher chlorinated congeners were the most abundant congeners.

Tables 3.38 and 3.39 summarize the dioxin concentrations obtained for different types of soil (forest, grass, residential, urban, and transitional) in samples collected during runoff conditions and prior to runoff sampling, respectively. Concentrations of 0.82 ± 0.80 , 1.18 ± 1.34 , 1.19 ± 0.93 , 0.92 ± 0.37 , and 2.73 ± 5.67 ng TEQ/kg-dry wt. were measured for the aforementioned types of soil, respectively. The congener 2378-TCDD was detected only in the following soils and sites: Grass (SS-8), Residential (SS-16), Urban (SS-15), and Transitional (SS-16), at concentrations of 0.94, 0.51, 0.19, and 0.51 ng/kg-dry wt., respectively. Profiles for each type of soil are illustrated in Figures 3.83 through 3.87. Similar to runoff and sediment samples, the profiles were dominated by the higher chlorinated congeners, especially OCDD.

A database of storm water sampling results reported by PSC Philips Analytical Laboratory and of the soil/sediment results reported by Pace Analytical is included in Appendix B4.

3.2.3 Flow Measurements in Support of Modeling Activities

As mentioned in Section 3.1.3, flow measurements were collected at least once per day during the course of a 1-week period using the RiverCat. Each time flow was measured, a minimum of 4 different flow readings was collected to assure data of adequate quality. In

Figure 3.82 Fraction Contribution of Dioxins in Houston Sediment during Runoff and Dry Conditions

F 3-82 (2)

Table 3.38 Dioxins in Houston Soil collected during Runoff Conditions

Table 3.39 Dioxins in Houston Soil Prior to Runoff Sampling

Figure 3.83 Fraction Contribution of Dioxins in Houston Grass Soil during Runoff Conditions

Figure 3.84 Fraction Contribution of Dioxins in Houston Forest Soil during Runoff Conditions

Figure 3.85 Fraction Contribution of Dioxins in Houston Residential Soil during Runoff Conditions

Figure 3.86 Fraction Contribution of Dioxins in Houston Transitional Soil during Runoff Conditions

Figure 3.87 Fraction Contribution of Dioxins in Houston Urban Soil during Runoff Conditions

addition, flow measurements were collected under a variety of tidal conditions, including rising and falling tides. Tide elevation data were collected with either a YSI probe or downloaded from the NOAA website. The YSI tide elevation data were recorded at 5 minute intervals and the NOAA data were reported at 6 minute intervals over the 1-week period. These data were then transformed into either 15-minute or 18-minute time intervals to simulate the change in tide elevations. The tide elevation data were broken down into several periods (15, 30, 45, 60, 75, 90 minute, etc.). This was done, for example, by subtracting the tide elevation at 15 minutes from the tide elevation at 0 minutes, etc.

Since several flow measurements were taken during one sampling period, the flows were averaged together after being viewed and checked for quality in the SonTek RiverSurveyor Software V4.30. The average flows for each sampling period are shown in Table 3.40. The time shown in Table 3.40 corresponds to the average time of the day that the flow measurements were taken.

Data from each flow event were matched to the corresponding tidal elevation data. A linear regression was performed using the data analysis package in Excel to find the best relationship between measured flow and the change in tidal elevation. The regression results (R^2 , intercept and X1 variable) for each flow sampling location are shown in Table 3.41. These data were then used to form an equation to predict the flow at a change in tide elevation as follows:

$$Q = a + b * dt(T) \quad (3.8)$$

where Q = Predicted Flow (m^3/s), a = Y-Intercept (m^3/s), b = X- variable (m^2/s), and $dt(T)$ = the change in tidal elevation for a given time period T (m).

The predicted flows were then plotted at each sampling location along with the measured and average flows (Figure 3.88). The figures show that the predicted flows are in good agreement

Table 3.40 Average Flows for Each Event

T 3-40 (2)

T 3.40 (3)

Table 3.41 Regression Results

Figure 3.88 Measured and Predicted Flow in the HSC

with the measured and average flows.

Since the RiverCat requires at least 3 feet of water to measure a representative flow reading, the data from sampling location 11273 was not processed due to the shallow water levels during sampling times (flows not included in Figure 3.88).

A summary of the regression outputs for each of the stations is included in Appendix D.

3.3 COLLECTION OF SEDIMENT DATA TO SUPPORT MODELING ACTIVITIES

While data on the sources of dioxins and furans are limited, it is expected that a substantial portion of the inputs to the Houston Ship Channel (HSC) is associated with particulate matter in runoff flows. This analysis provides estimates of the annual runoff loads of Total Suspended Solids (TSS) and Volatile SS (VSS) from tributaries to the HSC. These loads may be significant sources of dioxins to the HSC. Also included in this section is an analysis of sediment accumulation and removal from the HSC. In the analysis the loads removed from the HSC through dredging are calculated and compared with source estimates.

3.3.1 Background

Sediment loads to the channel have been studied in the past and measurements continue to be made. For example, the US Army Corps of Engineers (1987) analyzed sediment loads as part of its studies for improving the channel. Estimates were made by the Corps to determine the changes in sediment accumulation as a result of making the channel deeper and wider. As part of a major wastewater study for the City of Houston (1988), Pate and Espey, Huston & Associates (EH&A) analyzed sediment sources and removal from the HSC. The 1988 study of sources employed data from Winslow and Associates (1986) as well as the Corps and other sources. The 1988 study calculated the TSS and VSS loads by two methods. One was based on tributary

sampling data and the other was based on estimates of individual components such as load per unit area for various land use types.

Loads to the HSC in metric tons per year, from the area including Greens Bayou and above were:

	TSS	VSS
Tributary sampling method	318,500	55,500
Individual Component method	142,700	45,590

The load by the tributary method for the watershed from Greens Bayou to Morgan's Point

was

	90,950	15,860
--	--------	--------

thus,

Total tributary method	409,450	71,360
------------------------	---------	--------

Total Individual component method	233,650	61,450
-----------------------------------	---------	--------

As can be seen, the tributary method gives higher loads than the individual component method.

This same City of Houston (1988) study also reviewed the Corps dredging records and found that on average the solids removal from Morgan's Point and up was 431,000 metric tons per year. That is roughly equal to the 409,450 tons per year obtained using the tributary sampling method estimate. However, there are a number of points considering the distribution of TSS and VSS sources that were considered in the 1988 analysis. Accordingly, the relevant portions of this analysis are included with this document as Appendix E.

In addition to the above mentioned resources, the Galveston Bay National Estuary Program commissioned a study to estimate nonpoint source loads to Galveston Bay (Newell et al., 1992). The study assembled event mean concentration (EMC) values for a variety of parameters,

including TSS. Defined as the total constituent mass divided by the total runoff volume, the EMC is a parameter used to represent the flow-weighted average concentration of a given parameter during a storm event. It is usually measured by analyzing flow weighted composite samples of runoff. VSS EMC information was not included in the GBNEP report. Table 3.42 presents the TSS EMC values used in the GBNEP analysis:

Table 3.42 EMC TSS Values for Various Land Uses

Land Use Category	TSS EMC (mg/L)	Land Use Category	TSS EMC (mg/L)
High Density Urban	166	Forest	39
Residential	100	Wetlands	39
Agricultural	201	Water	0
Open/Pasture	70	Barren	2200

Source: Newell et al., 1992

Using the above EMC values, land use coverages obtained from a LANDSAT image obtained in November 1990, and runoff volume estimates using the Soil Conservation Service (SCS) curve number method, three pollutant loading rates were determined for sub-watersheds defined in the study. Loading rates were determined for an "average" precipitation year, a wet year, and an individual average size storm. The estimated loads to the Houston Ship Channel are presented in Table 3.43. The study estimated average TSS load of 217,000 metric tons per year, somewhat lower but in the same range as calculated in the 1988 City of Houston study.

The *Storm Water Joint Task Force (JTF)*, which is made up of the City of Houston, Harris County, Harris County Flood Control District, and TxDOT presently conducts storm water runoff sampling to obtain EMC values for a variety of parameters including TSS. The JTF members are

Table 3.43 TSS Loads to the Houston Ship Channel from Newell et al. (1992)

**Table 3.44 Summary of TSS EMC Data from Storm Water Management Joint Task
Force**

joint permittees who have a federally issued municipal separate storm sewer system (MS4) National Pollutant Discharge Elimination System (NPDES) storm water permit. The permit has required the JTF to monitor total suspended solids (TSS) on a quarterly basis since 1998. The TMDL project team has requested all TSS EMC data from the JTF along with drainage area boundaries and sampling sites. Table 3.44 presents a summary of the TSS EMC information. There is considerable variation with the means of the EMC values as would be expected from runoff data. Means of TSS EMC range between 12 mg/L and 647 mg/L. The overall average runoff event EMC value is 144 mg/L, which is within the range of EMC values used in Newell et al. (1992).

3.3.2 New Sediment Source Calculations

Since these earlier studies were performed, there has been considerable new data collected and some changes in the watershed. To produce updated information, the basic procedure was to analyze the relationship between bayou flow and TSS-VSS concentrations at available flow gages. The resulting relationships were used to estimate loads from the entire watershed, including the unaged areas.

The USGS stream flow gages employed are shown on Figure 3.89. These gages recorded hourly flow observations for the period October 1991 to September 2003, although there are periods with missing data at some gages. Samples for TSS and VSS were collected by several agencies in close proximity to the gaging stations. In rare cases, samples were collected by the USGS at the gage itself, but more often, samples were collected by either the TCEQ or one of the City of Houston agencies at stations at or nearby the flow gaging station. To obtain the best

Figure 3.89 Locations of USGS Gages and Sampling Stations

relationship with flow, regressions were produced using all available data at stations in close proximity to the flow measurements. The adjacent stations are also shown in Figure 3.89.

Figures 3.90a-e show the regressions of log flow against TSS. The regressions that have slopes that are significantly different from zero at the 95% confidence level are labeled as significant. Note that all of the plots show a great deal of scatter, reflecting grab sample data where the limited number of higher flow observations are subject to major uncertainties including whether the sample is a first-flush or a trailing limb observation. Even with a low r^2 and excessive scatter, the data indicate a relationship between flow and TSS. Even though most of the stations have a significant correlation between TSS and flow, several factors must be kept in mind. One is that the low flow end of the flow distribution for most stations is maintained by wastewater flow. Another is that the Buffalo Bayou stations are affected at higher flows by Barker and Addicks Reservoirs that allow settling of TSS so that it is not uncommon for the highest flow observations to have some of the lowest TSS concentrations. Other stations that do not show a relationship are Sims Bayou at Telephone Road (possible tidal influence) and Lake Houston (flow from spillway rating curve but concentrations obtained from Lake near dam). All the remaining gages exhibit statistically significant albeit noisy relations.

A similar but even noisier pattern is shown with the log flow versus VSS observations in Figure 3.91a-d. In general, there tend to be fewer VSS observations than TSS, and there also seems to be somewhat more variability in the data. Because these VSS data are limited, a tabulation was made of the paired TSS and VSS observations. Overall it was found that VSS averaged 27% of the TSS values, and this was used in the calculations that follow.

Figure 3.90 Relationship between TSS and Flow

F 3.90 (2)

F 3.90 (3)

F 3.90 (4)

F 3.90 (5)

Figure 3.91 Relationship between VSS and Flow

F 3.91 (2)

F 3.91 (3)

F 3.91 (4)

The illustrated regression relationships while useful do not capture some key points. For example, it is typical in a runoff event for the first part of the hydrograph to exhibit higher concentrations associated with runoff, while the declining limb of the hydrograph typically exhibits lower concentrations. This basic relationship is ignored in the correlation approach. However, to take that into account would require the development of a more sophisticated runoff model.

To calculate the overall TSS and VSS loads to the HSC, a multi-step analysis was performed. The first step was the regressions with hourly flow described above. These regressions provided a means to estimate the sediment load from flow data.

Next, the flow distributions for each of the gages were produced to examine the effects of different watershed characteristics. Figure 3.92 shows the flow distributions from all of the gages considered, after normalizing by the watershed area of each gage. The first point to be noted from this figure is that gages that are tidally influenced only report results when the flows are high enough to remove the tidal effect. In this case, the flow distributions are offset upward. This is the case with Greens Bayou at Ley Road that shows markedly higher flows per unit area than the other bayous. Another point is that the low flow values for many of the streams are affected by wastewater discharges and never get below set values. This is the case to varying degrees with most of the bayous, with Brays Bayou being the most affected. The only bayou that appears to show no upstream wastewater discharge effect is Vince Bayou.

The flow gage and concentration measurements exist for only part of the HSC watershed. To calculate the TSS and VSS loads for the entire HSC, a common procedure is needed. The modeling was developed as follows:

Figure 3.92 Distributions Of Flow Normalized W.R.T. Drainage Area

First, since the goal was to analyze TSS and VSS loads and the point source flows contributed little in the way of these parameters and are monitored separately, it was deemed appropriate to use the Vince Bayou unit flow distribution, as it appears to be the one that is least affected by point source discharges.

Second, the average slope of the significant TSS regression line for the non-*Buffalo Bayou* streams was used. The stations on *Buffalo Bayou* have statistically significant but flatter slopes that reflect the reservoir effect in a part of their watersheds. For this analysis the decision was made to represent the area of the gages below the reservoirs in the same way as other areas, and the reservoirs themselves with a different approach described below. Figure 3.93 shows all the regressions for TSS plotted versus a normalized flow (flow/watershed area). It can be seen that the slope of the TSS-log Q relation is generally similar for most of the streams, and somewhat lower for the *Buffalo Bayou* stations that are affected by the upstream flood reservoirs. The dashed line shown is the average slope of the regressions for the stations without upstream flow regulation (excluding *Buffalo Bayou* stations) and the *Greens Bayou* at *Ley* which has tidal effects.

Annual average TSS and VSS loads for locations along the channel were then calculated and presented in Table 3.45. These were done using the watershed areas of each of the major tributaries, the unit flow distribution without point sources obtained from the *Vince Bayou* gage refined to one percentile intervals at the high flow end, and the average concentration-flow regression (dashed line in Figure 3.93). The inputs from *Lake Houston* were taken from the 1988 study, which were in turn taken from a 1982 publication by *Baca, Bedient and Olson* (*Baca et. al., 1982*). The *Barker* and *Addicks* reservoir watersheds were average inputs based on this *Lake*

Figure 3.93 Regression Lines of TSS Against Normalized Flow

Table 3.45 Estimated Annual TSS and VSS Loads to the Houston Ship Channel

Houston rate. This is probably an underestimate because the settling time in these flood control reservoirs is much less than that of Lake Houston.

Also included in Table 3.45 is an estimate of the point source TSS and VSS loads. This estimate is conservative as the actual concentrations tend to be lower than those assumed. The annual average TSS load shown in Table 3.45, 189,997 metric tons/year, is somewhat lower than those computed in the 1988 study (233,650 - 409,450 mt/year) or the 1992 Galveston Bay NPS study, 217,000 mt/year. Given the inherent noise in runoff data, the limited amount of data actually available, and differences in calculation methodology, the differences are to be expected. It is also possible the sediment loads themselves may have reduced over time as the rate of development in the area has slowed from the extreme pace of the 1960s and 70s, and erosion control has become more of a priority in construction work. The changes over time are also addressed in the section dealing with dredging loads. Another factor to consider is the calculation procedures. In August 2000, the USGS published an analysis of over 3,200 paired TSS and suspended sediment concentration (SSC) data and concluded that SSC is a more reliable measure of solid phase material in natural waters than TSS. This finding was based upon the following observations (Grey, et. al., 2000):

SSC is determined from the entire water sample whereas TSS is determined from a sub-sample collected in inconsistent and unrepresentative ways from the original sample. This introduces significant errors and frequently yields underestimates of solids content;

- SSC values tend to be larger than their paired TSS values as the percentage of sand-size material exceeds about a quarter of the mass of sediment in the sample,

- TSS values for paired samples tend to be more equal for samples with finer solids (< 0.062 μm);
- the tendency for SSC values to exceed their paired TSS values has important ramifications for computations of suspended solid-phase discharges; those computed using TSS data will often underestimate solid-phase discharges. This is particularly true for sites when the percentages of sand-size material in the water samples exceed about a third of the total and where concentrations and percentages of sand-size material in transport increase with flow;

Review of the literature indicates that the TSS method originated as an analytical method for wastewater, presumably for samples collected after a settling step at a wastewater treatment facility. The results of this evaluation do not support use of the TSS method to produce reliable concentrations of solid-phase material in natural-water samples. The TSS method is being misapplied to samples from natural water.

In fact, Grey et al., (2000) state:

“The TSS method, which was originally designed for analyses of wastewater samples, is shown to be fundamentally unreliable for the analysis of natural-water samples. In contrast, the SSC method produces relatively reliable results for samples of natural water, regardless of the amount or percentage of sand-size material in the samples. SSC and TSS data collected from natural water are not comparable and should not be used interchangeably. The accuracy and comparability of suspended solid-phase concentrations of the Nation's natural waters would be greatly enhanced if all these data were produced by the SSC analytical method.”

The USGS findings strongly suggest that the use of historical TSS will under-predict the true sediment load to the HSC. The degree of under-prediction appears to depend upon the fraction of particles in the load of sand or larger size. As the soils in the study area have a high silt and clay content, with relatively little sand, the error in using TSS data may not be extreme but still needs to be considered. The dioxin TMDL QAPP calls for the use of SSC to characterize the sediment in runoff events. These data will be reviewed to further refine our estimates of sediment load to the HSC.

3.3.3 Sediment Accumulation and Removal

Dredging records of the Galveston District, US Army Corps of Engineers, were retrieved and analyzed to establish the long-term pattern of sediment accumulation and removal. This section describes the data and analysis methods. The dredging records are an especially valuable data source for sediment loads as they reflect the great bulk of sediment that enters the system, concentrated into a small place. While the channel bottom is a small part of the total drainage area, it is by far the deepest and most conducive to settling. Areas to the side of the channel such as the side bays are not dredged and have exhibited no significant sediment accumulation.

The Houston Ship Channel (HSC) is a federal navigation project, and the Corps is charged with the responsibility to maintain the channel at its authorized depth for safe navigation. To do this, the Corps makes regular hydrographic surveys to track the situation. As sediments accumulate and depths are decreased, the Corps dredges the appropriate reaches and places the material in designated areas. The amount of material actually removed down to the specified dredging depth can be estimated using the difference between before dredging and after dredging

(BD and AD) surveys. Records of these surveys, and the in situ material removed from the HSC bottom, are the basis for this analysis.

Figure 3.94 shows the channel distances in kilometers from Morgan's Point, and the major landmarks in the HSC. Figure 3.95 illustrates the dredging reaches and the years when maintenance dredging contracts were completed. The period 1968 through 2003 was used. The 40 ft project depth by 400 ft width over most of the channel was completed in 1964, and work on the 45 ft x 530 ft project began at the end of the 90s, but has been excluded from the analysis. Only contracts marked as maintenance dredging were employed in the analysis. Each dot in Figure 3.95 is an end point to a reach. Between each dot a volume of material was removed during the specified year.

The first step in the analysis was to compute an accumulation rate for a channel reach between two successive dredging operations. This was done by dividing the volume of material removed in dredging a reach by the channel bottom area of the reach, to get an overall average depth of sediment removed in feet. The calculated value was then divided by the time between dredging to get a rate for the reach in feet per year. The volume of material accumulated between the two operations is the sum of the over-dredged volume of the first operation and the prescribed volume of the second operation. This accounts for differences in overdredging amounts from one cycle to the next. There is some inaccuracy in the accumulation rate because the dates of the historical dredging contracts are only recorded to the year. Figure 3.96 shows the individual rate calculations over the period of record along the channel from Morgan's Point to the most upstream Turning Basin. Each value is plotted at the center of the reach, and further identified by the decade in which the work was performed. The values for the 70s include some dredging

Figure 3.94 Map of Houston Ship Channel

Figure 3.95 Maintenance Dredging Contract Reaches and Periods

Figure 3.96 Sediment Accumulation Rates in the Houston Ship Channel

performed in the late 60s while the values for the 90s include some dredging performed in the early 00s.

The highest accumulation rates occur at both ends of the channel. There also appears to be a difference in accumulation rates by decade. To further explore this, Figure 3.97 shows the average rate for each 5 kilometers of channel for each decade in the dredging record. In averaging, the exceptionally high value at about 24 km in the 90s group was excluded. This value was calculated with 2003 data (see Figure 3.95) of a short reach that may not be representative. From this it appears that in most areas the accumulation rates were markedly higher in the 1970s than in either the 80s or 90s. The reasons for this difference are not clear, but a possible reason may be higher growth rates in the metropolitan areas in the 60s and 70s compared to the last two decades in the twentieth century. With more growth and development there would be greater exposed soil for erosion during rains. Because of the apparent difference, the analysis for present and future conditions will use the data from the 80s and 90s, and not the higher rate data from the 70s.

The higher sediment accumulation rates in the upper channel may be due to the fact that the most upstream Turning Basin, being a relatively wide spot that receives drainage from a substantial portion of the basin, is a natural sediment accumulation point. It has been referred to as the stormwater settling basin for Houston. Further down the HSC the dredging contracts cover a longer reach of channel relative to the drainage area so the accumulation rate is lower. The reasoning for the upper channel high rates do not apply to the high accumulation rates in the lower channel, as these areas have a much smaller drainage area and thus much less input from runoff. This higher rate may be due to a combination of local erosion and resuspension of

Figure 3.97 Average Sediment Accumulation Rates by Decades

sediments from the smaller side bays in this reach, and the effect of sediments suspended by wind waves in Galveston Bay that are carried into the confined and sheltered waters of the upper channel during flood tides.

The dredged volume in cubic yards was converted to a mass of solids that can be compared with the tributary loads. Table 3.46 is a summary of sediment data collected in early August 2002 and late May 2003 at a number of stations in the HSC. The left part of the table contains the data for each station, and the right part groups data by channel reach. The upper channel sediments tend to have a higher organic content and a lower bulk density than the lower channel stations. These parameters are reflected in the solids removal calculations in Table 3.47. The basic procedure is to get the total and volatile solids considering the higher organic content and lower bulk density of the upper channel sediments.

As solids, both mineral and organic, settle into the HSC, there is a process of decay in which organic matter is mineralized anaerobically. In 1988 this was estimated at about 4,000 metric tons from Morgan's Point up. See Appendix E, Table 5.2.2-4, for calculation methods.

3.3.4 Solids Balance

In comparing the sediment source in Table 3.45 and the sediment removed in Table 3.47, in the channel down to Morgan's Point there is considerably more material removed than supplied. This is shown in Table 3.48. However, the amount of solids input to the upper channel is much closer to that removed in dredging when compared to the lower channel. There are several factors that contribute to this difference. In the lower channel, there is a relatively small drainage area to contribute sediment, but large dredging volumes. One of the sources of the lower channel sediment accumulation is likely to be the contribution of Galveston Bay sediments

Table 3.46 Sediment Data from 2002 and 2003 Intensive Surveys

**Table 3.47 Estimated Annual Volume and Mass of Solids Accumulation in Houston Ship
Channel**

Table 3.48 Sediment and Organic Balances

	Channel reach		Total
	Turning Basin to Greens Bayou	Greens Bayou to Morgan’s Point	
Sediment			
TSS Sources (mt/yr) ^a	119,298	70,699	180,997
TSS Sinks (mt/yr) ^b	157,220	495,355	652,575
Balance	(37,922)	(424,656)	(462,577)
Source % of Sink	76%	14%	29%
Organics			
VSS Sources (mt/yr) ¹	33,960	19,856	53,816
VSS Sinks (mt/yr) ²	10,267	15,840	26,106
Balance	23,694	4,016	27,710
Source % of Sink	331%	125%	206%

^a Sources as calculated in Table 3.45

^b Sinks as calculated in Table 3.47. VSS Sinks include organics in-situ decay, values from 1988 Study.

suspended by wind waves that are carried above Morgan's Point during flood tides and can settle in the more protected waters. Another source in this reach is erosion of the shorelines, particularly on the shallow side bays. Moreover, some of the material in larger rain events from the upper channel watershed would be carried into the lower channel before settling.

Another dimension that may be playing a role is the difference between TSS and SSC. The data do not exist that would allow quantification of this difference, but it would not be surprising to find that an analysis that captures the larger particles more completely would indicate a substantially higher runoff load. This would tend to make the sources and sinks in closer agreement.

With the organic load, VSS source and sink, the calculated sources exceed the amount removed by a substantial margin. One possible reason is that the estimate of organic decay in the sediments is low. While the runoff solids average 27% VSS, the channel sediments have only about 3% of the dry weight as volatile material. A higher estimate of biological decay of organic matter would bring the source and sink values closer together.

CHAPTER 4

DATA ANALYSIS

4.1 SITE-SPECIFIC BIOACCUMULATION FACTORS AND WATER QUALITY TARGETS

4.1.1 Development of Site-specific Bioaccumulation Factors

The BAF is defined by the USEPA (2003) as the ratio (in liters per kilogram of tissue) of the concentration of a chemical in the tissue of an aquatic organism to its concentration in water, in situations where both the organism and its food are exposed and the ratio does not change substantially over time. As is typical, in this project only the dissolved concentration in water, rather than the total water concentration (including the chemical associated with suspended particulate and colloidal material), was used in calculating the BAF.

$$BAF = \frac{C_{tissue}}{C_{water,diss}} \quad (4.1)$$

Because BAFs have been shown to vary in direct proportion to the lipid content of the tissue (USEPA 2003), the lipid-normalized tissue concentration is often used in lieu of the total tissue concentration in calculating a BAF. These BAFs are called lipid-normalized BAFs or BAF_l

$$BAF_l = \frac{C_{tissue} / F_{lipid}}{C_{water,diss}} \quad (4.2)$$

where F_{lipid} is the lipid fraction of the tissue by weight.

BAFs for catfish and crabs were calculated for each of the paired water and tissue samples collected in the spring, summer, and fall seasons from 2002 through 2004. Each fish or crab sample was a composite tissue sample from 3 to 5 animals. Because lipid normalization increased the variability in the BAF relationships, and the lipid measurement method used was imprecise, all BAFs were based on whole tissue concentrations and were not lipid-normalized. An effort was made to collect the fish, crab, and water samples from a given station on the same day. However, in practice this proved difficult and the samples from various media for a station were often collected several days apart.

BAFs⁴ for PCDD/F congeners measured in 111 catfish and water samples from the HSC system are shown in Figure 4.1, and those measured in 106 blue crab and water samples are shown in Figure 4.2. BAFs varied widely both among and between congeners. The individual log BAF patterns are similar between catfish and crabs, indicating the importance of chemical properties in controlling BAFs. However, on average the BAFs for crabs were lower than those in fish for most congeners. For the dioxin congeners, a systematic decline in BAF with increasing hydrophobicity (as indicated by size and chlorination) was evident, which is consistent with independent observations that for very hydrophobic chemicals such as the larger PCDD/Fs, dietary uptake efficiencies decline with increasing hydrophobicity (Opperhuizen and Sijm 1990; Gobas et al. 1988). This pattern was not evident to the same extent in the furan congeners.

More importantly, and for a given congener, the log BAFs vary over a wide range. Possible factors accounting for the variability include seasonality, spatial factors, tissue properties

⁴ BAFs were calculated as the ratio of the tissue concentration to the dissolved concentration for each individual data point.

Figure 4.1 Distribution of Individual log BAFs for Catfish from the HSC

Figure 4.2 Distribution of Individual log BAFs for Crabs from the HSC

(species, size, lipid content, etc), water properties (salinity, temperature, TOC, etc), and random error due to the fact that many of the reported values were non-detects or between the detection limit and the reporting limit (Non-detects were assumed equal to half of the detection limit).

Preliminary non-parametric correlations between tissue concentrations of 2378-TCDD and a number of explanatory variables are summarized in Table 4.1. Overall, there are few significant correlations between 2378-TCDD concentrations and other factors. For example, concentrations in catfish and crabs are correlated to the lipid content but the correlation coefficients are not very large. Table 4.2 summarizes correlation coefficients between log BAF for 2378-TCDD and some explanatory variables. It can be seen in Table 4.2 that while tissue lipid content did not explain a significant amount of variation in the tissue concentrations, BAFs did exhibit a small but statistically significant relationship with a measure of the “fatness” of the fish: the average weight to length ratio. Seasonal variations in BAF were not statistically significant. While the catfish species sampled included some gafftopsail catfish, blue catfish, channel catfish and black bullheads among the hardhead catfish, there was no significant variation in BAF among species.

In general, BAFs measured at less contaminated sites with low PCDD/F concentrations tended to be higher than those from sites with high water concentrations (Figure 4.3). This may be explained by the fact that fish are exposed to PCDD/F concentrations that vary over several orders of magnitude. Spatial variation in PCDD/F concentrations spans several orders of magnitude in the HSC system. Fish and crabs are of course mobile, and most leave the system for deeper waters between late November and March (USFWS 1983). Also, fish and crabs accumulate PCDD/Fs from direct exposure to PCDD/Fs in sediments and water, and from their

diet of multiple prey species residing in those media. Tissue concentrations are expected to be substantially less dynamic than the concentrations in other media, resulting in a relative

**Table 4.1 Spearman Correlation Coefficients for Concentrations of 2378-TCDD in
Tissue and some Explanatory Variables**

**Table 4.2 Pearson Correlation Coefficients for log BAFs of 2378-TCDD and some
Explanatory Variables**

Figure 4.3 Variation in Catfish BAF with Dissolved Concentration in Water

“flattening” of the tissue:water concentration ratio and the observed decline in BAF with increasing dissolved concentration.

The next section describes the detailed methodology for estimating BAFs for the 17 congeners.

4.1.1.1 Estimation of BAF for 2378-TCDD

As a first step, regressions of 2378-TCDD concentrations in tissue and water were completed in order to establish the most appropriate regression model for estimating BAFs for the remaining congeners. Since dioxins and furans are members of a class of chemical compounds known as nonpolar hydrophobic organic compounds (HOCs), they partition preferentially into lipid matter. It is often found that the variability of BAFs or BCFs between species and individuals for HOCs is reduced if they are first normalized by the tissue lipid content (USEPA, 1995). The lipid-normalized bioaccumulation factor (BAF_l) is defined by Equation (4.2).

Combining Equations (4.1) and (4.2), the concentration of an HOC in tissue of biota can be predicted using:

$$C_b = BAF_l * F_l * C_w \quad (4.3)$$

The USEPA (1995) advises that BAFs and BCFs (bioconcentration factors) for organic compounds should be calculated from lipid-normalized tissue concentrations and dissolved concentrations in water.

BAFs are also typically adjusted to correct for chemical bioavailability. The water concentration of a chemical includes portions associated with suspended and colloidal particles and dissolved organic matter, as well as portions truly dissolved in water. However, only the freely dissolved concentration is bioavailable for uptake across gill membranes or external body

surfaces (USEPA, 1995). It is likely that the dissolved data collected using the high-volume sampling technique correspond to the freely dissolved concentrations, as the colloidal fraction most probably passes through the XAD-2 resin.

In order to determine the strongest partitioning relationship for the HSC data (the USEPA (1995) suggest using either freely dissolved or total water concentrations), an analysis of correlation between the different measurements in water and tissue was performed and is included in Table 4.3. As indicated in Table 4.3, the strongest partitioning relationship was observed between measured 2378-TCDD in not lipid-normalized tissue and the dissolved concentrations. Thus, BAFs were calculated using regressions between tissue and dissolved concentrations.

Dissolved water concentrations and catfish data for 2378-TCDD were analyzed using different regression methods to determine the best-fit BAF. In general, linear regression is

Table 4.3 Pearson Correlation Coefficients between Water and Catfish Concentrations of 2378-TCDD

		2378-TCDD dissolved	2378-TCDD in water-total
2378-TCDD in catfish	Pearson coefficient	0.434	0.188
	Sig. (2-tailed)	0.000	0.087
	N	84	84
2378-TCDD in catfish-lipid	Pearson coefficient	<i>0.244</i>	0.349
	Sig. (2-tailed)	0.026	0.001
	N	84	84

Pearson coefficients in bold indicate that the correlation is significant at the 0.01 level (2-tailed).
Pearson coefficients in italics indicate that the correlation is significant at the 0.05 level (2-tailed).
 Shading indicates the strongest correlation.

preferred because it would yield a BAF directly from the slope. However, since the HSC data do not meet the assumptions of constant variance and normality of the residuals for the Ordinary

Least Square Method (OLS), and because there are outliers due to the various reasons cited earlier, alternative robust linear regression models were investigated. These alternative methods for regression include Robust Least Trimmed Squares (LTS)⁵, Robust MM Regression, and Iterative Weighted Least Squares (WLS)⁶. Robust methods help to control the disproportionate influence of outliers that could well be legitimate data points (Helsel and Hirsch, 2002). In addition, a curve representing the average log BAF from individual measurements was also included in the analysis.

Figures 4.4 and 4.5 present the HSC 2378-TCDD data as well as the best-fit lines derived using the previously mentioned methods. A summary of the test statistics for each of the regression models for both catfish and crabs is included in Table 4.4. Two non-linear regressions (power and polynomial as indicated in Figures 4.4 and 4.5 and Table 4.4) were also evaluated for comparison purposes. As can be seen in Figures 4.4 and 4.5, there was a lot of variance in the relationships. It is noted that a simple linear BAF regression between tissue concentrations and dissolved concentrations does not work well to explain the data collected in the Houston Ship Channel. The linear BAFs have low r^2 and F values and high standard errors. The polynomial and power (log-transformed data) models seem to better represent the data but they have the disadvantage that a BAF cannot be directly derived from the equations. This might suggest the need for developing a multivariate regression model or it might indicate that the congener-specific BAF approach cannot be used for the HSC.

⁵ See [Appendix F](#) for a brief description of the used robust regression methods.

⁶ Other methods such as Reduced Major Axis (also known as Geometric Mean Regression) and Least Median of Squares were also considered. However, results are not included due to the difficulty in obtaining test statistics to compare with the other methods employed in this analysis.

- Figure 4.4** **Partitioning of 2378-TCDD between Catfish and Dissolved Phase in the HSC**
Figure 4.5 **Partitioning of 2378-TCDD between Crabs and Dissolved Phase in the HSC**

**Table 4.4 Summary of Regression Statistics and Parameters for Tissue-Water
Relationships**

It is noted that non-detects were assumed to be equal to half of the detection limit.

Because the detection limits were variable, this should not have introduced a large bias towards a single value. It is noted, however, that those values have high uncertainty associated with them. The BAF regressions for 2378-TCDD presented earlier were compared to those completed assuming non-detects as zeros but no significant differences were evident and the relationships were not stronger.

To aid in selecting the linear regression method that would be used to estimate BAFs for all the 2378-substituted congeners, residuals versus fit plots for the different models were prepared and visually inspected (Figures 4.6 and 4.7 for catfish and crabs, respectively). The residuals present some clustering but, in general, they were distributed randomly in both directions. At the higher end of the predicted values, there were a few outliers that produced curvature. This confirmed the need for using a robust regression method. Figures 4.8 and 4.9 present histograms plotted along the probability mass function for a normal distribution for each set of residuals. As expected, the residuals of log-transformed data (power regression) are normally distributed. However, due to difficulties in calculating BAFs from non-linear regressions, the robust LTS regression was selected as the model to use for bioaccumulation factor estimation. As suggested by the data in Figures 4.8 and 4.9, residuals from the robust LTS had the distribution that differs the least from a normal distribution among all the linear methods.

The last step followed prior to completing regressions for all the congeners was to examine the plots of catfish residuals versus other explanatory variables. This helped in determining if other variables could have been included in a multiple regression model to explain the noise in the data. Figure 4.10 shows scatterplots of residuals versus sampling date, catfish

Figure 4.6 Residuals vs Fit Plots for Regressions between Catfish and Dissolved 2378-TCDD Concentrations

Figure 4.7 Residuals vs Fit Plots for Regressions between Crab and Dissolved 2378-TCDD Concentrations

**Figure 4.8 Histograms of Residuals for Regressions of Catfish and Dissolved
Concentrations of 2378-TCDD**

Figure 4.9 Histograms of Residuals for Regressions of Crab and Dissolved Concentrations of 2378-TCDD

Figure 4.10 Residuals from Catfish BAF Regressions Plotted by Additional Explanatory Variables

characteristics (weight, length, and lipid content), sampling location (distance from Morgan's Point), water properties (salinity, temperature, DOC, and pH), and suspended and bottom sediment 2378-TCDD concentrations. In addition, Figure 4.11 presents boxplots of the residuals by two categorical explanatory variables: fish species and water quality segment. In both cases, the goal was to identify a pattern that would pinpoint a variable affecting the relationship between catfish and dissolved concentrations. No obvious trend was inferred from the scatterplots in Figure 4.10. The residuals seem to be randomly distributed without being affected by seasonality or any other explanatory variable. The boxplots in Figure 4.11 indicate that the magnitude of the residuals is similar for the different segments, although segment 2421 seems to present slightly lower residuals. Regarding fish species, residuals from hardhead catfish appear to be considerably higher than those from blue catfish. However, sample sizes are very different which complicates comparison between the two datasets.

4.1.1.2 Estimation of BAF for All Congeners from Regressions

As mentioned earlier, because the dioxin congeners have a wide range of bioaccumulation potentials, it was considered necessary to estimate BAFs for each compound. As mentioned in the previous section, the robust LTS regression method was selected to fit the dioxin data in the HSC. While a non-linear model could represent the data more accurately, it would fail to provide a direct estimate of the bioaccumulation potential.

The following guidelines were used for BAF estimation:

1. The BAF was derived from linear regression between tissue concentrations and dissolved concentrations measured at the same location and approximately at the same time.
2. An effort was made to analyze all the data using the same regression method. However, if

Figure 4.11 Distribution of Residuals from catfish BAF Regressions by Categorical Variables

the BAF for a particular congener could not be derived using the LTS regression (i.e., the slope was not statistically significant or it was negative), the regression was performed using the WLS method.

3. All the test statistics and confidence intervals were calculated for a 95% confidence level ($\alpha=0.05$).

Figures 4.12 and 4.13 present the best-fit lines along with the confidence intervals for dioxins in catfish and crabs, respectively. The relevant test statistics are summarized in Table 4.5. Estimated BAFs vary from 38 ± 20 to 32617 ± 13925 for catfish and from 15 ± 41 to 26680 ± 7030 for crabs. Bioaccumulation factors varied within 2 orders of magnitude among the different congeners and were generally higher for catfish than for crabs. This may be the result of higher lipid content in fish than in crabs. It is noted that for some congeners the relationships were not statistically significant at the 95% confidence level (e.g., 123478-HxCDD in catfish, p -value =0.23) and, thus, the uncertainty in the estimated bioaccumulation factors for these compounds is high. An attempt was made to fit the field data for those congeners using all the above-mentioned methods, but in all cases the regressions were weak.

It is important to point out that the best-fit regression yielded negative slopes for congeners 123478-HxCDF, 234678-HxCDF, 123789-HxCDF, 1234678-HpCDF, and OCDF for catfish data and 123678-HxCDD, 123789-HxCDD, 23478-PeCDF, 123478-HxCDF, 123478-HpCDF, and OCDF for crab data. These negative slopes could be interpreted as a lack of bioaccumulation of the particular congeners in the sampled species or as the need for a more appropriate non-linear model.

It is noted that BAFs are equilibrium concepts. Aquatic animals are not infinite sinks for chemicals. As they take up chemicals, they also eliminate them via urine, feces, biochemical

Figure 4.12a Bioaccumulation Factors for Dioxins in Catfish from the HSC

Figure 4.12b Bioaccumulation Factors for Furans in Catfish from the HSC

Figure 4.13a Bioaccumulation Factors for Dioxins in Crabs from the HSC

Figure 4.13b Bioaccumulation Factors for Furans in Crabs from the HSC

Table 4.5a. Estimated Bioaccumulation Factors for HSC Catfish

Table 4.5b Estimated Bioaccumulation Factors for HSC Crabs

reactions (in some cases), and other mechanisms. Elimination processes are grouped in the term "depuration". When an animal is exposed to a new chemical, its BAF will increase until the chemical uptake rate is balanced by the chemical depuration rate. As a general rule, when the term BAF is used, it can be assumed to refer to the steady-state, equilibrium BAF. However, because the uptake and elimination rates for large animals, such as fish and crabs, are slow relative to the dynamically changing concentrations in water, it is expected that individual measured BAFs always incorporate some disequilibrium. This may help explain the high scatter observed in the data.

4.1.1.3 Determination of BAF using Measures of Central Tendency

Since the linear regressions to estimate BAFs did not fit the observed data very well, an alternative approach was used. This approach uses measures of central tendency (i.e. mean or median) of the ratios of tissue concentrations to dissolved concentrations (Figures 4.1 and 4.2) rather than BAFs estimated from linear regressions. For tissue to water ratios, it was considered that the log BAF datasets followed a fairly normal distribution. Thus, the average log BAF is an appropriate measure of central tendency. Line fit plots for BAFs comparing fish and crabs for several important congeners are shown in Figure 4.14.

4.1.2 Development of Site-specific Biota-Sediment Accumulation Factors

The BSAF is defined by the USEPA (2003) as the ratio (in kilograms of sediment organic carbon per kilogram of lipid) of the lipid-normalized concentration of a chemical in the tissue of an aquatic organism to its organic carbon-normalized concentration in surface sediment, in situations where the ratio does not change substantially over time, both the organism and its food

Figure 4.14 Line Fit Plots of BAF for Selected Congeners in Tissue from the HSC

are exposed, and the surface sediment is representative of average surface sediment in the vicinity of the organism.

$$BSAF = \frac{C_{tissue} / F_{lipid}}{C_{sed} / F_{oc}} \quad (4.4)$$

where F_{oc} is the organic carbon fraction of the sediment by weight.

BSAFs for catfish and crabs were calculated for each of the paired water, tissue, and sediment samples collected in the spring, summer, and fall seasons from 2002 through 2004. Because lipid normalization increased the variability in the BAF/BSAF relationships, and the lipid measurement method used was imprecise, all BSAFs were based on raw tissue concentrations and were not lipid-normalized.

BSAFs for PCDD/F congeners measured in 130 catfish and sediment samples from the HSC system are shown in Figure 4.15. BSAFs for PCDD/F congeners measured in 131 blue crab and sediment samples from the HSC system are shown in Figure 4.16. As with the calculated BAFs, these BSAFs are calculated from the bulk tissue concentration, and not normalized to the tissue lipid concentrations. BSAFs exhibited many of the same patterns as BAFs, which is expected as they are based on the same tissue concentrations.

4.1.2.1 Estimation of BSAF for 2378-TCDD

Based on measurements from the Houston Ship Channel system, it was observed that the tissue lipid normalizations decrease the strength of the relationship between tissue dioxin concentrations and organic carbon-normalized sediment dioxin concentrations. Thus, BSAF relationships were developed using whole tissue dioxin concentrations.

Regressions for catfish and sediment-organic carbon concentrations of 2378-TCDD were

Figure 4.15 Distribution of Individual BSAFs for Catfish from the HSC

Figure 4.16 Distribution of Individual BSAFs for Crabs from the HSC

performed using the linear models employed to estimate BAFs. Again, two non-linear models (power and polynomial) were included for comparison purposes. Figure 4.17 shows the best-fit lines for the various regression methods and Table 4.6 summarizes the test statistics. Similar to what was observed with tissue-water relationships, linear models did not provide the best fit for the field data. However, they were preferred over the non-linear ones because a biota to sediment accumulation factor could be directly derived. Figure 4.18 presents residuals versus fit plots for the various models. Clustering of the residuals is more evident for the sediment data. However, for low to medium predicted concentrations, the residuals seem to be varying randomly around zero for most of the models. It is noted that all the models in this case (including the non-linear ones) exhibit tailing of the residuals. This is due to very high concentrations of 2378-TCDD in some of the sediment samples. The histograms for the residual datasets are presented in Figure 4.19. Data in Table 4.6 and Figures 4.18 and 4.19 suggest that the LTS model best describes the field data among the linear regressions and fairly meets the assumptions of normality of residuals and constant variance. Thus, this method was selected to estimate the BSAFs for the remaining congeners.

Prior to calculating BSAFs for the different dioxin and furan congeners, scatterplots of residuals versus several explanatory and categorical variables were examined to look for possible correlations (Figures 4.20 and 4.21). No evident patterns were observed in the data.

4.1.2.2 Estimation of BSAF for All Congeners

Biota to sediment accumulation factors were estimated using the robust LTS regression method and following the guidelines outlined in the BAF section. Plots of tissue concentrations of each congener versus the measured concentration in organic carbon-normalized sediment along

Figure 4.17 Partitioning of 2378-TCDD between Catfish and Carbon-normalized Sediment in the HSC

**Table 4.6 Summary of Regression Statistics and Parameters for Catfish-Carbon
Normalized Sediment Relationships**

Figure 4.18 Residuals vs Fit Plots for Regressions between Catfish and Sediment-Organic Carbon 2378-TCDD Concentrations

Figure 4.19 Histogram of Residuals for Regressions of Catfish and Sediment Concentrations of 2378-TCDD

Figure 4.20 Residuals from Catfish BSAF Regressions Plotted by Additional Explanatory Variables

Figure 4.21 Distribution of Residuals from Catfish BSAF Regressions by Categorical Variables

with the best-fit line and the confidence intervals are presented in Figures 4.22 and 4.23 for catfish and crabs, respectively. Table 4.7 summarizes the test statistics for each regression. Biota to sediment accumulation factors varied within 2 orders of magnitude among the different congeners and were generally higher for catfish than for crabs. This may be the result of higher lipid content in fish than in crabs. It is noted that for some congeners the relationships were not statistically significant at the 95% confidence level and, thus, the uncertainty in the estimated BSAFs for those compounds is high.

4.1.2.3 Determination of BSAF using Measures of Central Tendency

Similarly to the observations for BAFs, linear models did not fit BSAF relationships well. Thus, a measure of central tendency (i.e. mean or median) of the ratios of tissue concentrations to sediment concentrations (Figures 4.15 and 4.16) was used instead of BSAFs estimated from linear regressions. The tissue to organic carbon-sediment do not follow a normal distribution as indicated by large skewness and kurtosis (up to 8 and 40, respectively). Thus, the median was selected as the most appropriate measure of central tendency. Figure 4.24 shows organic carbon-normalized sediment and tissue data and the BSAF fitting lines calculated for selected congeners in both catfish and crabs.

4.1.3 Combined Bioaccumulation and Biota to Sediment Accumulation Factors

In theory, the estimated BAFs include the effects of all routes of chemical exposure in the aquatic ecosystem. Thus, they do not assume simple water-biota partitioning but are an overall expression of the bioaccumulation using the concentration of the chemical in the water column as a reference point (USEPA, 1995). However, this holds true only if the dissolved and bed sediment

Figure 4.22a Biota to Sediment Accumulation Factors for Dioxins in Catfish from the HSC

Figure 4.22b Biota to Sediment Accumulation Factors for Furans in Catfish from the HSC

Figure 4.23a Biota to Sediment Accumulation Factors for Dioxins in Crabs from the HSC

Figure 4.23b Biota to Sediment Accumulation Factors for Furans in Crabs from the HSC

Table 4.7a Estimated Biota to Sediment Accumulation Factors for HSC Catfish

Table 4.7b Estimated Biota to Sediment Accumulation Factors for HSC Crabs

Figure 4.24 Line Fit Plots of BSAF for Selected Congeners in Tissue from the HSC

concentrations are at equilibrium, in which case sediment concentrations are related to the dissolved concentrations by an isotherm (linear or non-linear). For the HSC, it is unclear if the equilibrium assumption is valid, since the correlation between dissolved and bed sediment concentrations is rather poor.

Estimating BAFs and BSAFs independently using water-tissue and sediment-tissue data, respectively may overestimate their values. Thus, an alternative method that uses a combination of the two factors was used to account for all routes of exposure and eliminate overlapping effects. This method consists of multiple linear regressions among dissolved, organic carbon-normalized sediment, and tissue concentrations. It is noted, however, that a multiple regression assumes that the independent variables (dissolved and organic carbon-normalized sediment) are not correlated and that assumption is not completely valid for the HSC. The best-fit line equations will be of the form:

$$C_b = b_0 + BAF' * C_{w,diss} + BSAF' * C_{soc} \quad (4.5)$$

where b_0 is a coefficient and BAF' and $BSAF'$ are the factors calculated using both water and sediment-oc data. A prime notation is used to differentiate between the independently calculated factors and the combined factors. The robust LTS regression method was used to minimize the effect of outliers. Figures 4.25 and 4.26 show the results of the multiple regressions for the congeners that contribute more than 1.5% to the TEQ in catfish and crabs⁷. Table 4.8 summarizes the test statistics for each regression. The resulting BAF' s were lower than their respective BAFs calculated in Section 4.1.1.2, with the exception of 123678-HxCDF in catfish. The estimated

⁷ 2378-TCDD, 12378-PeCDD, 2378-TCDF, 23478-PeCDF, and 123678-HxCDF for catfish and 2378-TCDD, 12378-PeCDD, 2378-TCDF, and 23478-PeCDF for crabs.

Figure 4.25 Line Fit Plots of Multiple Regressions for Selected Congeners in Catfish from the HSC

Figure 4.26 Line Fit Plots of Multiple Regressions for Selected Congeners in Crabs from the HSC

**Table 4.8a Estimated Combined Bioaccumulation and Biota to Sediment Accumulation
Factors for HSC Catfish**

**Table 4.8b Estimated Combined Bioaccumulation and Biota to Sediment Accumulation
Factors for HSC Crabs**

BSAF’s for catfish were lower than the BSAF calculated in Section 4.1.2.2, while BSAF’s for 12378-PeCDD and 23478-PeCDF in crabs were higher than their respective BSAFs. Note that in some cases, the best-fit line coefficients were negative (e.g., 12378-PeCDD in catfish). This was interpreted as a lack of bioaccumulation of the congener in biota from the HSC.

4.1.4 Texas Statewide Water Quality Criterion

Texas Surface Water Quality Standards (30 TAC §307.1-307.7) include a human health water quality criterion for dioxins/furans of 9.33×10^{-8} µg/L water (0.0933 pg/L), based on saltwater fish consumption. This criterion is based on 2378-tetrachloro-dibenzo-*p*-dioxin (TCDD) equivalent concentrations (TEQs) for the following congeners that are the toxic forms regulated by the Texas Commission on Environmental Quality (TCEQ):

Table 4.9 Toxicity Equivalent Factors (TEFs)

Congener/Isomer	TEF
2,3,7,8 TCDD	1
1,2,3,7,8 PeCDD	0.5
2,3,7,8 HxCDDs	0.1
2,3,7,8 TCDF	0.1
1,2,3,7,8 PeCDF	0.05
2,3,4,7,8 PeCDF	0.5
2,3,7,8 HxCDFs	0.1

The dioxins/furans human health water quality criterion was calculated by the TCEQ from the following equation and risk-based assumptions:

$$(RL \times BW) / (CSF \times CR \times BAF) \tag{4.6}$$

where: *RL* = risk level = 10^{-5} or 1 in 100,000

BW = adult body weight = 70 kg

CSF = cancer slope factor = 10^5 kg-day/mg

CR = consumption rate of fish/shellfish = 0.015 kg/day

BAF = bioaccumulation factor for dioxins = 5000 L/kg

The human health criterion for dioxins in water is then:

$$(10^{-5} \times 70 \text{ kg}) / (10^5 \text{ kg-day/mg} \times 0.015 \text{ kg/day} \times 5000 \text{ L/kg}) = 9.33 \times 10^{-11} \text{ mg/L, or } 0.0933 \text{ pg/L}$$

This criterion applies to the total dioxin concentration in water, including the suspended particulate plus dissolved fractions.

As stated previously, TMDLs are required for water bodies not meeting water quality standards. It is worth noting that the water bodies addressed by this project were not found to exceed this water quality standard, but instead were not expected to meet the water quality standard because high levels of dioxins were found in fish and crab tissue by the Texas Department of Health. Results of water sampling undertaken in this project, however, confirm that the water quality standard is indeed not met in many of the water bodies.

There are several inherent problems with using this human health water quality criterion as a water quality target for a TMDL. First, it is difficult to measure 0.0933 picograms per liter in ambient water, and it requires complex and expensive sampling equipment. Thus, it is difficult and expensive to evaluate compliance with this criterion. Also, some assumptions used to derive this water-based criterion, such as the BAF, are questionable. The applicability of the BAF of 5,000 L/kg used by the TCEQ in calculating this criterion was not known, and the USEPA recommends determination of site-specific field-measured bioaccumulation relationships

(Sections 4.1.1 and 4.1.2). Thus, a waterbody meeting the TCEQ human health water quality criterion for dioxins/furans in water does not necessarily guarantee that fish and shellfish tissue concentration levels will be safe for human consumption.

The primary advantage of using a water concentration as the water quality target for the TMDL is that it facilitates calculations of loadings and permit limits. Water quality targets based on tissue or sediment concentrations offer other advantages. For example, it is easier and less expensive to sample and analyze concentrations in tissue and sediment to evaluate compliance.

The following sections are focused on using the data from this project for developing a WQ target that is based on a site-specific bioaccumulation factor as well as a sediment-based WQ target.

4.1.5 Tissue Residue Criterion

The fish or shellfish tissue residue criterion (TRC) is the target concentration in tissue considered acceptable for saltwater fish consumption and is calculated using the following equation and the TCEQ risk management assumptions:

$$TRC = RL \times BW / CSF \times CR \quad (4.7)$$

Note that Equation (4.7) is identical to Equation (4.6) except that it leaves out the BAF, which translates the tissue concentration to a water concentration. Thus, the target concentration for dioxins (TEQ) in fish or crab tissue based on TCEQ assumptions is:

$$(10^{-5} \times 70 \text{ kg}) / (10^5 \text{ kg-day/mg} \times 0.015 \text{ kg/day}) = 4.7 \times 10^{-7} \text{ mg/kg} = 0.47 \text{ ng/kg}$$

4.1.6 Water Quality Target Calculations for Dissolved PCDD/Fs in Water

The water quality targets for dissolved PCDD/Fs can be calculated from the TRC and the BAF from the following relationship:

$$C_{w,d} = \frac{TRC}{BAF} \quad (4.8)$$

While the tissue residue criterion is based on TEQ, a composite measure of toxic contributions from twelve dioxin and furan congeners, each of the congeners contributing to the dioxin TEQ has different physical and chemical properties and different bioaccumulation potentials. Given that the BAFs of the various congeners vary so widely, use of a composite BAF for dioxin TEQ seemed inappropriate. Thus, water quality targets for each of the major congeners contributing to the total equivalent concentration are desirable. However, no formal guidelines exist on developing targets for mixtures of compounds that contribute to an exceedance of a WQ criterion.

The fraction of the total TEQ attributable to a given congener f_i^{TEQ} can be calculated as:

$$f_i^{TEQ} = \frac{C_i * BAF_i * TEF_i}{\sum_{i=1}^{17} C_i * BAF_i * TEF_i} \quad (4.9)$$

Then the water quality target for a given congener can be calculated as:

$$C_{w,d} = \frac{TRC * f_i^{TEQ}}{BAF_i * TEF_i} \quad (4.10)$$

In this way, each congener was assigned a water quality target concentration that corresponded to their average fraction of the total TEQ in catfish and crab tissue in the system⁸.

⁸ For instance, if 2378-TCDD had contributed, on average, 80% of the TEQ in catfish, and 23478-PeCDD had

These congener-specific targets calculated for all congeners were summed to calculate the water quality target for dioxin TEQ. Note that only the targets for congeners contributing, on average, more than 2% of the TEQ (2378-TCDD, 12378-PeCDD, 2378-TCDF, 23478-PeCDF) were used to calculate exceedance rates in Section 4.1.9 below.

Site-specific water quality targets for dissolved PCDD/Fs in the HSC system calculated from the measured BAFs using Equation (4.10) and the average log BAF (Section 4.1.1.3) for all the data collected for this TMDL project are shown in Table 4.10. Because log BAFs exhibited a normal distribution, the average log BAF for each congener measured in the HSC system was used. The calculated water quality targets were lower for catfish than crabs for most congeners, and the lower target for the two species was selected as the overall water quality target.

Typically, 2378-TCDD comprised half or more of the TEQ in all media. The water quality target for dissolved 2378-TCDD was calculated to be 0.0024 pg/L. The water quality target for dioxin TEQ dissolved in water was calculated to be 0.0081 pg/L. The 95% confidence limits for the average BAF also were calculated and used to identify the 95% confidence limits around the water quality target.

4.1.7 Water Quality Target Calculations for PCDD/Fs in Water

Since BAFs were calculated from dissolved concentrations, it is necessary to estimate partitioning relationships to calculate targets that would apply to total water concentrations (dissolved + suspended). Aquatic sediments take up PCDD/Fs just as aquatic animals do, and

contributed 20%, the WQ target for 2378-TCDD would be calculated from a catfish TEQ of $0.47 * 80\% = 0.376$ ng/kg TEQ_{tcdd}, or 0.376 ng/kg TCDD, and the WQ target for 23478-PeCDD would be $0.47 * 20\% = 0.094$ ng/kg TEQ_{tcdd}, or 0.188 ng/kg PeCDD (TEF=0.5).

PCDD/Fs associated with suspended sediments typically exceed those dissolved in a given water sample. Partitioning between the suspended and dissolved phases can be quantitatively

**Table 4.10a Summary of BAFs and the Resulting Water Quality Targets for Catfish in the
HSC**

**Table 4.10b Summary of BAFs and the Resulting Water Quality Targets for Crabs in the
HSC**

characterized by the linear partitioning coefficient (K_p) or by the partitioning constants derived either from the Freundlich or Langmuir sorption equations (Mansour 1993).

The partition coefficient, K_p , describes the ratio of a chemical's concentration in sediment and water at steady-state equilibrium conditions.

$$C_s = K_p * C_{w,d} \quad (4.11)$$

where C_s is the concentration of the chemical in the solid phase, in pg/kg, and $C_{w,d}$ is the dissolved concentration in water, in pg/L. It was noted, however, that the linear partitioning coefficient did not fit the observed HSC data for many congeners (Figure 4.27). Thus, log-transformed data were used to estimate suspended-dissolved partitioning. This is equivalent to using the Freundlich isotherm:

$$C_s = K * C_{w,d}^{1/n} \quad (4.12)$$

where K is the adsorption constant and $1/n$ is another constant providing a rough estimate of the intensity of adsorption (Mansour 1993). The linear partitioning approach is equivalent to the Freundlich isotherm with an exponent ($1/n$) of 1. Congener-specific partitioning constants for the HSC are summarized in Table 4.11.

Water quality targets for total water concentrations (dissolved + suspended) were calculated assuming the average measured suspended particulate matter concentration in the HSC system of 26 mg/L and Equation (4.13):

$$C_{w,total} = C_{w,d} + K * C_{w,d}^{1/n} * [SPM] \quad (4.13)$$

where $C_{w,total}$ is the water quality target concentration for whole water samples, $C_{w,d}$ is the water quality target for dissolved concentrations in water, and $[SPM]$ is the concentration of suspended particulate matter. Site-specific water quality targets for PCDD/Fs in water samples from the

Figure 4.27 Partitioning of Dioxins between Suspended and Dissolved Phases

Table 4.11 Summary of Suspended-Dissolved Partitioning

HSC system are shown in Table 4.10. The water quality target for 2378-TCDD in water was calculated to be 0.011 pg/L, and the water quality target for dioxin TEQ in water was calculated to be 0.070 pg/L. These targets are several times higher than for dissolved concentrations, indicating that a large portion of the total dioxin is associated with the suspended particulate phase in water. This calculated target for dioxin TEQ in water is approximately 75% of the state water quality criterion of 0.093 pg/L.

4.1.8 Water Quality Target Calculations for PCDD/Fs in Sediments

The water quality target concentration in sediment can be calculated using the following equation:

$$C_{\text{sed,oc}} = \frac{\text{TRC}}{\text{BSAF}} \quad (4.14)$$

The water quality targets for individual congeners contributing to the composite TEQ concentration can be calculated as:

$$C_{\text{sed,oc}} = \frac{\text{TRC} * f_i^{\text{TEQ}}}{\text{BSAF}_i * \text{TEF}_i} \quad (4.15)$$

Site-specific sediment quality targets for PCDD/Fs in the HSC system calculated from the measured BSAFs using Equation (4.15) and the entire database collected for this TMDL project are shown in Table 4.12. For BSAFs, which exhibited non-normality, the median BSAF was selected as the most appropriate measure of the typical BSAF for each congener. Also note that this target is based on the organic carbon-normalized sediment concentration, calculated as the bulk sediment concentration divided by its organic carbon content. The calculated targets were lower for fish than crabs for most congeners, and the lower target for the two species was selected

as the overall water quality target. Typically,

Table 4.12a Summary of BSAFs and the Resulting Water Quality Targets for Catfish in the HSC

Table 4.12b Summary of BSAFs and the Resulting Water Quality Targets for Crabs in the HSC

2378-TCDD comprised half or more of the TEQ in all media. The sediment quality target for 2378-TCDD was calculated to be 43 ng/kg oc. The water quality target for dioxin TEQ in sediments was calculated to be 115 ng/kg oc. The 95% confidence limits for the average BSAF also were calculated and used to identify the 95% confidence limits around the water quality target.

4.1.9 Observed Target Exceedance Rates

The water quality targets are summarized in Table 4.13 below.

Table 4.13 Summary of Site-Specific Water Quality Targets in Various Media

Congener	Water – Dissolved pg/L	Water - Total pg/L	Sediment ng/kg-OC
2378-TCDD	0.0024	0.011	43
12378-PeCDD	0.0007	0.016	13
2378-TCDF	0.0207	0.087	182
23478-PeCDF	0.0015	0.010	23
Total TEQ	0.0081	0.070	115

For each congener, the lower target for the two species (catfish and crab) was selected.

Water and sediment data collected in Phases II and III of the project were compared to the estimated media-specific water quality targets to evaluate the current state of impairment of the HSC system, and the concentration reductions required to meet the water quality targets. Table 4.14 summarizes the percent target exceedances by congener for both water and sediment samples. Water quality targets are exceeded in most samples for most congeners, and overall exceedance rates are currently greater than 90%. Note that for many congeners, these exceedance rates may be high, as the exceedance status for nonquantifiable measurements could not be compared to the targets unless the quantitation limit was less than the target. The percent reductions in ambient dioxin levels required to meet the water quality targets in various media are shown in Table 4.15. Overall, it appears that an 85-90% reduction in concentrations, or one order

of magnitude, will be required for the water quality targets to be met.

Table 4.14 Summary of Exceedances of the Estimated Water Quality Targets

Congener	Dissolved Water Samples^a	Total Water Samples^a	Sediment Samples^a
<i>Number of samples</i>	<i>148</i>	<i>148</i>	<i>173</i>
2378-TCDD	96% (84)	83% (93)	84% (167)
12378-PeCDD	100% (64)	39% (127)	95% (86)
2378-TCDF	93% (147)	89% (148)	76% (174)
23478-PeCDF	100% (93)	91% (95)	88% (154)
Total TEQ	100% (148)	91% (148)	93% (174)

^aValue in parentheses represents the number of samples that could be used for determination of target exceedance because either the concentrations were quantifiable or, if the concentrations were not quantifiable, the quantitation limits were below the water quality target

Table 4.15 Median Measured Congener Concentrations and Percent Reductions Required To Meet Water Quality Targets by Media

Congener	Dissolved Water Samples		Total Water Samples		Sediment Samples	
	Median Concentration	% Reduction	Median Concentration	% Reduction	Median Concentration	% Reduction
<i>Number of samples</i>	<i>148</i>		<i>148</i>		<i>173</i>	
2378-TCDD	0.027	91%	0.106	90%	621	93%
12378-PeCDD	0.0043	84%	0.016	0%	75	83%
2378-TCDF	0.13	84%	0.40	78%	1,582	88%
23478-PeCDF	0.0095	84%	0.030	67%	147	84%

Total TEQ	0.066	88%	0.23	69%	1,065	89%
-----------	-------	-----	------	-----	-------	-----

4.2 SPATIAL TRENDS

4.2.1 Longitudinal Profiles

A summary of average TEQ concentrations in water, sediment, and tissue by segment is presented in Tables 4.16a and b for TEQ and 23478-TCDD, respectively. It can be observed in Table 4.16a that for the Summer 2002 samples, segment 1006 exhibited the highest average concentrations of dioxins in sediment, while segment 2430 showed the highest average concentration in water, segment 1007 showed the highest average concentration in catfish, and segment 1005 showed the highest average TEQ for crabs. Similarly, for the Fall 2002 samples, segment 1006 exhibited the highest average TEQ in water, segment 1007 showed the highest dioxin average in sediment, segment 2430 in catfish, and segment 2429 in crabs. It is also noted that the average dioxin concentrations in water and sediment measured in the Fall 2002 samples were for the most part higher than the ones measured in Summer 2002 by factors up to 7.1. Average TEQ concentrations in catfish and crab for Fall 2002 are higher than their counterparts for the Summer event only in 50% of the cases with ratios up to 1.8 and 2.2, respectively. It is noted, however, that during Fall 2002 samples were collected at fewer locations than during Summer 2002 and, thus, results from this comparison may not be conclusive.

Results from the Spring 2003 samples indicate that the highest average TEQ concentrations in water and sediment were found in segment 1001, while segments 2429 and 2427 showed the highest average TEQ concentration in catfish and crab, respectively. For the

Spring 2004 event, the highest average TEQ concentrations were calculated for segment 1006 in water, for segment 1007 in sediment, for segment 2430 in catfish, and for segment 2429 in crab. It

Table 4.16a Summary of Average TEQ Concentrations by Segment

Table 4.16b Summary of Average 2378-TCDD Concentrations by Segment

is noted, however, that the highest catfish and crab average TEQs for the Spring 2004 event correspond to a single sample collected in the mentioned segments. Finally, the highest average TEQ concentrations in water, sediment, catfish, and crab measured in fall 2004 were calculated for segments 1001, 1007, 1005, and 1001, respectively.

Data in Table 4.16b indicate that the maximum average 2378-TCDD concentration in water was measured in the Fall 2002 in segment 1006, while the maximum average in sediment was measured in Fall 2004 in segment 1007. The maximum average 2378-TCDD concentrations for catfish and crabs were measured in Fall 2004 in segments 1005 and 1001, respectively.

Figure 4.28 shows concentration profiles along the main channel for total water dioxin concentrations measured in 2004 (WO7) compared to those measured in 2002-2003 (WO4). These data provide an indication of spatial patterns. As can be seen in Figure 4.28, the longitudinal profile was fairly consistent for all events: the water concentrations start low, they then increase until reaching the highest dioxin concentration and then concentrations decrease downstream. For all the events the profiles show peak TEQ concentrations in segment 1006 (at station 15979) and most of the side bays and tributaries at or above the levels observed in the main channel at the confluence segments. In addition, the dioxin concentration at station 11193 in the San Jacinto River (segment 1001) is higher than those measured at the confluence with the main channel and higher than that those measured at station 15979. The only discrepancy was observed in the Fall 2004 profile which presented an additional “peak” in segment 1005.

Figure 4.29 depicts concentration profiles along the HSC for sediment samples collected in WO4 and WO7. Figure 4.29 shows similar profiles for the Spring and Fall 2004 samples: OC normalized TEQ concentrations start low and increase to a peak at station 11280 (segment 1007),

Figure 4.28 Total Water TEQ Concentration Profiles

Figure 4.29 Total Organic-carbon Normalized Sediment TEQ Profiles

then they show a dramatic drop at station 15979 (segment 1006), in segment 1006 concentrations maintain a general increasing trend up to station 16618 (segment 1005) to finally decrease towards Galveston Bay. Dioxin concentrations were lower for most of the locations (upstream and downstream of station 11280). Sediment TEQ concentration for station 11193 in the San Jacinto River (segment 1001) was the only exception, with a concentration almost as high as that measured at station 11280. Concentrations in side bays were, in general, higher than those measured at the receiving main channel. The concentrations measured in WO4 showed similar behavior but the peak was at station 15979 in segment 1006.

Figures 4.30 and 4.31 present concentration profiles along the HSC for catfish and crab samples, respectively. Catfish and crabs exhibited relatively “flat” profiles with in-stream levels that are greater than those for side bays. The Fall 2004 profile, however, showed a significant peak at Morgan’s Point (11252) for both catfish and crab.

4.2.2 Multivariate Analysis

In order to test for spatial variability within the PCDD/F data set collected, two different classes of analysis technique were employed: Principle Component Analysis (PCA), and clustering analyses. Background information on PCA and cluster analysis is included in Appendix F. The data sets for summer, fall, and spring did not include all the same sampling points. Therefore, only the summer dataset was used as it contains the most complete set of sampling points. A map with the locations sampled during Summer 2002 is included in Appendix F. There were eight sub-sets of data within the summer dataset: sediment, air, and suspended/dissolved concentrations for water, runoff, and effluent.

Figure 4.30 Total Catfish TEQ Concentration Profiles
Figure 4.31 Total Crab TEQ Concentration Profiles

In order to complete these analyses, the homologue profile and/or the 17 dioxin-like congener profile of the samples was compared. The profiles, or fingerprints, are the basis for the spatial variability testing that is presented below.

4.2.2.1 Methodology

In order to normalize the data prior to PCA and cluster analysis, the PCDD/F totals from each homologue group were divided by the sum total of all PCDD/Fs for that sampling point. To view the 17 dioxin-like congener profiles, two different methods were tested and compared. In the first method, the individual congener concentrations were divided by the total homologue group for that congener. OCDD and OCDF were divided by the sum total of PCDD and PCDF, respectively (Gotz and Lauer, 2003). This method would show the spatial relationship of toxic congeners as compared to the homologue groups. In the second method, the individual congener concentrations were divided by the sum total of the seventeen 2378-substituted congeners. This method would give a spatial pattern of the 17 congeners with respect to each other.

Regarding non-detects, for the Principle Components Analysis and Cluster Analysis, the same procedure was followed when deciding which data points to include in the analysis. Initially, a procedure was developed which would include most of the data, but excluded data with non-detects. In this method, homologue groups missing greater than 25% of the data due to non-detects were excluded from the analysis, and individual sampling stations missing data were excluded case-wise. Other methods for data inclusion have been presented in the literature, and include assuming non-detects (ND) as half the detection limit, or substituting a zero for the ND.

As a first step, PCA for sediment samples was completed in order to establish the most appropriate approach for determining the profiles and working with non-detects. Figure 4.32

Figure 4.32 Different Schemes for Normalizing Profiles of Sediment Data

shows the three different schemes for normalizing profiles discussed earlier. Figure 4.32a shows a biplot of sediment data using homologue profiles, this scheme is appropriate for analyzing data because it considers all the congeners present in the samples, not only the dioxin-like congeners. Figures 4.32b and c show biplots of sediment data using congener profiles for the 17 dioxin-like compounds. For analysis of congener profiles, the second normalization method (Figure 4.32c) was considered more applicable to this study than the one presented in Figure 4.32b because the question of interest is the spatial pattern of the 17 congeners with respect to each other. Also, the pattern found for the toxic congeners normalized by the sum of the 17 congeners (Figure 4.32c) resembled the spatial patterns for homologue groups (Figure 4.32a). This may allow for interchangeability between homologue groups and dioxin-like congener analysis. For this study, however, only the homologue groups were used in subsequent analyses.

Figure 4.33 shows biplots of PCA results using three different methods for dealing with non-detects. In the first method (Figure 4.33a), non-detects were excluded from the database. However, it was decided that this method excluded too much data. Figure 4.33b shows the results when non-detects are substituted by half of the detection limit. For this study, it was decided that including ND at $\frac{1}{2}$ the detection limit might lead to unreliable results because of two reasons. First, the detection limit was not the same for all samples, and second the inclusion of these points would result in a different homologue profile. Because the profile is what is compared between samples, it was decided that a substitution of a zero for ND was the best method (Figure 4.33c). This resulted in the ability to include all data in the analysis, and did not change the profile of homologue concentrations.

Figure 4.33 Different Methods for Treating Non-detects

Based on the previous analyses, PCA and cluster analysis testing for the remaining media were completed using homologue profiles normalized by the total dioxin concentration (Σ PCDD/PCDF) and assuming non-detects as zeros.

The first step in completing a PCA is creating a covariance matrix. SPLUS statistical package was used for this and all other aspects of PCA testing. Covariance is the default SPLUS choice, and it was chosen instead of a correlation matrix because the data were all of the same type and had previously been normalized. The scores of the loadings generated from the creation of components were utilized to generate scatter plots. Principle Components one and two were graphed together to look for possible patterns, or clusters. As a way to further validate or explain clustering in the PCA, cluster analysis was employed to explore the relationships within clusters.

Several different types of cluster analyses were examined for this project. It is important to note that cluster analysis utilizes a dissimilarity matrix, while the PCA algorithm generates a similarity matrix. Four major types of cluster analysis were explored: k-means, partitioning around medoids (pam), fuzzy, and agglomerative hierarchical. With k-means, pam, and fuzzy methods, the analysis was carried out in SPLUS. Background information on the different cluster analysis techniques is included in Appendix F.

When considering the PCDD/F data from the Houston Ship Channel, all three cluster analysis methods (fuzzy, k-means, and pam) were utilized and the results compared. For these three clustering techniques, the number of clusters must be chosen (see Appendix F for details on how this was accomplished). It was found that the k-means method was not very effective and so it was discarded. Using pam and fuzzy analysis gave different cluster memberships, and no

apparent pattern was evident, indicating that a more robust method was needed in order to generate results.

Agglomerative Hierarchical Clustering (AHC) was selected as another alternative, since the number of clusters is not pre-chosen in order to run the analysis. SPSS was also used to complete this analysis. The method begins with all the data points in their own cluster, and then combines the points with the next point least dissimilar, or more similar, until there is one large group. Ward's method was chosen as the measure of similarity between points in a cluster. This method was chosen as it gives the same amount of variance within clusters. It also assumes that the clusters are spherical in hyperspace. This may not be true, but it seems reasonable to look for clusters which have the same variance within them when looking at this data. It would be difficult to interpret the cluster results if the clusters had different amounts of variation within them.

The output from the AHC method is a clustering tree. This is a graph that looks something like a family tree. This visual aid makes it easy to interpret the clustering results. It is possible to see how much the sample points vary from each other, or how much the clusters differ from each other based on the height of the dividing branch. One downfall of this method is that if a point is miss-classified in the first cluster step, it continues to be placed in that cluster throughout the analysis. It is important to be discerning when analyzing the results.

4.2.2.2 Results

As mentioned in the previous section, principle components analysis and cluster analysis were employed to discover the spatial patterns (if any) of PCDD/Fs in the different media in the Houston Ship Channel. The results of these analyses are presented below.

Dissolved Data

Figure 4.34 shows that most of the sampling stations for dissolved water homologue profiles are clustered in the bottom right-hand corner. The clustering is not tight, however. Looking at Figure 4.35, the hierarchical cluster analysis output shows that there is only one station outlier, which is 13340. This means that although station 11287 also looks like an outlier, it is actually part of a cluster which is not much different from the other points in the analysis.

Suspended Sediment Data

The patterns of suspended sediment PCDD/F homologue profiles do not seem to be distinct. It appears that the points are spread out somewhat randomly on the scatter plot of PCA scores (Figure 4.36). Looking at Figure 4.37, the hierarchical cluster output, shows that although stations 15464, 11200, 13343, and 16622 appear to be closely related they are somewhat spread out on the PCA scatter plot. This means that the results are not a tight, true cluster.

Bottom Sediment

Sediment was the medium studied most thoroughly, as the properties of PCDD/Fs indicate that dioxins would be more likely to attach to particles. Sediment also tends to move less over time, and so would be a better indicator of homologue fingerprints throughout the HSC area than a medium that is constantly in motion. It was hoped that a clear pattern of side bays and main channel would be found. This was not the case.

However, it was found that there are some stations which clearly do not have the same homologue pattern as the rest of the stations. Figure 4.38 shows these stations to be 11273, 15979, 11193, and 11300. This analysis is borne out by the cluster analysis output (Figure 4.39), which shows 11273 and 15979 as a distinct group. Although station 11193 and 11300 appear to

Figure 4.34 PCA Analysis for Dissolved Concentrations

Figure 4.35 Dissolved Concentrations Dendogram using Ward Method

Figure 4.36 PCA Analysis for Suspended Sediment Concentrations
Figure 4.37 Suspended Concentrations Dendogram using Ward Method

Figure 4.38 PCA Analysis for Sediment Concentrations

Figure 4.39 Bottom Sediment Concentrations Dendogram using Ward Method

be a separate group in the PCA scores scatter plot (Figure 4.39), the cluster analysis shows that while the stations are somewhat different from the other stations, they are not highly dissimilar. This statement can be made based on the height of clustering branch declaring the two stations a separate cluster.

The homologue fingerprints for the stations 11273 and 15979 show much higher percentages of the furan homologue groups, which differs somewhat from the majority of stations that exhibit higher levels of dioxin homologue groups in their fingerprints. The homogeneity found between and among the stations is most likely due to the abundance of different sources for dioxin, and the re-suspension of sediment which would tend to create a pattern remaining consistent up and down the channel.

Effluent

Effluent is divided into two groups, as the PCDD/Fs were analyzed as either dissolved or sorbed to suspended solids within the effluent. Figure 4.40, which is a scatter plot of the PCA scores for a combined test of suspended and dissolved effluent, shows that while there is some overlapping of homologue patterns, most of the dissolved effluent is in the lower right hand corner, and most of the suspended effluent is in the bottom left. The outliers of 46, 34, and 40 suspended effluent show the same pattern that they have when included with the sediment and suspended solids analysis. The cluster analysis, Figure 4.41, shows that three samples, along with 80 dissolved effluent samples do in fact constitute a separate cluster. This is to be expected, because the different physical properties of the 10 homologue groups lead to different homologue profiles in different media.

Figure 4.40 PCA Analysis for Effluent Concentrations

Figure 4.41 Total Effluent Concentrations Dendogram using Ward Method

An individual analysis of dissolved and suspended effluent was also completed.

Dissolved effluent did not exhibit strong clusters in the PCA analysis (Figure 4.42), but did show strong clustering with the hierarchical cluster analysis (Figure 4.43). This means that the clusters should be interpreted with some caution.

Suspended effluent (Figure 4.44) does indicate one distinct cluster, again numbers 34, 40, and 46 and a less distinct cluster of 1,7,8,19,24,25,28, 42, and 43. This supports the analysis that the three samples (34, 40, and 46) do in fact form a cluster. That is most likely due to the high percentages of furans in the homologue patterns for those. The hierarchical cluster analysis is presented in Figure 4.45.

Runoff

A map showing the locations sampled for runoff is included in Appendix F. Runoff was divided up in a way similar to effluent samples. An analysis of suspended and dissolved runoff together shows that the homologue profile of the two groups is very different. Figure 4.46 illustrates this, as the dissolved runoff samples are in their own cluster in the bottom center of the PCA scores scatter plot. This is further supported by the clustering in the hierarchical cluster analysis, Figure 4.47, which shows the dissolved runoff samples in their own cluster. The majority of the remaining samples are shown in Figure 4.46 on the middle right side, which constitutes the suspended cluster.

There are four samples which are located in the top left hand corner of Figure 4.46, and these four constitute their own cluster. This analysis is, again, supported by Figure 4.47, the hierarchical cluster analysis. This analysis shows that Samples SS-9 and SS-8 are separated from the rest of the suspended and dissolved samples. It is interesting that the dissolved and suspended

Figure 4.42 PCA Analysis for Dissolved Effluent Concentrations

Figure 4.43 Dissolved Effluent Concentrations Dendogram using Ward Method

Figure 4.44 PCA Analysis for Suspended Effluent Concentrations

Figure 4.45 Suspended Effluent Concentrations Dendogram using Ward Method

Figure 4.46 PCA Analysis for Runoff Concentrations

Figure 4.47 Runoff Concentrations Dendogram using Ward Method

samples for stations SS-8 and SS-9 are clustered together when the rest of the samples from other stations are split between the suspended and dissolved clusters. According to Figure 4.47, the dissolved runoff samples are more like the other suspended solids samples than SS-9 and SS-8. Figure 4-48 shows fingerprints for suspended concentrations at samples SS-8 and SS-9 along with sample SS-17 for comparison. It can be seen that samples SS-8 and SS-9 differ from other samples in that almost 100% of the dioxin concentration is due to OCDD, while for other samples (e.g SS-17), OCDD comprises about 70% of the total dioxin concentrations and there is a significant contribution of the higher chlorinated furans.

The dissolved and suspended runoff samples were also analyzed separately, and when examined in this manner there are actually two clusters in the dissolved runoff samples. This is observed at in the PCA scores scatter plot, Figure 4.49, and confirmed with Figure 4.50, the hierarchical cluster analysis. Figure 4.50 shows that there is a high degree of dissimilarity between the cluster of SS-8/SS-9 and the rest of the samples.

The suspended runoff analysis also shows that stations SS-8 and SS-9 form their own cluster much different than the rest of the samples. This is illustrated in the PCA scatterplot in Figure 4.51 and confirmed with Figure 4.52, the cluster analysis.

Air

A map showing the locations sampled for air is included in Appendix F. Air is an interesting media to analyze for PCDD/F homologue profile patterns. The data for this analysis consist of three samples for each of five stations for the months of June, July, and August of 2002. Furthermore, the samples at stations C403 and C408 were divided into PUF and filter

concentrations. This gives 27 total variables to input into the analysis. These three months were selected because the data for the other media were from Summer 2002 as well. As before, a

Figure 4.48 Fingerprints of Suspended Runoff Concentrations for Selected Stations

Figure 4.49 PCA Analysis for Dissolved Runoff Concentrations

Figure 4.50 Dissolved Runoff Concentrations Dendogram using Ward Method

Figure 4.51 PCA Analysis for Suspended Runoff Concentrations

Figure 4.52 Suspended Runoff Concentrations Dendogram using Ward Method

PCA was completed along with a hierarchical cluster analysis. The PCA scatter plot of scores, Figure 4.53, seems to show that C603_JUNE is an outlier when compared to the other samples. This is supported when the hierarchical cluster analysis is considered, and it shows that the homologue fingerprint for C603_June has a very high percentage of OCDF. Figure 4.54 shows the fingerprint of this sample. It is also possible to see the other clusters in the air PCA scatter plot of scores. The PUF samples show a very different homologue distribution from the other samples. This is illustrated in Figure 4.55, the hierarchical cluster analysis, which shows that the PUF samples are quite different from the rest of the samples. The homologue fingerprint for all samples in this cluster is shown in Figure 4.56. These samples are all low in heavy homologues. This is most likely because of the high vapor pressure of the lighter PCDD/Fs compared to the more highly chlorinated homologues. It is more likely to find these homologue groups in the vapor phase than sorbed to particulate matter because of their high vapor pressure. This would also account for the different clusters found using both PCA and hierarchical cluster analysis.

4.3 TEMPORAL TRENDS

4.3.1 Historical versus Current Data

No historical in-stream water data for dioxin were available for comparison with the data obtained in this project. Therefore, this analysis of temporal trends only includes sediment and tissue data.

Dioxin concentrations in sediments from samples collected in Work Orders No. 4 and No. 7 were compared to data gathered by others in 1993 and 1994 (see University of Houston, 2001

for a summary of historical data) and 2001 (PBS&J and Parsons, 2001). It is noted, however, that differences

Figure 4.53 PCA Analysis for Ambient Air Concentrations

Figure 4.54 Homologue Profile for Sample C603-June

Figure 4.55 Summer Ambient Air Concentrations Dendogram using Ward Method
Figure 4.56 Homologue Profiles of Air Vapor (PUF) Concentrations

in sampling and analytical methods used in the 1993-1994 study may limit the results of such comparison. The average TEQ concentration in sediment from previous studies (1993-2001) was 27.05 ng/kg dry wt., while the average TEQs measured in this study are 25.23, 18.70, 17.58, 42.70, and 68.80 ng/kg dry wt. for Summer-02, Fall-02, Spring-03, Spring-04, and Fall-04, respectively.

Figure 4.57a shows a comparison of total TEQ concentrations in sediment from previous studies and data from this study at selected stations. Overall, current sediment TEQs in segments 1006 and 1001 (San Jacinto River) were higher than the values measured in previous studies, whereas they were lower in segments 1007 and 1005.

A comparison of the levels of dioxins in tissue samples to historical data was also conducted. Table 4.17 presents a summary of tissue data from previous studies by segment and Table 4.18 shows the average total toxicity equivalent of the tissue samples segregated by species for each of the segments in the study area for both previous and current studies. The TEQ was calculated for historical data using the Texas TEF. The data in these tables are not normalized for lipid content of the sample as information on percent lipids was not available for all the historical data gathered. Table 4.18 shows that overall the concentrations measured in 2002, 2003, and 2004 are similar to those observed during the Summer 2001 sampling and higher than the ones observed prior to 1996 for most cases (especially catfish).

Figures 4.57b and c show average TEQs in catfish and crab for a number of segments in the study area. It can be seen from Figure 4.57b that average TEQ concentrations in catfish measured in the current study are higher than those measured previously for segments 1001 and 2421, but not for segment 1005, 1006, or 2426. The mean of the total TEQ (using data for the

Figure 4.57 Comparison of Past and Current TEQ Levels

Table 4.17 Summary of Total TEQ in HSC Tissue between 1989-2001

Table 4.18 Average Texas TEQ for Tissue Samples for All Segments

T 4.18 (2)

T 4.18 (3)

T 4.18 (4)

stations measured both in previous studies and in this study) was found to be 8.46 and 6.10 ng/kg wet wt. for the previous and current studies, respectively. Overall, total TEQ concentrations from previous studies were significantly higher than their counterparts from this study (p -value=0.04). Similar observations were made for crabs (Figure 4.57c). The average TEQ in crabs from previous studies is 5.94 ng/kg-wet wt., while the average TEQ in crabs from this study is 3.84 ng/kg wet wt. The two TEQ datasets, however, were not found to be significantly different (p -value=0.29) when compared using the t -test.

In another analysis, the temporal trends for each of the dioxin congeners in catfish at a location near the San Jacinto Monument (station 11261) were evaluated (Figure 4.58). This analysis was conducted using the data collected from 1992 to 2001 by the GCWDA/Donohue facilities and includes results from Summer 2002, fall 2002, Spring 2003, Spring 2004, and fall 2004. Overall, PCDDs were higher than PCDFs with 2378-TCDD showing the highest levels throughout the entire period. It can be seen from Figure 4.58 that the PCDD lines remain relatively parallel from 1992 to 2002, with the exception of that for 123678-HxCDD, for which the 1997 measurement did not follow the trend. Conversely, the PCDF lines did not follow the same trends, especially those for congeners 12378-PeCDF, 123678-HxCDF, 234678-HxCDF, 1234678-HpCDF and OCDF, which differ substantially from the remaining curves after 1995. This may suggest a change in dioxin sources around 1995. Data in Figure 4.58 also indicate that, in general, there has been little change in congener concentrations with time. Linear regressions for each of the curves showed that, for most of the congeners the slope of the best-fit line was not significantly different from zero. The only exceptions were the congeners 12378-PeCDD, 123789-HxCDF, and 1234789-HpCDF, which exhibited a slightly increasing trend over time (p -

Figure 4.58 Time Series of Dioxin Concentrations in Catfish at Location 11261

values between 0.005 and 0.04 and r^2 between 0.31 and 0.46). Results from a Mann-Kendall test for this data set confirmed the results from the linear regressions. The total TEQ showed no significant trend with time (p -value=0.16).

4.3.2 Time Trends of Current Data

Concentrations at the locations sampled during all five sampling events (Summer 2002, Fall 2002, Spring 2003, Spring 2004, and Fall 2004) of this project were analyzed using the Mann-Kendall test to evaluate possible trends over time. The Mann-Kendall test was selected because it allows for analysis of non-normally distributed data. The test was completed for all congeners at the selected stations for all media. The result was considered significant if the value associated with a given Mann-Kendall statistic (S) was less than the alpha value of 0.05. This would only occur for a value of S greater than 7. A summary of the procedure to compute S values is included in Appendix F.

Table 4.19 presents a summary of the data trends. Each data “series” is comprised of five data points that correspond to the measurements during each of the sampling events. Because the concentrations were ordered chronologically, the results are showing trends over time. The values in the table are the resultant probability given by the S-value derived from the critical values table presented in Appendix F. Only at a value less than 0.05 would a trend be considered significant. In Table 4.19, the values highlighted in orange indicate a significant upward trend in the concentrations of that congener over the five-sample time period. Values highlighted in light blue show a significant downward trend in concentrations of that congener for the sampling period. The value 0.592 is highlighted in white and indicates that there is no trend over time.

Table 4.19 Values Probability Results for Mann-Kendall Test for Trend

Values in yellow indicate a general (non-significant) upward trend, and values highlighted in light green indicate a general downward trend in concentrations over time.

It appears that furans are decreasing more over the sampling period than dioxins. A majority of the green highlighted cells are on the furan half of the table. Also, all but one of the blue highlighted cells are on the furan side of the table. This is an interesting finding. In addition, thirteen of the 23 significantly increasing congeners were dioxins. At sediment station 11280, the TEQ is showing a significant upward trend, mainly because the concentrations measured in 2004 are dramatically higher than the ones measured in the previous events. Of the 24 congeners showing significant decrease over time, all but one, 2378-TCDD sampled at sediment station 11252, are furan congeners. When congeners showing no trend, (S=0) are taken into account, the overall trend of all data at all stations appears to be downward. OCDD is the only congener which appears to be holding steady with a slight increase at most sampling stations and sampling media.

4.4 SEASONAL TRENDS

Seasonal trends in data collected in this project were also analyzed. Figure 4.59 shows the average congener profiles for the different media/season for the stations that were sampled during each event. In general, the profiles did not change significantly from one season to another. Exceptions to note are 2378-TCDD and 2378-TCDF in fish and crab samples, whose averages showed a considerable increase in Fall 2004. To evaluate changes with season, data sets 1 (Summer-02), 2 (Fall-02), 3 (Spring-03), 4 (Spring-04), and 5 (Fall-04) for selected compounds (i.e., 2378-TCDD, OCDD, 2378-TCDF, 123678-HxCDF, OCDF, and TEQ) were compared to

Figure 4.59 Seasonal Variation of Dioxins in the Houston Ship Channel

each other using a Wilconox Signed Rank test⁹. The goal was to find if there was a significant difference between any data sets. Dataset one was compared to five, four, three, and two.

Dataset two was also compared to datasets three, four, and five, dataset three was compared to four and five, and dataset four was compared to five. This resulted in a comparison between all datasets. This test was performed purely to discover differences, if any, between data of different time periods. A trend analysis was performed to check for differences over time and the results of that analysis were presented in the previous section.

An examination of the results for all five media considered in this analysis show some surprising similarities. As shown in Table 4.20, in all media except sediment, the test results show that there is a significant difference between sampling events one and four, three and four, and five and four for OCDD.

Overall, most of the differences in the congener concentrations between time periods occur with OCDD. This congener occurs in concentrations much higher than the other congeners, in part due to its chemical characteristics and in part due to sources of OCDD. A more complete analysis of the differences occurring in each media is presented below. All results are summarized in Table 4.20.

Dissolved

Using the Wilconox Signed Rank test, there are significant differences in OCDD concentrations between time periods 1-2, 2-3, 3-4, and 1-4. OCDD is generally the most common congener found in the environment, and it is not surprising to find differing

⁹ Non-parametric alternative to the paired *t*-test that uses both sign and magnitude to determine differences between samples.

Table 4.20 Results of Wilconox Test for Seasonality

T 4.20 (2)

concentrations of this congener different at different time periods. Unless there is a constant source of OCDD, expected levels of this congener in the dissolved phase of water would be expected to be different depending on such factors as temperature, humidity, UV strength, etc., since OCDD is enriched in atmospheric particulate deposition and also possibly created in the atmosphere.

Suspended

Again, concentrations in a media such as water are expected to vary widely based on the source of the contamination, and environmental factors such as temperature, turbidity of the water, and sunlight. In this case, there are significant differences in the concentrations of OCDD between time periods 1-4, 3-4, and 4-5. There is also a significant difference between sampling events 2-3 for OCDF.

Sediment

Analysis of sediment data using the Wilconox test showed that there is a significant difference in OCDD concentrations between time periods one and two. There are also differences in OCDF concentrations between periods 1-2, and 2-3. Sediment was the media that presented the least variability among seasons, in fact no differences were found for any of the congeners in organic-carbon normalized sediment concentrations.

Catfish

There is a surprising amount of concentration differences in catfish. The congener 2378-TCDD is significantly different in concentration between time periods 3-4, 5-1, 5-2, and 5-4 (based on positive ranks), and the test results for 2378-TCDF show a significant difference from periods 1-2, 1-4, and 5-2. OCDD is, again, significantly different between time periods 1-4, 2-4,

3-4, and 5-4. The total TEQ results, which should follow the 2378-TCDD results closely, also show a difference between time periods 3-4, 5-1, 5-2, and 5-4. This was somewhat surprising because concentrations in catfish would be expected to remain somewhat constant over time. However, different fish of different size and sex were collected for each sampling event. This could explain the significant differences for 2378-TCDD, OCDD, 2378-TCDF and total TEQ for the different sampling events. Lipid content may play an important role in the differences found as indicated by much fewer differences found in the lipid-normalized sets. To further evaluate the role of lipid content and size (expressed as the weight/length ratio) on the measured dioxin concentrations, their relationship was plotted in Figure 4.60. The 2378-TCDD curve seems to mimic the lipid content curve, specially at stations 11261, 11280, and 11292. The relationship with fish size is less marked but present.

Crab

The results of the Wilcoxon Signed Ranks test for this medium show that there are significant differences in concentration of OCDD between time periods 1-4, 3-4, and 5-4. Concentrations of 2378-TCDF are also significantly different between time periods 1-3, 5-1, and 5-3. Looking back at the Mann Kendall test for trends over time (Section 4.3.2), OCDD showed no significant upward or downward trend at any station for crabs. However, when using the Wilcoxon test to look for differences between sampling events, differences between events are found. One of the sampling events (Fall 2002) had much higher concentrations of OCDD than the other times, but a significant difference of concentration between two sampling events cannot be interpreted as a significant trend upward or downward. There is so much variability in the concentrations that the results of paired testing should be interpreted with caution. Again, the

Figure 4.60 Relationship between Lipid Content/Fish Size and 2378-TCDD Concentrations

relationship of lipid content and crab size with the measured 2378-TCDD concentrations was evaluated (Figure 4.61). The relationships seem much weaker than those observed for catfish, especially for the weight/length ratio.

To further analyze if dioxin patterns changed with season, the relationship between the sum of PCDDs and PCDFs¹⁰ was plotted for all the sampled media (Figure 4.62). Overall, the PCDD contribution is higher for most of the samples, with average $\Sigma\text{PCDD}/\Sigma\text{PCDF}$ ratios of 24.9, 24.2, 2.2, and 1.2 for water, sediment, catfish, and crab, respectively. Data in Figure 4.62 indicate that for sediment samples, the concentration patterns seem equivalent, with slightly different $\Sigma\text{PCDD}/\Sigma\text{PCDF}$ average ratios. Water and tissue data, on the other hand, exhibited different ratios for the various sampling events, especially catfish for which the slope of the best-fit line for data collected in the Summer was much greater than the ones for the other four events.

4.5 COMPARISON OF DIOXIN DATA AMONG THE THREE SAMPLED MEDIA

4.5.1 All data

Tables 4.21a and b summarize the average TEQ and 2378-TCDD concentrations measured in this study¹¹, respectively. In terms of TEQ, station 11273 (Patrick Bayou) was the most contaminated location in this study, with the highest average TEQ in water, and the second highest in sediment and crab. Among the stations located in the main channel and Upper Galveston Bay, station 15979 shows large contamination, with the third highest average TEQ

¹⁰ This ratio includes both dioxin-like and non dioxin-like PCDDs and PCDFs. All the samples collected were included in this calculation.

¹¹ TEQ calculated as the average of the available Summer-02, Fall-02, Spring-03, Spring-04, and Fall-04 concentrations at each location.

Figure 4.61 Relationship between Lipid Content/Crab Size and 2378-TCDD Concentrations

Figure 4.62 Relationship between PCDDs and PCDFs for the Various Sampling Events

Table 4.21a Average TEQ Concentrations by Media

Table 4.22b Average 2378-TCDD Concentrations by Media

concentration in sediment and water and the second highest average concentration in catfish.

Other dioxin "hot spots" were located at stations 11280 and 13344¹². Station 11193 in the San Jacinto River (segment 1001) exhibited the second highest average TEQ in water and the fourth highest TEQ in sediment.

In terms of 2378-TCDD, the two most contaminated locations were 11193 and 15979, with average concentrations in water and sediment among the three highest. Stations 11273 and 11265 were additional "hot spots."

4.5.2 Principal Component Analysis

As mentioned in a previous section, principal components analysis and cluster analysis were employed to analyze the spatial patterns (if any) of PCDD/Fs in the Houston Ship Channel. It was also thought that by considering various media together in one PCA, and then using hierarchical cluster analysis to confirm/deny clusters, it would be possible to see if the homologue profile patterns for one media could be correlated to those in another media.

All Media Analyzed Together

As was expected, the patterns of homologue profiles differ by media. This was anticipated because of the different partitioning properties of the different homologue groups. The heavier homologues (OCDD and OCDF) have lower vapor pressures and so tend to be found sorbed to particles. The lighter homologue groups, like TCDD and TCDF, have the highest vapor pressures and so tend to volatilize rather than be found sorbed to a particle. This means that homologue profiles, or fingerprints, at samples of different media will be different. This can be

¹² Hot spots defined as stations with average TEQs among the highest for 3 or more media.

readily seen by looking at Figure 4.63, which is a scatter plot of PCA for all the media together. The obvious outliers are station 11273 and facilities with water quality permits number 00749-001, 02097-001, and 00305-001. Another small group appears to include station 15979.

Dissolved Water, Dissolved Runoff, Dissolved Effluent, Air Vapor

Because the partitioning of PCDD/Fs is highly dependent upon vapor pressure, it was thought that perhaps the homologue profiles would be similar when comparing all of the dissolved media. Dissolved Water, dissolved runoff, dissolved effluent, and air vapor were analyzed together in one PCA, to establish common patterns among the different media. Figure 4.64 shows the scatter plot of the scores output from this analysis. Components one and two are graphed in terms of each other, since most of the variability is now explained by these two components. What the figure shows is that Dissolved Water, which is from the Houston Ship Channel, and Dissolved Effluent seem to be somewhat independent of each other. The dissolved runoff, however, is right in the middle of the dissolved water points. The air vapor fingerprints for stations C403 and C408, which are the only two air sampling stations in which air vapor and air particulate matter were separated, show that there is a relationship in the pattern of homologue groups with the effluent dissolved stations nearest but not with runoff or in-stream water. Although, looking at the cluster output, Figure 4.65, the cluster which includes the air homologue profiles does not differ much from the next cluster.

Suspended Water, Runoff, Effluent, Sediment

The same reasoning for dissolved PCDD/F patterns was the basis for this analysis. Because dioxins are hydrophobic, it could be possible to find similar patterns of homologue groups between media groups which contain suspended solids. One would expect dioxins to sorb

Figure 4.63 PCA Analysis for Concentrations in All Media

- Figure 4.64 PCA Analysis for Dissolved and Air Vapor Concentrations**
Figure 4.65 Dissolved Mixed Media Dendogram using Ward Method

to particles and thus might have different patterns than those in the dissolved phase. It can be seen in Figure 4.66 that the sediment sampling points seem to cluster together, all except for stations 15979 and 11273. Closely related to those stations are suspended effluent samples from three sources. This result is further supported by Figure 4.67, which is the hierarchical cluster analysis output for the same variables.

The Effluent Suspended samples seem to exhibit less clustering when compared to the Sediment stations. This is most likely because of the variability in homologue profiles from different sources. Once, however, the effluent becomes mixed with the waters of the HSC, the patterns would merge into one homologue profile which is what is shown in Figure 4.66. The Suspended Water samples show little variability in their profile, and are located overlapping the Runoff Suspended sample points. As mentioned before, this is most likely due to the mixing in the Ship Channel which would tend to homogenize the profiles into one fingerprint common to the Ship Channel. As far as the clustering of the sediment samples, it would be expected that the homologue profiles would be similar for most points in the HSC, due to yearly dredging, sediment-mixing effects of daily tide ebb-and-flow, ship/boat traffic wakes, and stormwater runoff pulses. The dredging would tend to re-suspend sediment particles and this re-suspension would cause a homogenous mixture downstream. The sediment data seem to reflect this. The stations with nearby sources of input are the only ones that are different from the rest.

4.6 ANALYSIS OF AIR DATA

Dioxins and furans in ambient air were monitored in monthly events at five different sampling locations between September 2002 and April 2004 and in bi-monthly events between

December 2004 and April 2005 (see Final Report for WO4 and Chapter 3 of this report for results). The monitoring sites represent different levels of industrialization across the city (Figure

Figure 4.66 PCA Analysis for Suspended and Bottom Sediment Concentrations
Figure 4.67 Suspended & Sediment Mixed Media Dendogram using Ward Method

4.68). The monitors at Clinton Drive (C403) and Haden Road (C603) are located in an industrial area, whereas Mont Belvieu (C610) is in a semi-rural area and Lang Road (C408) and Bayland Park (C53) are located in mostly residential areas. Co-located samplers were set up at C403 and C408 to determine V/P ratios.

Overall, the total ambient air dioxin concentrations were found ranging from 546 to 1,711 fg/m^3 at Clinton Drive (C403), from 269 to 2,427 fg/m^3 at Lang Road (C408), from 546 to 2,198 fg/m^3 at Haden Road, from 288 to 2,345 fg/m^3 at Mont Belvieu, and from 447 to 1,304 fg/m^3 at Bayland Park. It is worth noting that the two “industrial” sites had the highest minimum concentrations, but the highest maximum concentrations were at the “semi-rural” and one of the “mostly residential” sites.

Averaging, total ambient air dioxin concentrations for the first (Sep/02-Aug/03), second (Dec/03-Apr/04), and third (Sep/04-Feb/05) sampling periods (mean \pm standard deviation) of 879 ± 359 , 1159 ± 342 , and $1083 \pm 387 \text{ fg}/\text{m}^3$ were observed at Clinton Drive. Similarly, average total ambient air concentrations for the first (Sep/02-Aug/03) and second (Dec/03-Apr/04) sampling periods of 1171 ± 647 and $972 \pm 497 \text{ fg}/\text{m}^3$ were measured at Lang Road; average total concentrations of 1532 ± 552 and $667 \pm 595 \text{ fg}/\text{m}^3$ occurred in the first sampling period (Sep/02-Aug/03) at Haden Road and Mont Belvieu, respectively. Finally, a concentration of 709 ± 319 was found at Bayland Park from March 2003 to August 2003.

The higher chlorinated congeners such as 1234678-HpCDD, 1234678-HpCDF, OCDF, and especially OCDD were consistently found at all sites as the congeners making the major contribution to the total ambient air dioxin concentration. In most of the cases, the contribution of OCDD was found to be $>50\%$ at all stations during the period sampled (see Figure 4.69).

Concentrations for OCDD of up to 1718 fg/m³ were measured in the Houston area at the Mont Belvieu site in the January/03 event. The congener 2378-TCDD made a very low contribution to

Figure 4.68 Air Monitoring Sites

Figure 4.69 Ambient Air Profiles of Dioxins and Furans in Houston, TX

F 4.69 (2)

F 4.69 (3)

F 4.69 (4)

F 4.69 (5)

F 4.69 (6)

F 4.69 (7)

the total dioxin concentration during the period sampled. A maximum concentration of 2 fg/m³ was detected for this congener at the Haden Road site (the site in the industrial area) in the October/02 event.

In terms of Σ Texas-TEQ concentrations, values were found fluctuating from 6 to 20 fg Texas-TEQ/m³ at Clinton Drive, from 5 to 21 fg Texas-TEQ/m³ at Lang Road, from 8 to 48 fg Texas-TEQ/m³ at Haden Road, from 3 to 28 fg Texas-TEQ/m³ at Mont Belvieu, and from 6 to 11 fg Texas-TEQ/m³ at Bayland Park. The congeners 1,2,3,7,8-PeCDD and 2,3,4,7,8-PeCDF were consistently found as the major contributors to the Σ Texas-TEQ concentration. Contributions of up to 23, 22, 25, 22, and 25 % were observed for 12378-PeCDD at Clinton Drive, Lang Road, Haden Road, Mont Belvieu, and Bayland Park, respectively. Similarly, contributions of up to 31, 33, 30, 60, and 25 % were found for 23478-PeCDF at the same sites, respectively. Finally, 2,3,7,8TCDD's contributions to the Σ Texas-TEQ of up to 15, 20, 13, 17, and 19 % were observed at the aforementioned sites, respectively.

4.6.1 Vapor-to-particle Partitioning

Tables 4.22 and 4.23 show the range in the percentage of the total concentration that was particle bound for individual congeners over the sampling period at Clinton Drive and Lang Road, respectively. A general gradation in partitioning behavior was observed from compounds found totally/almost exclusively in the vapor phase (e.g., 2378-TCDD), through those that had substantial concentrations in both phases (e.g., 123478-HxCDD), to those that were totally/almost exclusively found on particles (e.g., OCDD). Partitioning behavior is influenced by several factors, notably compound vapor pressure, temperature, level of chlorination, and nature of

**Table 4.22 Particle-bound (P) and Vapor (V) Phase Concentrations and Particulate
fraction (PF) of Dioxins and Furans at Clinton Drive**

**Table 4.23 Particle-bound (P) and Vapor (V) Phase Concentrations and Particulate
Fraction (PF) of Dioxins and Furans at Lang Road**

particles.

Most of the total mass of the 2378-substituted congeners of dioxins and furans was extensively found bound to particles (see Tables 4.22 and 4.23). Total particulate fractions ranging from 0.85 to 0.98 and from 0.71 to 0.97 were detected at Clinton Drive and Lang Road, respectively. In terms of Σ Texas-TEQ particulate fractions, values fluctuating from 0.28 to 0.74 and from 0.23 to 0.66 were calculated at Clinton Drive and Lang Road, respectively.

Another finding from the collected data is that the dioxin congeners tend to be more associated with the particle phase than the furan congeners. This characteristic is due to differences in the vapor pressure (a temperature-dependent property) between these two groups of compounds (For example, an average particle fraction of 0.40 for 1,2,3,7,8-PeCDD versus 0.31 for 1,2,3,7,8-PeCDF at the Clinton Drive site - see Table 4.24).

The correlation between the mass fraction of each congener and the Σ Texas-TEQ bound to particles was assessed by linear regression (see Table 4.24). In general, the analysis showed a negative correlation of the particulate fraction with ambient temperature. This negative correlation means that the mass of a specific congener bound to particles increases as temperature decreases.

4.6.2 Temporal Trend

The temporal trend for each dioxin and furan congener at each location is illustrated in Figure 4.70a through e where the detected monthly/bi-monthly ambient air concentrations were plotted over time. The mean ambient temperature was also included in Figure 4.70. These plots suggest that there is dependence of the concentration over time due to level of chlorination, the

Table 4.24 Particulate Fraction (PF) versus Ambient Temperature Correlation Results

**Figure 4.70a Monthly/Bi-Monthly Ambient Air Concentrations of Dioxins and Furan
Congeners at *Clinton Drive***

**Figure 4.70b Monthly/Bi-Monthly Ambient Air Concentrations of Dioxins and Furan
Congeners at Lang Road**

Figure 4.70c Monthly Ambient Air Concentrations of Dioxins and Furan Congeners at Haden Road

**Figure 4.70d Monthly Ambient Air Concentrations of Dioxins and Furan Congeners at
Mont Belvieu**

Figure 4.70e Monthly Ambient Air Concentrations of Dioxins and Furan Congeners at Bayland Park

type of congener (i.e., dioxin or furan) and, the time of year (i.e., ambient temperature). Dioxin and furan congeners tended to peak during the colder months (November – March). This seasonal behavior is likely due to seasonal sources of dioxins (e.g., combustion sources), atmospheric variations such as air mass movement patterns, temperature inversion conditions, and alteration of atmospheric removal processes such as chemical reactions occurring in the atmosphere and wet and dry deposition.

The variation of the Σ Texas-TEQ concentration over time (i.e., temperature) was statistically assessed using the Mann Kendall test for trend at Clinton Drive, Lang Road, Haden Road, and Mont Belvieu. Data collected over one year of sampling (September 2002 –August 2003) was analyzed for temporal trend. The data from Bayland Park was not included in the analysis because the sampling at this location was carried out for only 6 months (March 2003-August 2003), and therefore is not comparable. The test indicated a statistically significant trend (at $\alpha = 0.05$) of increasing Σ Texas-TEQ concentration with decreasing ambient temperature at the four monitoring locations.

4.6.3 Spatial Trends

The spatial variability among the data collected at the different air monitoring sites was analyzed using the *t*-test. Data obtained at Bayland Park (C53) was excluded from the analysis because the length of the sampling period (only six months) at this location does not make it comparable with the rest of the sites. Prior to the examination of the spatial variability, the coefficient of variation (CV) (the ratio between the standard deviation and the mean) at each site and congener was assessed to determine if the use of normal distribution parameters to estimate central tendency and variability was appropriate. The results of this analysis are summarized in

Table 4.25. In general, CV values less than 2 were obtained for all congeners at all sites, with the exception of 2,3,7,8-TCDF at Mont Belvieu site (C610). These results suggested that the use of normal distribution parameters was appropriate. The p -values of the pairs of monitoring sites were analyzed at an $\alpha=0.05$ significance level and the results are also summarized in Table 4.25. In this analysis, the null hypothesis (H_0) of equal means ($\mu_x=\mu_y$) was tested against the alternative hypothesis (H_A) of difference of means ($\mu_x\neq\mu_y$). Overall, significant statistical spatial differences were observed among the congener, total ambient air, and Σ Texas-TEQ concentrations. For example, 2378-TCDD was found to fluctuate among the air monitoring pairs C403-C603, C403-C610, C408-C610, and C603-C610. Similarly, 1,2,3,7,8-PeCDD, one of the major contributors to the Σ Texas-TEQ concentrations was found to show significant statistical differences among the pairs C403-C603, C403-C610, C408-C603, C408-C610, and C603-C610. In contrast, no significant difference was observed for OCDD among the pairs of sites analyzed. Finally, Σ Texas-TEQ concentrations showed significant differences among the pairs C403-C603, C408-C603, C408-C610, and C603-C610. From these results, it is concluded that the Houston data exhibit spatial variability based on the observed differences between the sampled sites.

The overall spatial variability in the Houston data was further confirmed by applying the Kruskal-Wallis non-parametric comparison test on Σ Texas-TEQ concentrations at an $\alpha=0.05$ level. This test also indicated that statistically different Σ Texas-TEQ concentrations exist among the four locations tested. These variations may be attributed to differences in air mass movement across the airshed and type of sources involved.

Table 4.25 Coefficient of Variation (CV) and p-value Results (September 2002 – August 2003)

4.6.4 Source Identification

The ambient air concentrations of dioxins were related to various emission sources of these compounds in order to explain the origin and contribution of these sources to the observed occurrence of these compounds in the Houston area. To identify the potential pollution sources, the ambient air concentrations were compared with (i) EPA's dioxin congener profile source database that contain the congener profiles of different sources of dioxin to the U.S. environment such as municipal, medical, and hazardous waste incineration, unleaded fuel combustion in vehicles, diesel fuel combustion in trucks among others, and (ii) EPA's Toxic Release Inventory Program (TRI) that contains information about the potential and confirmed sources of dioxins in Harris and surrounding counties. Figure 4.71 illustrates the potential sources of dioxins classified by SIC codes present in the area of study (e.g., industrial organic chemicals, petroleum refining, and pesticides and agricultural chemicals). Similarly, Figure 4.72 shows the potential and confirmed sources of dioxins for the year 2003 in the Harris and surrounding counties. A total of 35 industrial facilities out of 214 reported dioxin releases for the year 2003.

Historical air emission data of dioxins in Harris and surrounding counties from EPA's TRI program is depicted in Figure 4.73. As seen in Figure 4.73, a 53% decrease in air dioxin emissions occurred from 2000 to 2003, based on EPA's TRI program data.

Because the information from emission sources and receptors (ambient air) are expressed differently than data from this project, the data, prior to analysis, were normalized dividing the concentration of each 2378-substituted congener by the total sum of the 17 congeners at that specific sample (see Figure 4.69 for Houston profiles). The source profiles of the EPA's dioxin congener database are shown in Figure 4.74. This database includes profiles of municipal solid

Figure 4.71 Potential Sources of Dioxins Classified by SIC Codes (Year 2003)

Figure 4.72 Potential and Confirmed Sources of Dioxins in Harris and Surrounding Counties (Year 2003)

**Figure 4.73 Historical Air Emissions of Dioxins in Harris and Surrounding Counties from
Year 2000 to 2003**

Figure 4.74 EPA’s Dioxin Congener Profile Source Database.

F 4.74 (2)

waste incineration (MSWI), medical waste incineration (MWI), hazardous waste incineration (HWI), combustion of wastewater sludge at bleach chemical pulp mills (PULP), utility sector and industrial boilers (UTBO), utilities and industrial coal combustion (UTCC), petroleum refining catalyst regeneration (PETRO), primary ferrous metal smelting (PFE), secondary aluminum smelters (SAL), secondary copper refinery (SCU), and ferrous foundries (FEF). Table 4.26 lists the confirmed sources of dioxins in the Houston area (year 2003) from the EPA's Toxic Release Inventory Program (TRI).

Principal Component Analysis (PCA) was applied to the air data similar to the analysis for the other media (using SPSS for Windows Version 10.0.5).

Ambient Air Concentration versus EPA's dioxin congener profile source database

Profiles of the ambient air concentrations of Houston and EPA's dioxin source database were compared in order to determine the degree of correlation between dioxin concentrations at different receptors sites and typical emission sources of these compounds.

Figure 4.75 shows the two-dimensional score plots for the five ambient air stations in Houston and the EPA's dioxin congener profile source database. As seen in Figure 4.75, the data sets with similarities in the profiles were closely located, while those with divergent signatures were found further apart. The score plots revealed that the ambient air stations Clinton Drive, Lang Road, Mont Belvieu, and Bayland Park were consistently found in closeness with DFV (Diesel-fueled vehicles) and UTBO (utility sector and industrial boilers) profiles. Similarly, the ambient air profiles were found moderately connected with UFV (unleaded-fueled vehicles), PULP (pulp mills), HWI (hazardous waste incineration), MSWI (municipal solid waste incineration), and UTCC (utilities and industrial coal combustion). The profiles of these emission

**Table 4.26 Confirmed Sources of Dioxins in the Houston Area (year 2003) from the EPA's
Toxic Release Inventory (TRI) Program**

T 4.26 (2)

Figure 4.75 Score Plots from PCA When Comparing the Five Ambient Air Stations with the EPA’s Dioxin Source Database

F 4.75 (2)

F 4.75 (3)

sources are characterized by exhibiting considerable contributions of the higher chlorinated congeners (especially OCDD), similar to what is observed among the ambient air samples. No similarities were found between ambient air profiles and mineral smelting and refinery industries. The same cluster analysis was carried out using hierarchical cluster analysis (SPSS for Windows Version 10.0.5) and analogous results were obtained.

In contrast with these results, none of the ambient air profiles obtained at the Haden Road site seems to show any similarity with the EPA's dioxin congener source profiles with the exception of the events 2 (Oct/02), 3 (Nov/02), and 9 (May/03) that correlated with DFV (Diesel-fueled vehicles) and UTBO (utility sector and industrial boilers) profiles, and event 4 (Dec/03) that correlated with MSWI (municipal solid waste incineration) and UTCC (utilities and industrial coal combustion). These discrepancies among the Haden Road ambient air profiles may be attributed to higher levels of OCDF that are emitted in the proximity of the site. Ambient air profile contributions of up to 60% were observed for this congener (see Figure 4.69). This difference was explored comparing the Haden Road site with the confirmed sources of dioxins reported by EPA's TRI for Harris and surrounding counties as seen in the next section.

Ambient Air Concentration versus Confirmed Sources of Dioxins in Harris and Surroundings Counties

The dioxin ambient air profiles observed in Houston at the five different air-monitoring locations were also compared with confirmed sources of dioxins in the Houston area. The purpose of this analysis was to determine similarities, dissimilarities, and individual contributions to the dioxin pollution. The PCA analysis showed a consistent correlation at all of the air monitoring sites with emission sources # 2, 6, 16, 18, 31, and 35 listed in Table 4.26. These

emission sources are classified under the SIC code as sawmills and planing mills-2421 (#31), paper mills-2621 (#18), plastics, synthetic resins and nonvulcanized elastomers-2821 (#2, #16), industrial organic chemicals-2869 (#6), and electric services-4911 (#35). Figure 4.76 illustrates the clusters found at each air-monitoring site. In most of the cases, confirmed sources of dioxins in Houston are characterized by having a low contribution of 2378-TCDD as seen in the ambient air profiles. It is also noted that Haden Road (C603) seems to differ from the rest of the ambient air profiles with higher contributions of OCDF. This dissimilarity may be attributed to the fact that this site is located proximate to a pesticide plant (#10) where pesticides and agricultural chemicals are produced. As shown in Table 4.26, OCDF is a large component of dioxin emission for this type of industrial activity. Figure 4.76 shows that for the months where low concentrations of OCDF were detected, these months were located far apart from emission source #10. On the other hand, months with reported high concentrations of OCDF (April and June 2003) tend to be located in the vicinity of the emission source #10. However, it is important to note that despite these emissions, the profile observed at Haden Road tends to undergo a quick redistribution when low OCDF concentrations are detected (see Figure 4.69 for Haden Road site) (e.g., October event) therefore showing the higher chlorinated congener (especially OCDD) making the major contribution to the profile. Identical results were obtained using hierarchical cluster analysis (SPSS for Windows Version 10.0.5).

4.6.5 Dry Deposition versus Ambient Air Concentrations

A *t*-test demonstrated the existence of spatial variability of the dry deposition (Chapter 3). This finding differs with the no spatial variability observed among the ambient air concentration samples collected at these two locations (see Table 4.25 pair C403-C408). These differences may

Figure 4.76 Score Plots from PCA When Comparing the Five Ambient Air Stations with the Confirmed Sources of Dioxins in Harris and Surroundings Counties from TRI

F 4.76 (2)

F 4.76 (3)

be due to differences in the particle size distribution of associated dioxins, the existing meteorological conditions (e.g., wind speed and direction, atmospheric stability), and the type of sources.

The dry deposition fluxes for 1234678-HpCDD, OCDD, 1234678-HpCDF, and OCDF, obtained in the first and second deposition experiments (Results presented in Chapter 3), were correlated with their ambient air concentrations by linear regression. The r^2 values derived from this analysis are summarized in Table 4.27. In general, the results showed a poor correlation between the dry deposition fluxes and ambient air concentrations. This lack of correlation might be attributed to differences in the particle size distribution of associated dioxin congeners and the fact that dry deposition is governed by the size of the depositing particles. As discussed in Chapter 3, the particle size distribution samples demonstrated that most of the dioxin congener mass was concentrated in fine particles that exhibit low deposition.

Table 4.27 Dry Deposition Fluxes versus Ambient Air Concentration Results

Congener	r^2
1,2,3,4,6,7,8-HpCDD	0.15
OCDD	0.26
1,2,3,4,6,7,8-HpCDF	0.004
OCDF	0.13
Σ (PCDD+PCDF)	0.23

4.6.6 Analysis of Various Air Matrices

In order to evaluate possible similarities and/or difference among the different environmental matrices (particle and gas phases, and wet, dry and bulk deposition), PCA analysis

was applied. The results of the analysis are summarized in Figure 4.77 where three basic clusters of data can be distinguished. It is noted that the particle-phase profile more closely resembles the deposition profiles (dry, wet, and bulk) than the gas-phase profile. This evidences that deposition processes are governed by the fraction of dioxins that are bound to atmospheric particles.

Moreover, the results also evidence that the deposition processes are influenced by the level of chlorination for the 2378-substituted congeners. Dioxins with higher levels of chlorination (e.g., 1234678-HpCDD) are removed more efficiently from the atmosphere. The same analysis was made using Hierarchical Cluster Analysis (SPSS for Windows Version 10.0.5). Similar and comparable results were obtained (Figure 4.78).

4.6.7 Deposition Loads

Using the dry/wet deposition fluxes measured at Clinton Dr., loads for the entire Houston Ship Channel watershed were calculated assuming constant fluxes across the watershed (Table 4.28). Direct deposition (wet&dry) of TEQ and 2378-TCDD to the channel surface was estimated to be 1.05×10^8 and 1.42×10^7 pg/yr, respectively when non-detects are set equal to half of the detection limit and 4.66×10^7 and 0 pg/yr, when non-detects are equal to zero. Similarly, when non-detects are assumed equal to half of the detection limit, total deposition over the entire watershed was estimated to be 5.80×10^9 and 7.84×10^8 pg/yr for TEQ and 2378-TCDD, respectively. While if non-detects are assumed equal to zero, total deposition over the entire watershed was estimated to be 2.57×10^9 and 0 pg/yr for TEQ and 2378-TCDD, respectively.

Figure 4.77 Score Plot from PCA When Comparing Particle-Bound (p) and Vapor (v) Concentrations, Wet (wd) and Dry (d) Deposition, Bulk (b) Deposition Profiles

Figure 4.78 Hierarchical Cluster Analysis Dendrogram When Comparing Particle-Bound (p) and Vapor (v) Concentrations, Wet (wd) and Dry (d) Deposition, Bulk (b) Deposition Profiles

Table 4.28 Deposition Loads

4.7 ANALYSIS OF RUNOFF DATA

4.7.1 Runoff Concentrations versus Physical Properties

The observed TEQ concentrations in runoff were correlated with TSS, and TOC concentrations by linear regression (Figure 4.79, 4.80, and 4.81). Similarly, the Σ Texas-TEQ in the suspended phase was correlated with the Σ Texas-TEQ in the dissolved phase (Figure 4.82). The results showed that the Σ Texas-TEQ in the 40- μ m suspended phase was better correlated with TSS than the 1- μ m phase (r^2 of 0.4963 versus 0.0892). A weak correlation was obtained between the combined Σ Texas-TEQ (suspended + dissolved) and the TOC concentration. Finally, an r^2 of 0.7 was obtained when correlating the Σ Texas-TEQ observed in the suspended phase (1 and 40 μ m) with that of the dissolved phase.

4.7.2 Runoff versus Soil/Sediment Profiles

Similarities and differences between the suspended-phase runoff and sediment profiles were evaluated by PCA and Hierarchical cluster analysis (Figure 4.83 and 4.84, respectively). Results obtained using these techniques were comparable. The results showed that, in general, the profiles for the 1- and 40- μ m suspended phases are in proximity to the sediment profile at each site with the exception of site SS-8 that exhibited differences between the suspended and sediment profiles. It is also noted that the sites SS-9, SS-8 and SS-16 are each grouped in different clusters and separate from the remaining sites: SS-10, SS-13, SS-14, and SS-15. These dissimilarities among the sites may be attributed to the presence of different types of sources that have a specific impact at each site.

Figure 4.79 TEQ Concentration in the 1- μm Suspended Phase Versus TSS

Figure 4.80 TEQ Concentration in the 40- μm Suspended Phase Versus TSS

Figure 4.81 Combined TEQ Concentration Versus TOC

Figure 4.82 TEQ Suspended-Phase Concentration Versus TEQ Dissolved-Phase

Figure 4.83 Score Plot from PCA When Comparing 1- and 40- μ m Suspended Phases and Urban Sediment (During Runoff Conditions) Profiles

Figure 4.84 Hierarchical Cluster Analysis Dendrogram When Comparing 1- and 40- μ m Suspended Phases and Urban Sediment (During Runoff Conditions) Profiles

CHAPTER 5

MODEL DEVELOPMENT

The goal of this task is to use models to elucidate the sources and major processes controlling observed levels of dioxins in the Houston Ship Channel and to identify the maximum permissible loading that would not impair water quality. Development of a preliminary mass-balance of dioxins in the HSC was completed using the MEGA-TX model (a modification of the QUAL-TX model completed for this project) to ensure that all the sources and process had been identified. In addition, a steady-state WASP model of the HSC was developed and a 1-month transient WASP simulation is underway. A conceptual model for dioxins in the HSC is provided in Figure 5.1. Major sources of dioxin to the channel include wet/dry air deposition, direct discharges, tributary input, sediment resuspension, land runoff, and discharges from groundwater. Major sinks include biodegradation, sediment burial, sediment removal by dredging, volatilization, groundwater outflow, hydrolysis, and photolysis (Figure 5.1).

5.1 MEGA-TX MODEL OF THE HOUSTON SHIP CHANNEL

5.1.1 Conceptual Model and Schematic

The MEGA-TX model was used to create a preliminary mass balance of TEQ and 2378-TCDD in the system. The simplified conceptual model representation of the physical system for MEGA-TX is presented in Figure 5.2a. The MEGA-TX model has the capability of incorporating point source discharges, nonpoint source runoff that includes dioxins from atmospheric deposition, and direct atmospheric deposition to the receiving water bodies. In addition the

Figure 5.1 Conceptual Model for Dioxins in the HSC

Figure 5.2a MEGA-TX Conceptual Source Schematic
Figure 5.2b MEGA-TX Fate and Transport Schematic

model has the capability to simulate the transport and fate pathways and kinetics shown in Figure 5.2b. The MEGA-TX model also incorporates calibrated and accepted hydraulics for the receiving water bodies, and is easy to use and configure. It is noted that, because the mass balance was to be used as a preliminary, screening tool, only some of the dioxin sources/sinks identified in Figure 5.1 are included in the MEGA-TX model for dioxins in the HSC. Inclusion of all the processes will be completed using the WASP numerical model.

As a starting point, the same schematic that TCEQ employed for the recent nickel TMDL was used. The TCEQ nickel model schematic consists of a main model that encompasses the HSC system from the lower boundary at Morgans Point upstream to the approximate tidal limits of each of the tributaries and ten tributary models. The reasoning behind splitting the HSC system into eleven sub models lies in the historical limitations of the QUAL-TX model. The version of QUAL-TX currently in use by TCEQ is written in FORTRAN 77 and is dimensioned sufficiently to simulate the HSC main model on a typical PC.

A drawback resulting from splitting the HSC system into sub models is the effective blocking of dispersive transport from a downstream model to an upstream tributary model. The upstream tributary models are run first and their output is transferred to an intermediate file that is read as input by the downstream model at the appropriate location. Using this method, however, precludes any communication of dispersive or advective transport upstream from the lower model. The effect of this simplification is minimized by breaking the models at the approximate tidal limit where advective transport is theoretically downstream only and upstream dispersive transport is negligible.

Downstream to upstream dispersive transport was deemed of sufficient significance in the screening runs of QUAL-TX to justify modifying the model to eliminate the problem of interconnected sub-models. To provide this capability, some changes were made to the QUAL-TX code. The FORTRAN 77 code was updated to Fortran 95 and dynamic memory allocation was added. The new code is not constrained to a maximum size of model by static dimensioning, since it reads the input and dynamically allocates memory. The original QUAL-TX input decks for the TCEQ Nickel TMDL on the HSC were joined into a single model. The new model (MEGA-TX) is comprised of 481 model reaches that encompass 2100 individual calculational elements (Figure G-1 in Appendix G). The model has 172 headwater elements and a single lower boundary element to represent the main channel of the Houston Ship Channel/Buffalo Bayou and 171 tributaries.

In addition to being combined into a single model, the HSC nickel TMDL input decks were modified to simulate dioxin rather than nickel. In the dioxin TMDL HSC models, dioxin is modeled as a user-defined nonconservative parameter. Utilizing the MEGA-TX nonconservative parameter allows the inclusion of settling. Figure 5.3 is a schematic representation of the fate of dioxin in the MEGA-TX model.

5.1.2 Input Data

5.1.2.1 Hydraulic Model Input

The hydraulic and physical characteristics of each reach in the HSC model were obtained from the QUAL-TX model developed for the Nickel TMDL study (TNRCC, 2002). The upper boundaries are represented in the model by the headwaters. The lower boundary, on the other

Figure 5.3 MEGA-TX Dioxin Schematic

hand, was set in Channel Marker 75 (Km -8.0, station 14560) in Galveston Bay, with water concentrations measured in Summer 2002: 0.1124 pg/L for TEQ and 0.0501 pg/L for 2378-TCDD.

5.1.2.2 Point Sources

Input from point sources is simulated in MEGA-TX by a steady state flow and a dioxin (TEQ or 2378-TCDD) concentration. The MEGA-TX input contains permitted flow values, as included in the TCEQ permittee database (as of May 2003). A second input deck with the average self-reporting flow for the period 1997-2002 was also prepared and run for comparison purposes. Dioxin concentrations from point sources (PS) gathered in this project during Spring 2003 were used as model input. For the point sources that were not sampled for effluent, one of the following three approaches was used to estimate a dioxin concentration:

1. If the PS was sampled for sludge, the concentration in effluent was extrapolated from a regression between the concentration in sludge and the concentration in effluent for the point sources sampled for both, as shown in Figure 5.4.
2. If the PS was not sampled for sludge or for effluent and the SIC was among those identified as potential dioxin dischargers, the dioxin concentration in effluent was assumed equal to the average dioxin concentration for effluent from facilities with the same SIC code. If no facilities with the SIC code of the PS were sampled, the dioxin concentration was assumed as the average dioxin concentration of all the sampled industrial outfalls.
3. If the PS was not sampled and the SIC code was not among those identified as potential sources of dioxins, the concentration was assumed zero.

Figure 5.4 Relationship between Measured Dioxin Levels in Sludge and Effluent

The point source concentrations are entered into the model in femtograms per liter (fg/L). Figures 5.5a and b show the distribution of PS in the HSC system and the magnitude of the TEQ and 2378-TCDD concentration entered into the model, respectively. Figures 5.6 and 5.7 summarize the distribution of point sources entered into the MEGA-TX model by segment using permitted and average self-reported flows, respectively. The total load from PS to the HSC system using permitted flows is estimated to be 5.98×10^5 ng/day for TEQ and 1.11×10^5 ng/day for 2378-TCDD, excluding any loads from the San Jacinto River above the Lake Houston Dam or from Galveston Bay. Similarly, the PS load to the HSC system using average self-reported flows is estimated to be 3.42×10^5 ng/day for TEQ and 5.71×10^4 ng/day for 2378-TCDD. Appendix G includes the input files.

5.1.2.3 Non-point Sources

Non-point source pollutant loads on a daily basis for the HSC watershed were calculated using land cover information, the dioxin concentrations in runoff measured in 2002/2003, and the recorded rainfall in 2002.

Subwatershed Delineation

The HSC watershed covers a total of 1,208 square miles within the San Jacinto River basin in Texas. In order to better simulate the fate and transport of dioxins, the model area was divided into a total of 355 subwatersheds. Subwatershed delineation was performed using ArcView 3.2 and CRWR-PrePro (a watershed delineation system developed by the Center for Research in Water Resources at the University of Texas at Austin). The delineation was based upon digital elevation (DEM) Arc/Info grids; an Rf3 stream network; and the reaches established for the HSC Nickel QUAL-TX model.

Figure 5.5a Point Source TEQ Concentrations Input to MEGA-TX Model

Figure 5.5b 2378-TCDD Point Source Concentrations Input to mega-TX Model

Figure 5.6 Point Source Flows and Loads by Segment using Permitted Flows

Figure 5.7 Point Source Flows and Loads by Segment using Average Self-reported Flows

DEMS used for delineation were obtained from BASINS 3, USGS DEM elevations grids (1:250,000 scale). The DEM grid data provided with BASINS 3.0 have 3 arc second cell (approximately 90 x 90 meter). DEM grids from Hydrologic Unit Codes 12030203, 12040101, 12040102, 12040103, 12040104, 12040202, 12040203, 12040204, 12040205 were merged together to form one large Grid. The BASINS Rf3 stream files were used for initial stream burn-in and outlets were added at the beginning of the model reaches, when necessary, in order to determine the drainage area for each reach. Figure 5.8 shows the resulting subwatershed delineation. It is important to note that this delineation differed from that used by the Harris County Flood Control District (HCFCD) because of the different methods used for watershed delineation.

Rainfall Data

Rainfall data from January 1, 2002 to December 31, 2002 were obtained from the Harris County Office of Emergency Management (OEM) webpage for the rain gages in the HSC watershed (Figure 5.9). These gages were selected based on the completeness of the rain data and the proximity of the rain gages to the subwatersheds. Average daily rainfall data were calculated as the total amount of rainfall for the year 2002 divided by 365 days. Each subwatershed was assigned the rainfall data from the closest gage.

Runoff Volume

The amount of runoff for each subwatershed was calculated using the SCS runoff curve number method (Natural Resource Conservation Service, 1986). The SCS Runoff Curve Number (CN) method is described in detail in NEH-4 (SCS 1985). The SCS runoff equation is:

Figure 5.8 Subwatershed Delineation for the Houston Ship Channel

Figure 5.9 Harris County OEM Rain Gages

$$Q = \frac{(P - I_a)^2}{(P - I_a) + S} \quad (5.1)$$

where Q = runoff (in);

P = rainfall (in);

S = potential maximum retention after runoff begins (in); and

I_a = initial abstraction (in).

Initial abstraction refers to all the losses before runoff begins and includes water intercepted by vegetation, infiltration, evaporation, and water retained in surface depressions.

This parameter is very variable but is correlated to land cover and soil type (NRCS, 1986). The Natural Resource Conservation Service (1986) estimates I_a to be equal to

$$I_a = 0.2S \quad (5.2)$$

Substituting equation (5.2) into equation (5.1) gives a runoff estimate as a function of S and P :

$$Q = \frac{(P - 0.2S)^2}{(P + 0.8S)} \quad (5.3)$$

Finally, S is related to the curve number (CN) by

$$S = \frac{1000}{CN} - 10 \quad (5.4)$$

CN values range from 0 to 100 and are based on land cover and soil group. For this runoff calculation, all subwatersheds were assumed to be in soil group D (silts and clays) that generally has low infiltration rates. Land coverage data developed by the HGAC in 2002 (HGAC, 2003) were used. The classification system for the HGAC dataset and their corresponding runoff curve numbers are included in Table 5.1.

Table 5.1 Runoff Curve Numbers for the HSC Watershed

Land Cover Code	Land Cover Description	CN^a
1	Developed	96
2	Grass/Agriculture	89
3	Woodland	77
4	Open Water	0
5	Wetlands	30
6	Transitional/Bare	94

^a Obtained from “Urban Hydrology for Small Watersheds.” Natural Resources Conservation Service, Technical Release 55, June 1986.

Non-point Source Loads

The total TEQ and 2378-TCDD concentrations in runoff measured in 2002/2003 in this project were used to calculate NPS loads for the different reaches in the MEGA-TX model. Because the drainage areas of the stormwater ditches sampled in Spring 2003 are not composed of a single land cover category, it was not possible to determine a dioxin concentration for each land cover type. Therefore, the available runoff dioxin data were assigned to the different subwatersheds based on proximity between the sampled stations and the specific watersheds. For each reach, the corresponding runoff TEQ concentration was multiplied by the drainage area to

calculate the NPS load. The resulting daily loads, normalized by subwatershed area are shown in Figures 5.10a and b for TEQ and 2378-TCDD, respectively. The calculated subwatershed concentrations ranged from 0.05 to 15.22 ng/acre/day for TEQ and from 0.006 to 0.27 ng/acre/day for 2378-TCDD. The total loads of NPS to the HSC system were estimated to be 1.17×10^6 and 6.74×10^4 ng/day for TEQ and 2378-TCDD, respectively. These estimates are based on the results from the 10 runoff samples gathered in 2202/2003. It is noted that direct dry-deposition to the HSC streams was not included in the NPS load calculation.

5.1.2.4 Decay and Settling Rates

Dioxin decay from the water column (biodegradation, volatilization, and photolysis) was assumed negligible and, thus, a first-order decay rate of zero was used in the model. Settling rates were assumed equal to the sediment net accumulation rates calculated using historical TSS data and dredging records from the Corps of Engineers (see Section 3.3). Table 5.2 summarizes the sediment accumulation rates in the Houston Ship Channel for the 1990's decade from Morgan's Point to the Turning Basin. Settling rates for the tributaries were assumed as the average of the available rates for the main channel. It is noted that these settling rates are probably overestimates, because they are based on sedimentation into the actual narrow deep channel, which is probably dominated in some reaches by sediment transport from tributaries, the undredged sides of the channel, and adjacent side bays.

Figure 5.10a Non-point Source Loads of TEQ to the HSC

Figure 5.10b Non-point Source Loads of 2378-TCDD to the HSC

Table 5.2 Average Sediment Accumulation Rates

Channel Km	Sediment Accumulation Rate	
	(ft/yr)	(m/day)
2.5	0.897	0.0007
7.5	1.357	0.0011
12.5	0.699	0.0006
17.5	0.618	0.0005
22.5	0.413	0.0003
32.5	0.346	0.0003
37.5	0.745	0.0006
40.82	2.073	0.0017
Average for tributaries	0.893	0.0007

To track the fate of settled dioxin, the "Conversion to SOD" factor in the model is enabled and set to a value of 1.0. This option forces MEGA-TX to report the areal flux of dioxin to the sediments for each calculational element in the model.

5.1.3 Output Data

The total TEQ and 2378-TCDD water column concentration results from the runs of the MEGA-TX dioxin model are shown in Figures 5.11a and b, respectively, and the sediment flux results are shown in Figure 5.12. As can be seen, the modeled concentrations are lower than the measured ones in some reaches. Observed concentrations in the vicinity of stations 15979 and

11193 are elevated and could not be matched using data from known sources even when adjusting all model parameters. As a preliminary attempt to calibrate the model, a source of 5×10^6 ng/day for TEQ and 3.5×10^6 ng/day for 2378-TCDD (assuming no flow associated with such a source)

Figure 5.11a Total TEQ in Water Column

Figure 5.11b Total 2378-TCDD in Water Column

Figure 5.12 Dioxin Sediment Flux

was input to the model to match the measured concentration at station 15979 in Summer 2002 (Figure 5.13). This would suggest "possible unidentified/ unquantified sources" in the vicinity of this sampling station. Similarly, an additional source would have to be entered in the vicinity of station 11193 to match the peak observed at that location. Possible unquantified sources include road runoff, groundwater leachate, dredged material leachate, and localized contaminated sediments (e.g. old waste pit in San Jacinto River at I-10, currently under investigation). It is also noted that resuspension in general is likely to have been underestimated due to the fact that MEGA-TX has no mechanism for increasing the water column concentration from a bed load pool (due to scour or desorption). This may account for some of the difference between observed and modeled concentrations along the channel.

A preliminary mass balance using MEGA-TX results to date is presented in Table 5.3. It must be noted that the unknown/unquantified source (74% of the total TEQ load and 95% of the total 2378-TCDD load to the system) corresponds to that load that allowed matching the concentrations measured at station 15979 in Summer 2002. Concentrations at station 11193 were not matched using the MEGA-TX model.

**Figure 5.13 MEGA-TX Output Assuming Suspected Source in the Vicinity of Station
15979**

Table 5.3 Summary of Dioxin Loadings to the HSC

Source	TEQ		2378-TCDD	
	Load (ng/day)	Contribution to Total Loading	Load (ng/day)	Contribution to Total Loading
Permitted Point Sources	5.98x10 ⁵	9%	1.11x10 ⁵	3%
Stormwater Runoff	1.17x10 ⁶	17%	6.74x10 ⁴	2%
Unknown/unquantified	5.00x10 ⁶	74%	3.50x10 ⁶	95%
TOTAL	6.77x10⁶		3.68x10⁶	

Note: The unknown source does not include the source necessary to match concentrations at station 11193. If that were done, the estimated % of unknown/unquantified load would be higher.

5.1.4 Sensitivity Analysis

Sensitivity analyses were conducted to examine the effect of changing the settling rate, runoff loadings, and permitted point source loadings on the overall concentration profile. For loadings, model parameters (flow and concentration) were varied individually by factors equal to 0.1, 0.5, 2, and 10. For settling rates, uniform rates of 0, 0.05, 0.1, 0.2, 1, and 2 m/day were input (Base case rates in m/day were summarized in Table 5.2). In addition, a model run assuming a settling rate of 0.00004 m/day for tributaries was completed. Results from the sensitivity analysis are presented in Figures 5.14 and 5.15 for the main channel and San Jacinto River, respectively. None of the adjusted parameters produced a concentration profile that matched the measured concentrations as discussed previously.

5.2 WASP SIMPLIFIED MODEL

The Water Quality Analysis Simulation Program (WASP) is a dynamic compartment model that can be used to simulate contaminant fate and transport in surface water. For this study WASP version 7.1 (Wool et al, 2004) is being used. The model consists of a main program,

Figure 5.14 Results of Sensitivity Analysis - Main Channel

Figure 5.15 Results of Sensitivity Analysis - San Jacinto River

WASP7, and three subprograms: EUTRO5, TOXI5, and DYNHYD5. EUTRO5 is used to model BOD/DO eutrophication, TOXI5 is used to simulate toxic chemicals (tracers, organics, metals), and DYNHYD5 is used to simulate hydrodynamics.

WASP can be applied in 1-, 2-, or 3-D and can be linked to simulated hydrodynamics and sediment transport models. The model includes both the surface water column and the underlying benthic sediment layer. WASP simulates the varying processes of advection, dispersion, point and non-point mass loading, deposition/resuspension, and boundary exchange.

To model dioxin in the HSC, the TOXI5 model is used. TOXI5 can simulate up to six systems and 13 levels of complexity as summarized in Table 5.4. For the dioxin model, level 3 solids (simulated TSS), equilibrium level 3 (hydrophobic sorption), and kinetics 1 or 2 are needed. For this level of complexity, the equations used in the constituent mass balance are (for a 1-D system):

$$\frac{\partial C}{\partial t} = \frac{\partial}{\partial x} \left(-U_x A C + E_x A \frac{\partial C}{\partial x} \right) + A(S_L + S_B + S_K) \quad (5.5a)$$

where C = concentration of the water quality constituent (mg/L)

t = time (days)

A = cross-sectional area (m²)

U_x = longitudinal advective velocity (m/s)

E_x = longitudinal dispersion coefficient (m²/s)

S_L = direct and diffuse loading rate (g/m³-d)

S_B = boundary loading rate (g/m³-d)

S_K = total kinetic transformation rate (g/m³-d)

Table 5.4 TOX15 Systems and Levels of Complexity

or

$$\frac{\partial C}{\partial t} = -\frac{\partial}{\partial x}(UC) + \frac{\partial}{\partial x}\left(E_x \frac{\partial C}{\partial x}\right) - \frac{C_s}{S}W_d + \frac{C_{s,b}}{S_b}W_e + S_B + S_K \quad (5.5b)$$

where W_d = rate of sediment deposition ($\text{g}/\text{m}^3\text{-s}$)

W_e = scour rate of sediment ($\text{g}/\text{m}^3\text{-s}$)

C_s = constituent sorbed concentration in the water column (mg/L)

$C_{s,b}$ = constituent sorbed concentration in the bottom sediment (mg/kg)

S = concentration of suspended sediment (mg/L)

S_b = sediment concentration in bottom sediment (mg/kg)

and

$$C_s = K_p S C_w \quad (5.6a)$$

$$K_p = f_{oc} K_{oc} \quad (5.6b)$$

where C_w is the concentration of dissolved constituent (mg/L), K_p is the linear partitioning coefficient, f_{oc} is the organic carbon mass fraction of suspended sediment (g/g), and K_{oc} is the organic-carbon partitioning coefficient of the constituent (L/kg).

A list of WASP input requirements for the dioxin model is included in Table 5.5.

Table 5.5 Data Requirements for the Dioxin WASP Model for the HSC

Data Group	Description	Source
A	Model Identification and Simulation Control	Basic simulation information including variables to simulate obtained from the statement of the problem

Data Group	Description	Source
B	<p>Exchange Coefficients Dispersion coefficient (water column and pore water) Cross-sectional area Characteristic length</p>	<p>Calibration to a tracer or values from literature Channel data Channel data</p>
C	<p>Volumes Number of segments Type of segment (water column or benthic) Hydraulic geometry to derive depth and velocity as a function of flow</p>	<p>Conceptual model for the channel Conceptual model Hydrodynamic model, rating curves from existing models for the site, or empirical coefficients for a given cross-section derived from Manning’s equation</p>
D	<p>Flows - <i>Surface and Pore Water</i> Number of transport fields (up to six) Flow routing Flow time function - <i>Sediment Transport</i> Area for settling and resuspension Flow routing Velocity (settling or resuspension)</p>	<p>Conceptual model Channel data Historical data (steady-state or dynamic), hydrodynamic linkage Channel data Channel data Sediment load study for the HSC, initial settling velocities estimated using Stoke’s equation. Refine initial estimates with channel-specific calibration</p>
E	<p>Boundary Concentrations Concentrations for each system at segments that import, export, or exchange water with locations outside the network</p>	<p>Channel data</p>

Data Group	Description	Source
F	<p>Waste Loads Point source loadings</p> <p>Non-point source loadings</p>	<p>NPDES permit files, MEGA-TX model for the HSC, Spring 2003 effluent data, and regressions for non-measured outfalls Estimated using GIS and spreadsheets models (steady-state) or simulated using runoff models such as HSPF (dynamic)</p>
G	<p>Parameters Spatially variable characteristics of the water body that affect the particular processes being modeled. Dissolved organic carbon concentration Fraction organic carbon of solids Total lumped first-order decay rate</p>	<p>Channel data Channel data Literature values</p>
H	<p>Constants Organic carbon partitioning coefficient</p> <p>First-order loss rate constant Volatilization rate constant</p> <p>Water column biodegradation rate Benthic biodegradation rate Photolysis rate</p>	<p>Measured effective coefficients using data collected in this project (not needed if DOC and f_{oc} are input in Data Group G) Literature values Literature values or coefficients using data collected in this project Literature values Literature values Literature values</p>
I	<p>Kinetic Time Functions Not used in the dioxin model</p>	
J	<p>Initial Conditions Concentration of each modeled system (dioxin and TSS) for each segment</p>	<p>Channel data</p>

5.2.1 Conceptual Model

Two WASP implementations to simulate 2378-TCDD in the HSC are in progress. A simplified WASP model was setup using the 28 surface segments into which the entire channel

had been divided in a modeling study completed in 1971 (Espey et al., 1971). This segmentation had been used to setup a WASP5 model to simulate dissolved oxygen in the HSC (Benaman et al., 1996). The segmentation allowed the assumption of homogeneous hydrography. It is noted that since the geometry of the HSC has changed considerably between 1971 and present date, no attempt to calibrate the simplified model was undertaken. Similarly, the model was not used as a predictive model. The main goal of this simplified model was to determine data needs and to determine model sensitivity to the various input parameters. A more detailed, transient WASP model, still under development as discussed in Section 5.3, divides the HSC in more segments (55) with their corresponding underlying benthic segments.

5.2.2 Channel Segmentation

In the simplified WASP model, the HSC (from the Turning Basin to Morgan's Point) was divided into 28 hydrographic segments. Fourteen segments correspond to the main channel (as shown in Figure 5.16) and the remaining fourteen are comprised by tributaries, side bays, Barbours Cut, and Galveston Bay. Figure 5.17 shows a detailed schematic of the original HSC model developed by Espey et al., 1971. As can be seen in Figures 5.16 and 5.17, segments were defined between major tributaries to allow the input of fresh water inflows.

5.2.3 Input Parameters

5.2.3.1 Hydraulic Model Input

The hydraulic and physical characteristics for each reach in the HSC model were obtained from the Tracor model developed for dissolved oxygen in the HSC (Espey et al., 1971). Table 5.6 summarizes the physical characteristics of the segments in the main channel. As can be seen in

Table 5.6, the cross-sectional area in the Ship Channel was represented by Espey et al. (1971) as a series of two constant area sections. The upstream sections (Turning Basin to Shell Barge) have an average area of 1625.8 m², while the downstream sections (Shell Barge to Morgan's Point) have an average area of 2471.2 m². Table 5.3 also includes mean depth values measured in the Tracor Inc. modeling study.

Figure 5.16 Segmentation for the Simplified Model

Figure 5.17 Schematic of Segmentation used in the Tracor Modeling effort (Espey et al., 1971)

Table 5.6 Physical Characteristics of Main Channel Simplified Model Segments

Table 5.7 Physical Characteristics of Boundary Segments for the Simplified Model

The hydraulic coefficients that relate velocity and depth to flow as described in Equations (5.7) and (5.8) below were assumed to be those for rectangular channels [i.e., $a=0.004$, $b=0.4$, $c=1.2$, and $d=0.6$ (Ambrose et al., 1993)]. It is noted, however, that these coefficients are only important when calculating reaeration or volatilization and not for transport functions.

$$V = aQ^b \quad (5.7)$$

$$D = cQ^d \quad (5.8)$$

where V is the channel velocity (m/s), Q is channel flow (m^3/s), D is channel depth (m).

Dispersion coefficients were also obtained from the Tracor Inc. study. The study found that the magnitude of the dispersion coefficient varied with the magnitude of the net advective flow in the channel. The selected dispersion coefficients are presented in Table 5.6.

Segments that exchange water with locations outside the main network (tributaries, the lower downstream segment--Galveston Bay, and side bays) are represented in the model using boundaries segments. These boundary segments are included to account for inflows, outflows, and dispersive mixing. Table 5.7 includes the main characteristics for the boundary conditions. The bottom sediment layer was simulated as a single benthic segment with a total length equal to the sum of lengths of the segments in the main channel. A depth of 10 cm was assumed for this benthic segment as shown in Table 5.7.

5.2.3.2 Point Sources

Input from point sources is simulated in WASP7 by a series of loading versus time values. It is important to note that mass entered as loads is not directly accompanied with inflow. This simplification is acceptable as long as the inflow associated with a loading is small compared with the water body flow. For the simplified model, point sources discharging directly to the main channel were aggregated by segment to determine total loads and flow. New segments were

created in the advection section to account for the inflows and the respective loads were input in the loading section. For this model, only the outfalls discharging directly into the main channel segments were considered. This was to avoid duplication given that flows and concentrations for the boundary segments already include point sources discharging directly into the tributaries. Figure 5.18 shows the distribution of point sources discharging to the main channel and Figure 5.19 shows the schematic of the “point source” segments. The WASP7 input contains permitted flow values, as included in the TCEQ permittee database (as of May 2003). Dioxin data from point sources (PS) gathered in this project during Spring 2003 were used to calculate load input. For the point sources that were not sampled for effluent and the SIC was among those identified as potential dioxin dischargers, the 2378-TCDD concentration in effluent was assumed equal to the average concentration for effluent from facilities with the same SIC code. If the SIC was not among the potential dioxin dischargers, the 2378-TCDD concentration was assumed equal to zero. The TSS loads from point sources were calculated using the average of the TSS self-reported data. A summary of the point source data for the model is included in Table 5.8. The total load of dioxins from PS discharging directly to the HSC system (not to the tributaries) calculated in this manner was estimated to be 2.90×10^{-8} kg/d.

5.2.3.3 Non-point Sources

Non-point source pollutant loads on a daily basis for the HSC major watersheds were calculated using land cover information, the measured 2378-TCDD concentrations in runoff gathered in this project, and the amounts of rainfall in the year 2002.

Figure 5.18 Point Sources in the Model Area

Figure 5.19 Schematic of Loading Segmentation

Table 5.8 Point Sources for Simplified Model

Subwatershed Delineation

The watershed delineation completed recently by the HCFCD was used to determine drainage areas. Figure 5.20 shows the watersheds that correspond to the segments in the model.

Rainfall Data and Runoff Volume

See explanation presented in section 5.1.2.3 above.

Non-point Source Loads

The 2378-TCDD concentrations in runoff measured in this project were averaged and the mean value was used to calculate NPS loads of dioxins to the main subwatersheds. For each reach, the average runoff 2378-TCDD concentration (0.025 pg/L) was multiplied by the runoff volume to calculate the NPS load. For TSS, concentrations measured during runoff sampling were used to calculate solid loads. For the watershed with no sampling locations, the average of all the TSS measurements during runoff sampling was assumed (86 mg/L). Table 5.9 summarizes the loads from NPS. The total 2378-TCDD load from NPS to the HSC system is estimated to be 9.29×10^{-8} kg/d. This estimate is based on the results from the 10 runoff samples collected in 2002/2003. It is noted that direct dry-deposition to the HSC streams was not included in the NPS load calculation for the simplified model but will be incorporated in the detailed WASP model.

5.2.3.4 Initial Concentrations and Boundary Concentrations

Concentrations of 2378-TCDD in water and TSS measured in Summer 2002 were used as initial concentrations. For the benthic segment (i.e., segment 9), the average 2378-TCDD concentration in sediment for the Summer 2002 data was assumed. Table 5.10 summarizes the initial and boundary concentrations.

Figure 5.20 Segmentation and Drainage Areas for Simplified Model

Table 5.9 Non-point Sources for Simplified Model

Table 5.10 Boundary and Initial Concentrations

In addition to chemical concentrations, the dissolved fractions must be specified for each segment at the beginning of the simulation. For dioxin, the dissolved fractions was set to 0.25. This fraction is internally recalculated by the model at each time step using partition coefficients and sediment concentrations.

5.2.3.5 Solid Transport Parameters

Sediment transport is a very important process in modeling dioxins because dioxins sorb strongly to sediment and thus undergo settling, scour, and sedimentation. In addition, sorption affects the transformation rates. The suspended sediment was simulated as a single solid class. The major processes affecting sediment distribution are advection and dispersion between the water column segments, and settling to and scour from the benthic segment.

Water Column Transport

Sediment and particulate dioxin in the water column may settle and deposit to the surficial benthic layer. Settling and scour rates in WASP7 are described by velocities and surface areas. Particulate transport velocities are multiplied by cross-sectional areas to obtain flow rates for solids and the particulate fractions of dioxins.

Settling velocities should be set within the Stoke's range of velocities corresponding to the size distribution of suspended particles (Ambrose et al., 1993):

$$V_s = \frac{8.64g}{18\mu}(\rho_p - \rho_w) \cdot d_p^2 \quad (5.9)$$

where V_s = Stokes velocity for particle with diameter d_p and density ρ_p (m/d)

g = acceleration of gravity = 981 cm/s²

μ = absolute viscosity of water = 0.01(g/cm³-s) at 20 °C

ρ_p = density of the solid (g/cm³)

ρ_w = density of water =1.0 g/cm³

d_p = particle diameter (mm)

Benthic exchange of sediment and particulate chemicals is driven by the net scour and deposition velocities. WASP calculates benthic exchange as:

$$W_{BS} = A_{ij}(w_R S_i - w_D S_j) \quad (5.10)$$

where: W_{BS} = net sediment flux rate (g/d)

S = sediment concentration (g/m³)

w_D = deposition velocity (m/d). The deposition velocity can be calculated as the product of the Stoke's settling velocity and the probability of deposition: $w_D = V_s \alpha_D$ (α_D is probability of deposition upon contact with the bed).

w_R = scour velocity (m/d)

A_{ij} = benthic surface area (m²)

i = benthic segment

j = water segment

Grain size analyses of suspended particles have not been completed in this project, so it was assumed that the majority of the particles correspond to the size range for silt (0.0039-0.0625 mm). Thus, settling velocities should be within the range 0.716 and 183.9 m/day (8.29×10^{-6} to 0.002 m/s). Initial settling velocities were assumed equal to 0.001 m/s for the main channel segments and 0.002 m/s for the side bays. Settling within the side bays was assumed higher as they are less affected by disturbances created from ship traffic.

There are no sediment studies in the HSC that allow determination of scour rates. These rates were assumed to be 2 orders of magnitude lower than the settling rates (i.e. 1×10^{-5} m/s). It is noted that there are no special process descriptions for solids transport in WASP7. Scour rates, for example, are not programmed as a function of water column shear stress. Consequently, the TOXI5 sediment model is considered descriptive and must be calibrated to site data (Ambrose et al., 1993)

Sediment Bed

The selected sediment bed option was constant bed volume, which allows sediment concentration to change. It is a simplified assumption. However, the detailed model will be refined using a variable bed volume option to allow for checking of balance of fluxes and also to model contaminant burial (provided that data are available on rates and mechanisms). The variable bed volume allows 2 benthic layers (upper uncompacted and lower more compacted layer).

Water Column-Sediment Bed Exchange

A dispersion coefficient of $0.01 \text{ m}^2/\text{s}$ was assumed for the surface-benthic segment exchange (Table 5.7).

5.2.3.6 Parameters and Constants

In this model, the fraction organic carbon (f_{oc}) of the suspended sediments was the only parameter input to the model. Results of particulate organic carbon analyses for water samples were not available at the time of the simplified WASP model development (samples for POC analysis were collected in the Fall 2004 sampling event), thus, a value of 25% was assumed for

all the surface segments. The f_{oc} for the benthic layer was assumed equal to the average of the fractions measured in sediments collected in Summer 2002 (2.5%).

For this model, two constants were input. The first one corresponds to the logarithm of the organic-carbon partitioning coefficient (K_{oc}), which was estimated to be 7.11 (University of Houston, 2004). For the simplified model, transformation processes (biodegradation, photolysis, and volatilization) were modeled as a lumped first-order decay rate. The second constant corresponds to the lumped decay rate, which was assumed to vary between 1×10^{-6} and $1 \times 10^{-4} \text{ d}^{-1}$.

5.2.4 Model Runs

The base case for the simplified model was implemented with the following input parameters:

- Segment characteristics presented in section 5.2.3.1
- Point source flows and loads as summarized in section 5.2.3.2
- No non-point source loads
- Initial and boundary concentrations as described in section 5.2.3.4
- Settling and scour velocities as presented in section 5.2.3.5
- Linear hydrophobic sorption ($\log K_{oc}$) and no decay processes.

Figure 5.21 shows longitudinal profiles for TSS and 2378-TCDD modeled in the base case. As can be seen, TSS concentrations were relatively uniform along the main channel with values between 16 and 23 mg/L, and 2378-TCDD concentrations in water varied between 0.06 and 0.13 pg/L. The input dataset for the base case run is included in Appendix H.

It is noted again that no calibration was attempted for the simplified model. Instead, the focus was on determining which variables had most impact on model results. Thus, scenarios

were run assuming different conditions to determine the change in the output concentrations. The scenarios were divided into 8 main groups as summarized in Table 5.11.

Results from the model runs are presented in Figures 5.22a, b, c, and d for TSS, total 2378-TCDD in water, dissolved 2378-TCDD in water, and suspended 2378-TCDD in water, respectively.

Figure 5.21 Model Results for the Base Case

Table 5.11 Summary of Model Runs

Figure 5.22a Summary of TSS Results

Figure 5.22b Summary of 2378-TCDD Concentrations in Water

Figure 5.22c Summary of 2378-TCDD Dissolved Concentrations in Water

Figure 5.22d Summary of 2378-TCDD Suspended Concentrations in Water

Results indicate that TSS concentrations are most sensitive to settling/resuspension (benthic exchange) and dispersion processes as well as point and non-point source loadings (Figure 5.22a). Concentrations of 2378-TCDD in water showed sensitivity to most of the parameters (Figure 5.22b), with the greatest variation in model results corresponding to changes in the dispersion and benthic exchange coefficients. Total 2378-TCDD concentrations in water did not show sensitivity to either pore processes or decay.

5.3 WASP TRANSIENT MODEL

5.3.1 Channel Segmentation

The latest watershed and subwatershed delineations were obtained from Harris County Flood Control District (HCFCD). The channel was divided into 55 water segments (including tributaries) with their corresponding underlying benthic segments (Figure 5.23). The tributary segments correspond to the section between the flow gage and the mouth of the stream.

5.3.2 Hydraulic Input

The Dynamic Estuary Model Hydrodynamics Program (DYNHYD5) was used to simulate the transient hydrodynamics. DYNHYD solves the one-dimensional equations of continuity and momentum for a branching or channel-junction computational network. The simulations are driven by variable upstream flows and downstream heads (Ambrose et al., 1993). The DYNHYD5 model was selected because of its relatively easy interface with WASP. However, the model has the following limitations:

- It can treat fairly complex branching flow patterns but it cannot handle stratified waterbodies

Figure 5.23 Segmentation for the Transient WASP Model

- DYNHYD only allows up to 5 variable inflows (inputs)
- The variable inflow only allows up to 100 breaks in the flow series

The following sections describe the input and output series for the HSC DYNHYD model.

5.3.2.1 Model Parameters

Simulation Period and Time Step

Because DYNHYD cannot handle more than 100 breaks in the flow series, the model was run for a 24-day period, with 6-hr time steps. The period of the simulation was from August 1, 2002 to August 24, 2002. This time period was selected because it corresponds to the period with the largest dioxin dataset.

Model Network

The model network corresponds to that shown in Figure 5.23, for a total of 56 nodes and 55 water segments (links).

Junction and Channel Data

Summaries of the initial conditions at each junction and channel are presented in Tables 5.12 and 5.13, respectively. To determine the different geometry parameters two sources of data were relied upon: (i) HSC cross-sections from the Center for Operational Oceanographic Products and Services, available on-line at <http://www.co-ops.nos.noaa.gov/>, and (ii) cross sections for major tributaries from the Tropical Storm Allison Recovery Project (TSARP).

Inflow Data

Hourly flow data for all the major tributaries was obtained from the USGS and averaged using 6-hour intervals. The major tributaries considered in the model, from downtown Houston to Morgan's Point, are listed in Table 5.14 below.

Table 5.12 Junction Parameters for DYNHYD Model

Table 5.13 Channel Parameters for DYNHYD Model

Table 5.14 Major Tributaries and USGS Gages

Tributary	Station Description	USGS gage	Watershed Area (mi²)	Parameters Measured	Long-term median flow (cfs)
San Jacinto River	San Jacinto River at Sheldon	08072050	2,879	GH	1.95
Buffalo Bayou	Buffalo Bayou at Shepherd	08074000	358	Q, GH	66
Whiteoak Bayou	Whiteoak Bayou at Heights	08074500	86.3	Q, GH	30
Greens Bayou	Greens Bayou at Ley Rd	08076700	182	Q, GH	260
Brays Bayou	Brays Bayou at Houston	08075000	94.9	Q, GH	76
Sims Bayou	Sims Bayou at Houston	08075500	63	Q, GH	35
Vince Bayou	Vince Bayou at Pasadena	08075730	8.26	Q, GH	1.70
Patrick Bayou	None	None	4.4		NA
Carpenters Bayou	None	None	25.8		NA
Hunting Bayou	Hunting Bayou at IH-610	08075770	16.1	Q, GH	7.30
Goose Creek	Goose Creek at Baytown	08067525	15.8	GH	NA

Q = flow, GH = gage height

Because DYNHYD does not allow more than five variable-flow input data series, the USGS data were combined as follows: (1) Buffalo Bayou, Whiteoak Bayou, and 69th St. WWTP entering the channel at segment 2, (2) Brays Bayou entering the channel at segment 37, (3) Sims Bayou entering the channel at segment 38, (4) Vince, Hunting, and Greens Bayous entering the channel at segment 41, and (5) San Jacinto River entering the channel at segment 52. The San Jacinto River flow series was developed using the USGS gage data and regressions made with the flow measurements collected as part of this project (Section 3.2.3). Figure 5.24 shows the flow series input to the model.

Seaward Boundary

As of this writing, the downstream boundary for the model is at Morgan’s Point. Inclusion of a segment corresponding to Upper Galveston Bay is under consideration. Gage data for Morgan’s Point was obtained from NOAA in 6-minute intervals and averaged to 1-hour intervals. Data for a single tidal cycle was then fitted (by the model) to the following regression:

Figure 5.24 Flow Input Series for DYNHYD

$$H = A_1 + A_2 \sin(\omega t) + A_3 \sin(2\omega t) + A_4 \sin(3\omega t) + A_5 \cos(\omega t) + A_6 \cos(2\omega t) + A_7 \cos(3\omega t) \quad (5.11)$$

where H is head (m), ω is tidal period (hr), and t is time (hr).

Figure 5.25 shows the tidal data input to DYNHYD (5-day period) and the resulting modeled gage heights for the simulation period (24 days) are depicted in Figure 5.26.

5.3.2.2 DYNHYD Output

Preliminary flow data series for a number of segments in the HSC as simulated by DYNHYD are presented in Figure 5.27. The hydraulic model is currently being refined and calibrated. An updated version of the model will be presented in the next quarterly report.

5.3.3 WASP Model Development

The output from DYNHYD was linked to the WASP model and the benthic segments were added to complete the water quality simulations. The WASP model is currently under development and its results will be discussed in the next quarterly report.

Figure 5.25 Input Tidal data
Figure 5.26 Tidal Data Simulated by DYNHYD

Figure 5.27 Modeled Flows

CHAPTER 6

STAKEHOLDER/PUBLIC EDUCATION AND INVOLVEMENT

6.1 SUMMARY OF SUPPORT ACTIVITIES

The project team supported the stakeholder process facilitated by the Houston Galveston Area Council (HGAC) and the Environmental Institute of Houston at UH Clear Lake. The following support tasks were undertaken:

- Development of informational materials summarizing the technical aspects of the project for electronic and paper distribution at stakeholder meetings. These materials included documents, maps, and the QAPP for this project;
- Preparation of web based project informational briefs;
- Participation in three stakeholder meetings (01/07/2004, 02/02/2005, and 08/31/2005);
- Participation in two technical meetings with members of the stakeholder group. The first one was held at the Port of Houston Authority main office on May 17, 2004 and the second took place at the University of Houston on May 24, 2004;
- Preparation of responses to questions and information requests from stakeholders and providing rationale for whether or not certain requests by stakeholders for refinement in technical analysis can or cannot be achieved. After the January 2004 stakeholder meeting, the project team received comments from Lial Tischler and from Oxy Vinyls. It is noted that these two documents present differing perspectives regarding calculating site-specific BAFs and BSAFs. In response to Lial Tischler's comments, congener-specific BAFs,

BSAFs, and BEFs were calculated using the USEPA (1995) guidance document and are discussed in Chapter 4 of this report. In addition, the project team prepared a document in response to comments received from Oxy Vinyls on February 16, 2004. The document, included in Appendix I of this report, was discussed during the May 24 technical meeting; and

- Preparation of data to be submitted to H-GAC for development of informational map and brochure on the project.
- On February 22, 2005, new information from the Texas Parks and Wildlife indicated the presence of a potential source in the San Jacinto River near the I-10 bridge. More research was completed to investigate this issue and as a result additional high-resolution sediment sampling was conducted in Summer 2005.

6.2 TECHNICAL PRESENTATIONS AT STAKEHOLDER MEETINGS

Copies of the technical presentations given at the stakeholder meetings are included in Appendix I. The QAPP and other related documents can be found on the web at <http://www.hgac.cog.tx/intro/introtmdl.html>.

6.3 PUBLIC OUTREACH

In addition to stakeholder presentations, the following technical presentations were given:

- “Development of a Dioxin TMDL for the Houston Ship Channel in Texas” at the *WEF 2003 TMDL National Conference* held in Chicago, IL on November 15-19, 2003;
- “Site-Specific Water Quality Targets for Fish Contaminants: Application of Sediment, Water, and Tissue Targets based on Measured Partitioning Relationships” at the *WEF*

2003 TMDL National Conference held in Chicago, IL on November 15-19, 2003;

- “Assessment of Particulate and Dissolved Dioxin Concentrations in Storm Water Runoff to Houston-area Waterways Using High Volume Sampling” at the *WEF 2003 TMDL National Conference* held in Chicago, IL on November 15-19, 2003;
- “TMDL for Dioxin in the Houston Ship Channel” at the *Haden Road Community Advisory Panel* on March 22, 2004;
- “TMDL for Dioxin in the Houston Ship Channel” at the *Board Meeting of the Galveston Bay Estuary Program* on April 22, 2004;
- “TMDL for Dioxin in the Houston Ship Channel” at the *Baytown Area Community Advisory Panel* on May 17, 2004; and
- “TMDL for Dioxin in the Houston Ship Channel” at the *GBNEP State of the Bay Conference* on January 25, 2005.

CHAPTER 7

PCB ASSESSMENT

In January and July 1999, the Texas Department of Health (TDH) collected twenty-four finfish¹³ and eight composite blue crab samples from four sites in the Houston Ship Channel System to complete a Health Assessment. The locations included the Turning Basin, the Lynchburg Ferry/San Jacinto State Park, the San Jacinto River near I-10, and Tabbs Bay near Houston Point. Results from the 1999 Health Assessment showed the presence of PCBs (Aroclor 1260) in 3 out of 12 finfish samples from the Lynchburg Ferry and the San Jacinto River. The maximum and average concentrations for the samples above detection limits were 0.330 and 0.068 ng/g, respectively. Based on the results from the 1999 studies, it was recommended by the TDH to extend the existing advisory for the Houston Ship Channel to include all species of finfish due to the presence of pesticides and PCBs in concentrations that exceed health-based comparison values. The Health Assessment took into account potential cumulative noncancerous and carcinogenic health effects.

The scope for the dioxin project was, thus, expanded to include a preliminary assessment of PCB concentrations in all media in the channel and leverage the costs involved in dioxin sample collection. Unlike the TDH study, the dioxin TMDL project quantified both the 209 PCB congeners and the Aroclors in all media and results were presented in the Final Report for WO4. This chapter presents an analysis of the PCB data collected during the Summer 2002, Fall 2002,

and Spring 2003 sampling events to make recommendations regarding impairment and the need for initiating TMDL projects.

In February 2005, the Texas Department of Health issued a new advisory for the consumption of Speckled Trout from the HSC and Upper Galveston Bay.

7.1 PCB WATER QUALITY STANDARDS

Several national and state criteria and screening levels for PCBs in water and fish tissue exist. The state/federal Maximum Contaminant Level (MCL) for drinking water is 500 ng/L (ppt), while the human health water quality criteria based on uptake by fish consumption and water recommended by EPA is 0.17 ng/L (EPA, 1999).

The Texas Surface Water Quality Standards (§307.1-307.10) include human health water quality criteria for total PCBs (based on Aroclors) of 1.3 ng/L and 0.885 ng/L in freshwater and saltwater, respectively. These concentrations are lower than the MCL for drinking water due to the fact that the highest exposure potential of PCBs in waters is through the bioaccumulation potential and consumption of contaminated fish (Webster et al. 1998). Additionally, fresh and saltwater criteria differ because it is assumed that consumption rates are higher for saltwater species.

The Texas Department of Health based its health assessment of PCBs in the Houston Ship Channel (TDH, 2001) on a screening level of 47 ng-Aroclor/g-tissue. This screening value was derived from an EPA chronic oral reference dose (RfD) for Aroclor 1254 of 0.00002 mg/kg/day¹⁴.

¹³ Seven hybrid bass, five smallmouth buffalo, three sheepshead, three red drum, one freshwater drum, two southern flounder, two common carp, and one blue catfish.

¹⁴ This is the lower of the carcinogen and noncarcinogen comparison values. The comparison value using the EPA slope factor of 2 (mg/kg/day)⁻¹ to account for the carcinogen effects of PCBs was 270 ng/g. Assumptions: body

7.2 PCB ANALYTICAL QUANTIFICATION

PCBs may be quantified as individual congeners, as Aroclor equivalents, or as homologue groups (i.e. monochlorobiphenyl, dichlorobiphenyl, etc). Aroclors are identified as commercial mixtures of PCB congeners. Historically, the most common PCB analysis has been through Aroclor analysis (EPA Method 8082). However, the analysis of Aroclor may yield significant error in determining both total PCB and their total toxicity. This is because the Aroclor method assumes that the distribution of PCB congeners in environmental samples and parent Aroclor compounds is similar (U.S. EPA, 2000).

Cogliano (1998) found that bioaccumulated PCBs are more toxic and persistent than the original Aroclor mixtures. Thus, the U.S. EPA (2000) recommends analysis of homologue groups or PCB congeners. However, it acknowledges that all health-based assessments are based on Aroclors. EPA (2000) suggests summing 18 congeners to compare to total PCB or Aroclor-based screening values, as recommended by the National Oceanic and Atmospheric Administration (NOAA, 1989). The 18 congeners include PCB-8, PCB-18, PCB-28, PCB-44, PCB-52, PCB-66, PCB-77, PCB-101, PCB-105, PCB-118, PCB-126, PCB-128, PCB-138, PCB-153, PCB-169, PCB-170, PCB-180, and PCB-187.

7.3 SUMMARY OF PCB RESULTS IN THE HOUSTON SHIP CHANNEL

During the Summer 2002, concentrations of the 209 PCB congeners (EPA Method 1668A) were analyzed from 31 ambient water locations, 34 in-stream sediment locations, 45

weight 70 kg, consumption rate 30 g/day, exposure period 30 yr (for carcinogens), and excess lifetime cancer risk of 1×10^{-4} .

catfish and crab tissue locations, and 11 tributary sediment locations¹⁵. In addition, samples from 18 ambient water locations, 16 in-stream sediment locations, 13 locations for catfish tissue, and 13 locations for crab tissue were analyzed for PCBs (209 congeners) during Fall 2002. During the Spring of 2003, 4 water samples, 37 sediment samples, and 26 catfish samples were analyzed for the 209 PCB congeners. Table 7.1 includes a summary of the total number of samples collected during the three sampling events.

7.3.1 In-stream Water

Total concentrations of PCBs (calculated as the sum of the 18 NOAA congeners) in water (dissolved plus suspended fractions) for the three sampling events are summarized in Table 7.2. Figure 7.1 shows the distribution of total PCBs in water in the Houston Ship Channel System. Total Summer 2002 PCB concentrations ranged between 0.18 and 1.62 ng/L with a mean value of 0.56 ng/L for 31 stations, when non-detects were assumed equal to zero. Total PCB concentrations in Fall 2002 samples varied between 0.12 and 2.60 ng/L with an average of 0.68 ng/L for 18 locations. As can be seen in Table 7.2, only 5 out of the 31 (16%) locations sampled in Summer 2002 and 3 out of the 18 (17%) Fall 2002 locations exceeded the Texas Surface Water Quality Standard (WQS) for human health protection of 0.885 ng/L. In addition, the mean concentration is less than the WQS. The exceedances were observed at stations located in segments 1006, 1007, and 2427. During Spring 2003 PCBs in water were measured only for segments 1006 and 1007. Total PCB concentrations in Spring 2003 were between 0.96 and 1.8

¹⁵ Water samples were collected using the high-volume technique, which yielded samples sizes between 268 and 731 L. Sediment samples were composites of 3 to 5 grab samples at each location. Tissue samples were obtained by compositing 3 to 5 individuals from a given location; only the edible portion was used in the sample composite.

Table 7.1 Total Number of PCB Samples

Table 7.2 Total PCB Concentrations in Water

T 7.2 (2)

Figure 7.1 Total PCB Concentrations in Water

ng/L with an average of 1.36 ng/L. The four stations sampled in Spring 2003 exceeded the Texas WQS for total PCBs.

Figure 7.2 shows the concentration distribution for the 18 NOAA congeners and total PCBs in dissolved and suspended phases for the three sampling events. The dissolved concentrations for the individual PCBs ranged from 0.00002 to 0.453 ng/L, while the suspended concentrations varied between 0.00002 and 0.114 ng/L. Overall, congener concentrations in dissolved water were greater than those in the suspended phase for the lower chlorinated PCBs with the exception of PCB-8. Average suspended/dissolved ratios for PCB-18 through PCB-101 vary between 0.34 and 0.85, while the average suspended/dissolved ratio for PCB-8 is 3.64 and for PCB-105 to PCB-187 it varies between 1.16 and 3.44. Concentrations of PCBs with the same number of chlorines are similar. On average, up to 50% of the dissolved total PCB concentration is attributable to congeners 28, 44, and 52. The total PCB concentration in suspended sediments, on the other hand, is distributed almost evenly among all but 2 congeners.

7.3.2 Sediment

PCB results from the in-channel sediment samples collected in Work Order No.4 are included in Table 7.3. Total PCB levels in Summer 2002 sediment samples varied between 56 and 1,445,307 ng/kg-dry wt. with a mean value of 61,366 ng/kg-dry wt. Similarly, Fall 2002 sediment samples exhibited total PCB concentrations between 76 and 1,117,233 ng/kg-dry wt. with a mean value of 82,986 ng/kg-dry wt. Total PCB concentrations in sediment samples collected in Spring 2003 ranged between 70 and 810,877 ng/kg-dry wt. with an average value of 40,537 ng/kg-dry wt. Figure 7.3 shows the distribution of total PCB concentrations along the HSC system for the different sampling events.

Figure 7.2 Distribution of Individual PCB Congeners in the Dissolved and Suspended Phases

Table 7.3 PCB Concentrations in Sediment

T 7.3 (2)

Figure 7.3 Total TEQ Concentrations in Sediment

Figure 7.4 shows the concentration distribution for the 18 NOAA congeners and total PCBs in bottom sediments for the three sampling events. Sediment concentrations for the individual PCB congeners ranged from 20 to 317,000 ng/kg dry wt. The average contribution of individual congeners to total PCBs is below 10% for all the compounds with the exception of PCB-138 and PCB-153 that contribute on average 15 and 12%, respectively.

7.3.3 Tissue

PCB concentrations in catfish and crab tissue are included in Tables 7.4 and 7.5, respectively. Total PCB concentrations at the different locations sampled during Summer and Fall 2002 are mapped in Figures 7.5 and 7.6 for catfish and crab, respectively. Total PCB concentrations in catfish samples collected in Summer 2002 varied within the range 2.2- 866.1 ng/g wet wt. with an average value of 81.8 ng/g wet wt. Fall 2002 catfish samples showed concentrations between 36.2 and 115.9 ng/g wet wt. with an average of 64.4 ng/g wet wt. Finally, catfish samples collected during Spring 2003 exhibited concentrations between 8.0 and 303.8 ng/g wet wt. with an average of 104.2 ng/g wet wt. It was found that 59 out of 84 catfish samples (70%) exceeded the TDH Health Assessment Comparison Value (47 ng/g) using summed data of the 18 NOAA congeners.

Total PCB concentrations in crabs varied between 2.2 and 69.5 ng/g wet wt. in the Summer 2002 samples and between 1.9 and 20.2 ng/g wet wt. in Fall 2002 samples with respective averages of 18.2 and 10.9 ng/g wet wt. Only 1 out of 58 crab samples (3%) exceeded the TDH Health Assessment Comparison Value.

Figure 7.4 Distribution of Individual PCB Congeners in Bottom Sediment

Table 7.4 PCB Concentrations in catfish Tissue

T 7.4 (2)

Table 7.5 PCB Concentrations in Crab Tissue

T 7.5 (2)

Figure 7.5 Average Total PCB Concentrations in catfish

Figure 7.6 Average Total PCB Concentrations in Crabs

Figure 7.7 shows the concentration distribution for the 18 PCB congeners in catfish and crab samples. The concentrations for the individual PCBs ranged from 0.001 to 210 ng/g wet wt. for catfish and from 0.001 to 19 ng/g wet wt. for crabs. Most of the total PCB concentration in catfish can be attributed to PCB-138 and PCB-153 with average contributions of 20 and 21% to the total PCB sum, respectively. Similarly, the highest contributors to the total PCB concentration in crabs are also congeners PCB-138 and PCB-153, with average contributions of 18 and 23%, respectively. It is noted that congeners 138 and 153 are also the highest contributors to total PCB concentration in bottom sediments. PCB congeners 138 and 153 are not among the “dioxin-like” PCB congeners.

7.4 ANALYSIS OF PCB DATA IN THE HOUSTON SHIP CHANNEL

7.4.1 BAF/BSAF Calculations

PCB data collected during WO4 were used to calculate congener-specific bioaccumulation factors (BAFs) and biota to sediment accumulation factors (BSAFs) for the entire Houston Ship Channel System. Two approaches for calculating BAFs were used. The first approach uses measures of central tendency (i.e. mean or median) of the ratios of tissue concentrations to dissolved concentrations and of the ratios of tissue concentrations to sediment concentrations. The second approach uses ratios of average concentrations for the different media (EPA, 2003).

Figure 7.8 shows dissolved and tissue dioxin data and BAF fitting lines for selected congeners using both approaches. Similarly, Figure 7.9 shows organic carbon-normalized sediment and tissue data and the BSAF fitting lines calculated using both approaches. The two approaches give similar results for BAFs, but not for BSAFs. As seen in Figure 7.9, the BSAFs

Figure 7.7 Distribution of Individual PCB Congeners in Tissue Samples

Figure 7.8 Line Fit Plots of BAF for Selected PCB Congeners in Tissue from the HSC

Figure 7.9 Line Fit Plots of BSAF for Selected PCB Congeners in Tissue from the HSC

do not seem to fit the observed data very well, thus, a sediment-based water quality target was not calculated for PCBs.

Using the TDH screening value for PCBs (47 ng/g), a target concentration in water may be established using the following relationship:

$$WQ_{target,water} = TRC / BAF \quad (7.1)$$

Each of the congeners contributing to the total PCB concentrations has different physical and chemical properties and different bioaccumulation potentials. Using the estimated bioaccumulation factors, the PCB concentration in tissue (PCB_b) can be calculated using:

$$PCB_b = \Sigma (C_{diss})_i * BAF_i \quad (7.2)$$

Since the water quality criterion sets limits for the total equivalence of the mixture rather than the individual congeners and there are no guidelines to develop targets for mixtures of compounds that contribute to an exceedance of a WQ criterion, each congener was assigned a target concentration that corresponded to their associated fraction of the total PCB concentration that was observed historically (on average) in catfish and crab tissue in the system. This can be mathematically expressed as:

$$(C_{diss})_i = TRC * (PCB_b)_i / \Sigma PCB_b / BAF_i \quad (7.3)$$

Using the BAFs estimated from both approaches, and Equations (7.2) and (7.3), the target concentrations for individual congeners were calculated (Tables 7.6a and b).

These BAF ratios were calculated from dissolved water concentrations, so this target applies to the dissolved PCB concentration in water. Based on the average log BAFs for catfish, the water quality target for total PCB dissolved in water would be 0.335 ng/L. Based on the log of the ratio of the average catfish concentration to the average dissolved concentration, the water

Table 7.6a Summary of Average log BAFs, log BAFs from Average Concentrations, and the Resulting Water Quality Targets for PCBs in Catfish from the HSC

Table 7.6b Summary of Average log BAFs, log BAFs from Average Concentrations, and the Resulting Water Quality Targets for PCBs in Crabs from the HSC

quality target for total PCBs dissolved in water would be 0.289 ng/L. Using dissolved-suspended partitioning relationships presented in Figure 7.10, the water quality target for total PCBs in water would be 3.182 and 2.804 ng/L for the first and second approach, respectively. These targets are higher than the Texas WQS of 0.885 ng/L for marine waters. Crab data yielded higher water quality targets with respective concentrations in whole water of 11.483 and 10.194 ng/L for the first and second approach.

Water data collected in WO4 were compared to the estimated congener-specific targets derived using both approaches to evaluate the current state of impairment of the Houston Ship Channel. Table 7.7 summarizes the percent target exceedances by congener in the entire system. Data in Table 7.7 indicate that the water quality targets calculated using site-specific BAFs are not exceeded for most congeners. The congeners with most exceedances are PCB-44 and PCB-52 with 4 out of 58 samples exceeding the WQ target. The water quality target for total PCB is not exceeded in the HSC samples.

Figure 7.10 Partitioning of PCBs between Dissolved and Suspended Phases in the HSC

**Table 7.7 Summary of Exceedances of the PCB Water Quality Criteria Estimated using
Site-specific BAFs**

7.4.2 Spatial Trends

Figures 7.11, 7.12, 7.13, and 7.14 show total PCB concentration profiles along the main channel for water, sediment, catfish, and crabs, respectively; as well as the standard/screening values for the different environmental media. The total dioxin TEQ profiles are also shown for comparison. Figure 7.11 shows that average PCB concentrations in water start low (below the WQS) and they increase in segment 1006 to levels above the Texas WQS then start decreasing in the direction of Galveston Bay. A similar profile is obtained for average OC-normalized sediment concentrations (Figure 7.12), with the difference that the sediment profile exhibits a sudden decrease in concentration in station 11258 in segment 1005. Average OC-normalized sediment concentrations in the Side Bays are generally lower than those at the confluences with the main channel (Segment 1005).

Average catfish PCB concentrations exhibit a longitudinal profile that is fairly flat in the main channel prior to Galveston Bay (Figure 7.13). Most of the catfish concentrations exceed the TDH health-based screening level. Finally, average PCB concentrations in crab samples are somewhat stable in segments 1007, 1006 and beginning of 1005, with levels below the screening level (Figure 7.14). They then start decreasing towards Galveston Bay.

It is noted that for all the media, the PCB profiles mimic those for dioxin concentrations, confirming similar patterns for PCBs as for dioxins with one notable exception related to water PCB concentrations being below the standard in 1005 and 2421, whereas dioxin concentrations are not.

To further analyze spatial patterns, a Principal Component Analysis was completed for the Summer 2002 sediment dataset. The sediment dataset was selected because sediment

Figure 7.11 Total Water Dioxin and PCB Concentration Profiles in the HSC

Figure 7.12 Total Organic Content-normalized Sediment Dioxin and PCB Concentration Profiles in the HSC

Figure 7.13 Total Catfish Dioxin and PCB Concentration Profiles in the HSC
Figure 7.14 Total Crab Dioxin and PCB Concentration Profiles in the HSC

concentrations are expected to be more stable over time than concentrations in other media.

Figure 7.15a shows the biplot of the PCA. It can be seen that Figure 7.15a does not represent a good PCA, since it takes 6 components to explain 88% of the variability. Figure 7.15b shows a plot of the three main components. Station 11273 is still an outlier when compared to the other stations, similar to what was observed for dioxin data. With the three components, only 44% of the variance could be explained. The cluster analysis tree (Figure 7.16) indicates that the relative outliers are 11273 and 11292. They do not appear as outliers in either scatter plot, but that is most likely because most of the variance is not explained in the first two or three components.

7.5 SUMMARY OF AROCLOR RESULTS IN THE HOUSTON SHIP CHANNEL

In addition to the 209 PCB congeners, Aroclor concentrations (EPA Method 8082) were also quantified in all the media. During the Summer 2002, Aroclors were analyzed from 18 ambient water locations (using the high-volume sampling technique), 28 in-stream sediment locations, 23 catfish tissue and 27 crab tissue locations, and 11 tributary sediment locations. In addition, during Fall 2002 samples from 18 ambient water locations, 16 in-stream sediment locations, 11 locations for catfish tissue, and 12 locations for crab tissue were analyzed for Aroclors. Table 7.8 includes a summary of the total number of samples collected during the Summer and Fall of 2002. Results of Aroclor analyses for Summer and Fall 2002 are presented in Tables 7.9 through 7.12. A summary of measured Aroclor concentrations for the different media is included in Tables 7.13a and b. Overall, the majority of the samples (>90%) showed

Figure 7.15a PCA of PCB Concentrations in Sediment
Figure 7.15b Scores for Three Main Components of PCBs in Sediment

Figure 7.16 PCB Sediment Dendogram using Ward Method

Table 7.8 Total Number of Aroclor Samples

Table 7.9 Aroclors in Water

Table 7.10 Aroclors in Sediment

T 7.10 (2)

Table 7.11 Aroclors in Catfish Tissue

T 7.11 (2)

Table 7.12 Aroclors in Crab Tissue

T 7.12 (2)

Table 7.13a Aroclor Results for Summer 2002 Samples

Matrix/Units	Aroclor Mixture	#Detected/ # Sampled	Min	Max	Mean^a
Water (ng/L)	All	0/18	ND	-	NC
Sediment (ng/g)	1016	0/47	ND	-	NC
	1221	1/47	ND	61	NC
	1232	0/47	ND	-	NC
	1242	1/47	ND	61	NC
	1248	5/47	ND	2400	1469
	1254	7/47	ND	1200	520
	1260	7/47	ND	470	230
Catfish (ng/g)	1016	0/27	ND	-	NC
	1221	0/27	ND	-	NC
	1232	0/27	ND	-	NC
	1242	0/27	ND	-	NC
	1248	0/27	ND	-	NC
	1254	8/27	ND	160	107
	1260	8/27	ND	480	127
	Total Aroclors	10/27	ND	480	119
Crab (ng/g)	1016	0/30	ND	-	NC
	1221	0/30	ND	-	NC
	1232	0/32	ND	-	NC
	1242	0/32	ND	-	NC
	1248	0/32	ND	-	NC
	1254	1/32	ND	66	NC
	1260	9/32	ND	61	44
	Total Aroclors	2/32	ND	59	59

^a non-detects not included in calculation
 ND=not detected; NC=not calculable
 Detection limits included in Tables 7.9 to 7.12.

Table 7.13b Aroclor Results for Fall 2002 Samples

Matrix/Units	Aroclor Mixture	# Detected/# Sampled	Min	Max	Mean^a
Water (ng/L)	All	0/20	ND	-	NC
Sediment (ng/g)	All	0/17	ND	-	NC
Catfish (ng/g)	1016	0/15	ND	-	NC
	1221	0/15	ND	-	NC
	1232	0/15	ND	-	NC
	1242	0/15	ND	-	NC
	1248	0/15	ND	-	NC
	1254	8/15	ND	180	84
	1260	0/15	ND	-	NC
	Total Aroclors	7/15	ND	80	64
Crab (ng/g)	All	0/14	ND	-	NC

^a non-detects not included in calculation

ND=not detected; NC=not calculable

Detection limits included in Tables 7.9 to 7.12.

non-detectable levels during Summer 2002. All the Aroclors were below detection limits in water samples. In addition, Aroclor 1254 was at detectable levels in sediment from only 7 locations. Finally, the TDH Health Assessment comparison value (47 ng/g tissue) was exceeded in 32% of catfish samples and 6% of crab samples. The Fall 2002 samples showed similar low levels of Aroclors: water and sediment samples exhibited non-detectable levels for all the Aroclors, 6% of fish samples exceeded the TDH screening levels (only Aroclor 1254 was detected at 8 samples, all the other Aroclors were below detection levels), and none of the Aroclors were detected in crab samples.

7.6 USE SUPPORT AND RISK ASSESSMENT

In order to assess the current status of impairment of the HSC system by segment, total PCB concentrations calculated as the sum of the 18 NOAA congeners were compared to the

Texas human health water quality standard and screening criteria outlined in Section 7.2. When looking at the Aroclor analysis data, all water samples met the Texas WQS for total PCBs, and all but one were non-detects. A summary of results is presented in Table 7.14.

According to the “*Guidance for Assessing Texas Surface and Finished Drinking Water Quality Data, 2004*” to assess water quality attainment a minimum of 10 samples are required, and samples are usually evaluated on a station by station basis. The Guidance, however, establishes that exceptions to the 10-sample rule can be made for streams or reaches of streams that are 25 miles or less in length and for estuarine waters, where water quality conditions are similar. For these water bodies or portions of water bodies, field measurements, constituents in water, sediment, and fish tissue collected at multiple sites may be aggregated to meet the 10-sample minimum requirement. Thus, data for all the locations within a given water quality segment were pooled. To determine the use (fish consumption) support of a water quality segment, the average of the collected samples was compared to the human health criteria (WQS for water). If the average exceeded the criterion and the number of samples was equal or greater than 10, the segment was considered not supporting. If the average exceeded the criterion and the number of samples was between 4 and 9, a Tier-1 primary concern was identified.

To assess the status of impairment of tissue data, catfish and crab data were evaluated using the TDH 1999 Health Assessment procedure. Tables 7.15a and b present estimates of the hazard index (HI)¹⁶ and the cancer risk level for each tissue sample using the 18 PCB congeners and the Aroclors. In most cases (85%) using PCB congener data yields higher HI's and cancer

¹⁶ Hazard Index (HI) is the sum of the ratios of single substance exposure levels over a specified time period to a reference dose for that substance derived from a similar exposure period. If the HI is greater than 1, there may be concern for potential noncancer effects (EPA, *Risk Assessment Guidance for Superfund (RAGS) Part A: Chapter 8: Risk Characterization*, <http://www.epa.gov/superfund/programs/risk/ragsa/ch8.pdf>).

Table 7.14 Exceedances in Houston Ship Channel PCB Assessment for 2002-2003 Period

Table 7.15a Total PCBs and Health Effect Calculations for Catfish Samples

T 7.15a (2)

Table 7.15b Total PCBs and Health Effect Calculations for Crab Samples

T 7.15b (2)

risks. Maximum Hazard Indices using 18 congeners are 9.28 and 1.01 for catfish and crab tissue, respectively. The Hazard Index exceeded 1 in 9 catfish samples (in segments 1001, 1006, 1007, 1013, 2430, and 2427) and 1 crab sample (in segment 1006), suggesting a potential risk from noncarcinogenic effects.

The maximum cancer risks from consuming catfish and blue crabs from the Houston Ship Channel, also calculated using 18 congeners, are 3.71×10^{-4} and 4.05×10^{-5} , respectively using all the data. The TDH recommends that consumption of seafood contaminated with carcinogenic compounds be limited to amounts that result in an estimated lifetime cancer risk of 1×10^{-4} (1 excess cancer risk in 10,000 people exposed through seafood). Thus, two catfish samples (one in segment 1001 and the other in segment 1013) present a potential risk from carcinogenic effects.

Based on the total PCB water data collected in this project using the 18 NOAA congeners, segments 1006 and 1007 present a *Tier-1 primary concern* for the fish consumption use due to 86% and 50% exceedances of the 0.885 ng/L Texas WQS, respectively. However, if one calculated a site-specific water quality target based on site-specific BSAFs, the water quality target would not be exceeded.

The Draft 2004 Texas §303(d) List includes Segments 1006 and 1007 as impaired due to high concentrations of PCBs in fish tissue. It also includes the section of segment 1001 between US Hwy 90 and IH 10 and the portion of segment 1005 between I-10 and Lynchburg Ferry Road. The listings, however, are based on PCB concentrations from Aroclor analyses. Based on data on the 18 NOAA PCB congeners in tissue collected in this project and the TDH risk assessment procedure, segments 1001, 1006, 1007, 1013, 2430, and 2427 present a potential concern.

7.7 RECOMMENDATIONS

Analysis of PCB and Aroclor data gathered in this project led to the following conclusions:

- When evaluating congener-specific results, water concentrations showed a *Tier-1 primary concern* in segments 1006 and 1007; additional PCB congener in water samples are required to determine use support in segments 1006 and 1007. In contrast, when looking at Aroclor data, none of the segments showed a concern.
- Tissue data collected in this project confirms a concern of PCBs in catfish in segments 1001, 1006, and 1007 when evaluating congener data; whereas Aroclor data shows a concern in segment 1001 only.
- Congener-specific PCB data in catfish also showed potential concerns for stations located in the tidal portions of Simms Bayou, Vince Bayou, Patrick Bayou, Buffalo Bayou, and Whiteoak Bayou. These water bodies are also included in the Draft 2004 Texas §303(d) List.

The above mentioned conclusions indicate a need to evaluate both the Aroclor and congener specific data to determine if §303(d) listings and future TMDL projects are warranted. In addition, since the water quality standard and the TDH screening values are based on Aroclors and not on PCB congeners, a methodology to compare PCB data and to establish criteria to assess use support is needed. More investigation is warranted to address the new food consumption advisory for trout.

CHAPTER 8

SUMMARY AND CONCLUSIONS

This report summarizes the activities conducted by the dioxin project team during the period September 1, 2003 to August 31, 2005. These activities are part of Phase III of the dioxin TMDL project.

During WO7, 30 locations (19 in-channel and 11 tributaries) were sampled for ambient water, 55 in-channel locations were sampled for sediment, 28 locations were sampled for catfish and crab tissue, 8 locations for sediment cores, 2 locations were sampled for air deposition/ambient air, and 8 locations were sampled for stormwater runoff. Analytical results for the Spring 2004, Summer 2004, Fall 2004, and Summer 2005 sampling events are discussed in this report.

Results from the dioxin analyses showed concentrations in water that exceed the Texas Surface Water Quality Standard (0.0933 pg/L) in 94% of the samples. In addition, the health-based standard of 0.47 ng TEQ/kg (derived from the Texas WQS) was exceeded in more than 96% of the catfish and crab samples.

Results from deep and shallow water samples collected simultaneously showed that deep concentrations were generally higher than shallow concentrations, with average deep/shallow ratios of up to 1.69 and 1.54 for locations 11193 and 15979, respectively (maximum ratios were 2.85 and 2.67, respectively). An analysis of fugacity ratios suggested a lack of equilibrium at the suspended-dissolved and sediment-dissolved interfaces for most of the congeners. Data indicate that 2378-TCDD is close to equilibrium between the bottom sediments and the dissolved phase

(deep) at location 15979, whereas a bottom sediment→ dissolved flux is expected at location 11193. For almost all the remaining congeners, ratios lower than 1 were measured for the dissolved-suspended interface indicating flux of dioxins from the dissolved phase to the suspended phase. For the bottom sediment-dissolved interface, on the other hand, ratios greater than 1 were measured for some PCDFs and ratios lower than 1 for the higher chlorinated PCDDs.

Geochronology analyses performed on 7 sediment cores yielded sedimentation rates between 0.14 ± 0.08 and 113.10 ± 87.08 cm/yr. The longest time coverage of the sediment cores was about 150 years. Vertical distribution of dioxin concentrations in the collected cores versus the estimated year of deposition showed surprisingly that the oldest interval concentrations appeared to be as high or slightly higher than those measured in the surface intervals. This could indicate the presence of other sources prior to the construction of the HSC.

Measurements of dioxin concentrations in various media allowed the determination of site-specific partitioning relationships. These partitioning relationships are important not only to develop the model to support load allocations, but also to establish an appropriate water quality target for the TMDL, to allow for economical long-term monitoring of continuing progress toward the water quality target, and to facilitate implementation of the TMDL through water quality permitting. An estimation of congener-specific bioaccumulation factors (BAFs) using all the sampling data from this project yielded water quality targets for 2378-TCDD and TEQ of 0.011 and 0.070 pg/L, respectively. The calculated target for dioxin TEQ in water is approximately 75% of the state water quality criterion of 0.093 pg/L. Sediment quality targets calculated using site-specific BSAFs were calculated to be 43 and 154 ng/kg-oc for 2378-TCDD and TEQ, respectively. A comparison of sampling data to the estimated water quality targets

showed exceedance rates greater than 90%. It appeared that an 85-90% reduction in concentrations, or one order of magnitude would be required for the water quality targets to be met.

An analysis of dioxin data collected in Phases II and III of this project showed that segment 1001 exhibited the highest average concentrations of dioxins in water, segment 1007 showed the highest overall average concentration in sediment, while segment 1006 showed the highest average concentration in catfish and segment 1005 showed the highest average TEQ for crabs.

OCDD is the major contributor to the total dioxin concentration (the sum of the 17 2378-substituted congeners) in water, sediment, and catfish samples from the HSC, while 2378-TCDF is the major contributor in crab samples. However, 2378-TCDD is the major contributor to total TEQ in all cases with average contributions of 47%, 49%, 80%, and 68% for water, sediment, catfish, and crab samples, respectively.

In addition to dioxin analyses, PCB levels in water, sediment and tissue samples were determined to assess the level of impairment of the HSC system. In general, concentrations of individual PCB congeners were low and the Texas Standard for total PCB in water was exceeded only in segments 1006 and 1007 when utilizing PCB congener data. The TDH health-based PCB tissue target level (47 ng/g) was exceeded in more than 60% of the fish samples but was exceeded in only 4% of the crab samples. Aroclor data revealed mainly non-detect values for all media.

A screening quantification of relative source importance conducted using a QUAL-TX model showed that known sources (point sources and storm runoff) accounted only for 5% and 26% of the total 2378-TCDD and TEQ load in the HSC, respectively. A detailed WASP model is

underway to estimate contributions from sediment resuspension, direct deposition, and additional sources.

REFERENCES

- Ambrose, R.B., T.A. Wool, and J.L. Martin. 1993. “The Water Quality Analysis Simulation Program, WASP5.” Environmental Research Laboratory, US Environmental Protection Agency, Athens, Georgia.
- Appleby P.G. and Oldfield F., 1978. “The Calculation of Lead-210 Dates Assuming a Constant Rate of Supply of Unsupported ^{210}Pb to the Sediment.” *Catena*, 5: 1-8.
- Baca, E., P.B. Bedient and R. Olsen, 1982. “Urban Impacts of Water Supply Reservoir.” *Journal of Environmental Engineering*, 108(E1): 73-87.
- Benamen, J., N.E. Armstrong, and D.R. Maidment. 1996. “Modeling of Dissolved Oxygen in the Houston Ship Channel using WASP5 and Geographic Information Systems.” CRWR Online Report 96-2. Center for Research in Water Resources at the University of Texas, Austin, August 1996.
- Binford, M.W., 1990. “Calculation and Uncertainty Analysis of ^{210}Pb Dates for PIRLA Project Lake Sediment Cores.” *Journal of Paleolimnology*, 3: 253-267.
- City of Houston, 1988. “Wastewater Strategy Study, Volume IV, Stream Model.” Report prepared for City of Houston, Department of Public Works by Pate/EH&A Joint Venture.
- Cogliano, J.V., 1998. "Assessing Cancer Risks from Environmental PCBs." *Environmental Health Perspectives*, 106 (6):317-323.
- Craft, C.B. and Richardson, C.J., 1993. “Peat Accretion and N, P, and Organic Accumulation in Nutrient-enriched and Unenriched Everglades Peatlands.” *Journal of Applied Ecology*. 3: 446-458.

Espey, W.H., A.J. Hays, Jr., W.D. Bergman, J.P. Buckner, R.J. Huston, and G.H. Ward, Jr.,

1971. “Galveston Bay Project Water Quality Modeling and Data Management: Phase II Technical Report.” Tracor, Inc, Austin, Texas.

Gobas, FAPC, DCG Muir, and D Mackay, 1988. “Dynamics of Dietary Bioaccumulation and Faecal Elimination of Hydrophobic Organic Chemicals in Fish.” *Chemosphere*. 17(5): 943-962.

Gotz, R. And R. Lauer, 2003. "Analysis of Sources of Dioxin Contamination in Sediments and Soils Using Multivariate Statistical Methods and Neural Networks" *Environmental Science and Technology*, 37 (24): 5559-5565.

Grey, John R., Glysson, G. Douglas, Turcios, Lisa M., and Schwarz, Gregory E., 2000. “Comparability of Suspended-Sediment Concentration and Total Suspended Solids Data.” U.S. Geological Survey Water-Resources Investigations Report 00-4191.

Helsel, D.R. and R.M. Hirsch, 2002. “Statistical Methods in Water Resources. U.S. Geological Survey.” Available at <http://water.usgs.gov/pubs/twri/twri4a3/>.

Houston-Galveston Area Council, 2003. “2002 Land Cover Image Processing and Accuracy Assessment Protocol.” Prepared for Texas Commission on Environmental Quality - Texas Clean Rivers Program. Houston, TX, January 2003.

Huntley, S.L., Wenning, R.J., Su, S.H., Bonnevie, N.L., Paustenbach, D.J., 1995.

“Geochronology and Sedimentology of the Lower Passaic River, New Jersey.” *Estuaries*, 18 (2): 351-361.

Kim, J.G. and Rejmankova, E., 2002. “Recent History of Sediment Deposition in Marl and Sand based Marshes of Belize, Central America.” *Catena*, 48(4): 267-291.

- Mansour, M. (Ed), 1993. "Fate and Prediction of Environmental Chemicals in Soils, Plants, and Aquatic Systems." Lewis Publishers, Boca Raton, FL. 291 p.
- McFarland, V.A., and J.U. Clarke, 1989. "Environmental Occurrence, Abundance, and Potential Toxicity of Polychlorinated Biphenyl Congeners: Considerations for a Congener-Specific Analysis." *Environmental Health Perspectives* 81:225-239.
- Natural Resource Conservation Service, 1986. "Urban Hydrology for Small Watersheds." Technical Release 55. Conservation Engineering Division. June 1986.
- Newell, C. J., Rifai, H. S., and Bedient, P. B., 1992. "Characterization of Non-Point Sources and Loadings to Galveston Bay." GBNEP-15, Prepared for the Galveston Bay National Estuary Program, Houston, TX.
- NOAA (National Oceanic and Atmospheric Administration), 1989. "Standard Analytical Procedures of the NOAA National Analytical Facility." 2nd Edition. NOAA Tech. Mem. NMFS F/NWC-92, 1985-86. National Status and Trends Program, U.S. Department of Commerce, Rockville, MD.
- Opperhuizen, A, and DTHM Sijm, 1990. "Bioaccumulation and Biotransformation of Polychlorinated Dibenzo-*p*-dioxins and Dibenzofurans in Fish." *Environmental Toxicology and Chemistry*, 9: 175-186.
- PBS&J and Parsons Engineering, 2001. "Dioxin Sediment and Tissue Sampling in the Houston Ship Channel and Upper Galveston Bay." Prepared for Clean Rivers Program, Houston-Galveston Area Council, Houston, TX, September 2001.
- Robbins, J. A., 1978. "Geochemical and Geophysical Applications of Radioactive Lead." In *The Biogeochemistry of Lead in the Environment*. J. Nriagu (Ed.), Elsevier, 285-393.

Soil Conservation Service, 1985. "National Engineering Handbook." Section 4-Hydrology (NEH-4).

Texas Commission on Environmental Quality, 2003. "Guidance for Assessing Texas Surface and Finished Drinking Water Quality Data, 2004." Austin, TX, August , 2003.

Texas Department of Health, 2001. "Health Consultation - Houston Ship Channel and Tabbs Bay." Prepared by the Texas Department of Health under cooperative agreement with the Agency for Toxic Substances and Disease Registry. August 1, 2001.

Texas Natural Resources Conservation Commission, 2002. "Fourteen Total Maximum Daily Loads for Nickel in the Houston Ship Channel System." Prepared by the Strategic Assessment Division Water Permits and Resource Management Division. June 2002.

University of Houston, 2001. "Total Maximum Daily Load for Dioxins in the Houston Ship Channel – Final Report Work Order No. 1." Prepared for the Texas Natural Resources Conservation Commission. Houston, TX, June 2001.

University of Houston, 2004. "Total Maximum Daily Load for Dioxins in the Houston Ship Channel - Quarterly Report 2 Work Order No. 7." Prepared for the Texas Commission on Environmental Quality. Houston, TX, April 2004.

USACE (U.S. Army Corps of Engineers), 1987. "Final Feasibility Report and EIS, Galveston Bay Area Navigation Study." Volume 6. Appendix F, Plan Effects.

U.S. EPA, 1995. "Great Lakes Water Quality Initiative Technical Support Document for the Procedure to Determine Bioaccumulation Factors." EPA-820-B-95-005. Office of Water, Washington, DC.

U.S. EPA, 1999. "Polychlorinated Biphenyls (PCBs) Update: Impact on Fish Advisories." Fact Sheet, September 1999. EPA-823-F-99-019.

U.S. EPA, 2000. "Guidance for Assessing Contaminant Data for Use in Fish Advisories, Volume 1. Fish Sampling and Analysis." 3rd Edition.

U.S. EPA, 2003. "Methodology for Deriving Ambient Water Quality Criteria for the Protection of Human Health (2000). Technical Support Document. Volume 2: Development of National Bioaccumulation Factors." EPA-822-R-03-030, December 2003.

USFWS (United States Fish and Wildlife Service), 1983. "Species Profiles: Life Histories and Environmental Requirements of Coastal Fishes and Invertebrates (Gulf of Mexico): Sea Catfish and Gafftopsail Catfish." TR EL-82-4. October 1983.

Valero-Garces, B., Navas, A., Machin, J., Walling, D., 1999. "Sediment Sources and Siltation in Mountain Reservoirs: A Case Study from the Central Spanish Pyrenees." *Geomorphology*, 28: 23-41.

Walsh, J.P. and Nittrouer, C.A., 2003. "Contrasting Styles of Off-shelf Sediment Accumulation in New Guinea." *Marine Geology*, 196: 105-125.

Webster, C.F., Buchanan, T.A., Kirkpatrick, J. and Miranda R., 1998. "Polychlorinated Biphenyls in Donna Reservoir and Contiguous Waters - Results of Intensive Sediment, Water and Fish Sampling and Human Health Risk Assessment. Special Study Report No. AS-161." Field Operations Division, Texas Natural Resource Conservation Commission, Austin.

Winkels, H., Kroonenberg, S., Lychagin, M., Marin, G., Rusakov, G., Kasimov, N., 1998. "Geochronology of Priority Pollutants in Sedimentation Zones of the Volga and Danube Delta in Comparison with the Rhine Delta." *Applied Geochemistry*, 13(5): 581-591.

Winslow and Associates, Inc., 1986. “Houston Ship Channel Urban Runoff Nonpoint Source Study.” Report prepared for TDWR.

Wool, T.A., R.B. Ambrose, J.L. Martin, and E.A. Corner, 2001. “Water Quality Analysis Simulation Program (WASP) Version 6.0 - User’s Manual.” U.S. Environmental Protection Agency Region 4.

Yeager, K.M., Santschi, P.H. and Rowe, G.T., 2004. “Sediment Accumulation and Radionuclide Inventories ($^{239,240}\text{Pu}$, ^{210}Pb and ^{234}Th) in the Northern Gulf of Mexico, as Influenced by Organic Matter and Macrofaunal Density.” *Marine Chemistry*, 91: 1-14.

APPENDIX A - QUALITY ASSURANCE

**Appendix A1 - Approved Annual Update to the Quality Assurance Project Plan and July
2005 Amendment (Electronic)**

Appendix A2 - Field Duplicate Agreement for Dioxin Samples

APPENDIX B - DIOXIN LABORATORY RESULTS

Appendix B1 – Water, Sediment, and Tissue Results (File name: *DioxinWO7Data.mdb*)

Appendix B2 – Sediment Core Dioxin Results (File name: *SedimentCore.mdb*)

Appendix B3 – Air Results (File name: *Air Results.xls*)

Appendix B4 – Runoff Results (File name: *RunoffWO7.mdb*)

APPENDIX C - SEDIMENT CORE SUPPLEMENTAL DATA

APPENDIX D – FLOW REGRESSIONS

APPENDIX E – SEDIMENT LOAD STUDY

**APPENDIX F - BACKGROUND FOR
STATISTICAL ANALYSES**

Appendix F1 - Principal Component and Cluster Analysis Background

Principle Components Analysis is an exploratory data analysis method which reduces the dimensionality of a dataset by considering the characteristic vectors of a covariance matrix as orthogonal (perpendicular) linear combinations which explain the maximum amount of variance in the first few components. This means that instead of analyzing all of the original variables, the components can be used instead. This method allows a simpler analysis utilizing the first few components which capture most (approximately 90%) of the original variance of the dataset. Historically, this method has been used in anthropology, psychology, and college entry exam interpretation, among other fields of study. Presently, this method has been found useful to quantify the spatial variability in the distribution of a contaminant in the environment. Many researchers have found this method useful for explaining the concentration patterns of PCDD/Fs in the environment, including studies in British Columbia, Italy, and the Great Lakes.

"Cluster Analysis is a term used to describe a family of statistical procedures specifically designed to discover classifications within complex data sets." (Tinsley, Brown 2000) What this means is that cluster analysis is used to place variables or sample points into clusters that share the same relative characteristics as that sample point. This is done using multivariate observations and many different algorithms in statistical programs. There are many different clustering methods, and the methods chosen for this study will be further explained below.

The first step in completing a PCA is creating a covariance matrix. SPLUS statistical package was used for this and all other aspects of PCA testing. Covariance is the default SPLUS choice, and it was chosen instead of a correlation matrix because the data were of all the same

type and had previously been normalized. The scores of the loadings generated from the transposition of the data and creating of components was utilized as a way to generate scatter plots. Principle Components one and two were graphed together and patterns, or clusters, were looked for. As a way to further validate or explain clustering in the PCA, cluster analysis was employed to explore the relationships within clusters.

Several different types of cluster analysis were examined for this project. It is important to note that cluster analysis utilizes a dissimilarity matrix, while the PCA algorithm generates a similarity matrix. Four major types of cluster analysis were explored: k-means, partitioning around medoids (pam), fuzzy, and agglomerative hierarchical. With k-means, pam, and fuzzy analysis, the analysis was carried out in SPLUS.

For these three clustering techniques, the number of clusters must be chosen. This was accomplished by looking at a silhouette plot of the data. In order to create a silhouette plot, a silhouette value (s_i) was computed and represented the bar length in the plot (Mathsoft, 77). If $s_i=1$, then the point was well classified, if it was zero, the point did not fit into the cluster (Mathsoft, 78). By changing the number of clusters specified in the analysis, one can look at the overall silhouette width of the plot. The larger the width number, the better. However, if the bars lie to the left of zero, there are points which do not fit into any of the clusters. Utilizing this method, it was possible to determine the correct number of clusters for the data set.

When considering the PCDD/F data from the Houston Ship Channel, all three methods were utilized and the results compared. It was found that the k-means method was not very effective and so discarded. Using pam and fuzzy analysis gave different cluster memberships,

and no apparent pattern was evident. A more robust method was needed in order to generate results.

Agglomerative Hierarchical Clustering (AHC) was chosen as another alternative, since the number of clusters is not pre-chosen in order to run the analysis. SPSS was the statistical program used to complete this analysis. The method begins with all the data points in their own cluster, and then combines the points with the next point least dissimilar, or more similar, until there is one large group.

Ward's method was chosen as the measure of similarity between points in a cluster. This method was chosen as it gives the same amount of variance within clusters. It also assumes that the clusters are spherical in hyperspace. This may not be true, but it seems reasonable to look for clusters which have the same variance within them when looking at this data. It would be difficult to interpret the cluster results if the clusters had different amounts of variation within them.

There are several differences between k-means, pam, and fuzzy cluster analysis. First of all, k-means and pam are "crisp" clustering methods. This means that each point will be assigned to exactly one cluster, while fuzzy cluster analysis can give a data point partial assignment to more than one cluster. Secondly, there are differences in how the center of the cluster is determined. The k-means algorithm utilizes a centroid "the multidimensional version of the mean" and assigns each data point to the group with which it most closely resembles that number. The centroids change as more points are considered in the analysis and are determined using a least squared method. The partitioning around mediods (pam) partitions a set of objects into k clusters by finding k objects to represent the heart of each cluster (mediods). The mediods are

determined by minimizing the sum of dissimilarities instead of the sum of squared Euclidean distances (Mathsoft, 76).

Fuzzy cluster analysis is a little different than either k-means or pam cluster analysis. Because cluster assignments are not crisp, when looking at the output from a fuzzy cluster analysis, it is important to look at the Dunn's partition coefficient. If all the data points have multiple memberships, then the coefficient will be equal to $1/k$, (k =number of data points) and if each point belongs to only one cluster the coefficient will be equal to one (Mathsoft, 88).

Appendix F2 - Locations Sampled in 2002

Appendix F3 - Mann-Kendall Test Background

Resource: Statistical Methods for Detection and Quantification of Environmental Contamination

Robert D. Gibbons and David E. Coleman. John Wiley and Sons, NY, 2001, pp194-199.

The steps followed to perform the Mann-Kendall test were: " First, order the data by sampling date....where x_i is the measured value on occasion i . Second, record the signs of each of the $N!$ possible differences $x_{i'}-x_i$, where $i' > i$" (Gibbons and Coleman). This means that if the difference is positive, then record $a +1$, if it is negative, record $a -1$, and if there is no difference record a 0. The Mann-Kendall statistic is computed by subtracting the number of negative differences from the number of positive differences. Using the table values for the Mann-Kendall test, with a sample size of $n=5$, and $S = 0-10$, the probabilities are given in Table F1.

Table F1. Critical values for the Mann-Kendall Test for Trend

MK critical values		
S	df=5	<u>Trend</u>
0	0.592	No trend
1	0.500	Shows trend
2	0.408	
3	0.325	
4	0.242	
5	0.180	
6	0.117	
7	0.080	
8	0.042	Significant trend
9	0.035	
10	0.028	

This procedure was completed for all congeners at all sampling stations for all media. The result was considered significant if the value associated with a given S was less than the alpha value of 0.05. This would only occur for a value of S greater than 7.

APPENDIX G – HOUSTON SHIP CHANNEL MEGA-TX MODEL SEGMENTATION AND INPUT/OUTPUT FILES

Appendix G-1 Model Segmentation

Appendix G-2 QUAL-TX Input/Output Files

- TEQ simulation using permitted flows for PS (File names: *TEQ_permitted_base.inp* and *TEQ_permitted_base.out*)
- TEQ simulation using average self-reported flows for PS (File names: *TEQ_self_base.inp* and *TEQ_self_base.out*)
- TEQ simulation with additional source in 1006 (File names: *TEQ_suspected.inp* and *TEQ_suspected.out*)
- 2378-TCDD simulation using permitted flows for PS (File names: *TCDD_permitted_base.inp* and *TCDD_permitted_base.out*)
- 2378-TCDD simulation using average self-reported flows for PS (File names: *TCDD_self_base.inp* and *TCDD_self_base.out*)
- 2378-TCDD simulation with additional source in 1006 (File names: *TCDD_suspected.inp* and *TCDD_suspected.out*)

**APPENDIX H - INPUT DATASET FOR BASE CASE OF THE
WASP SIMPLIFIED MODEL**

APPENDIX I – SUPPORT OF STAKEHOLDER ACTIVITIES

Appendix I1 -Slides Presented at Stakeholder Meetings (Electronic)

Appendix I2 - Response to Comments from Oxy Vinyls on Final report WO4